PROBABILISTIC METHODS FOR ASSESSING RELIABILITY OF CONTAMINATED SEDIMENT VOLUME ESTIMATES

by

Mike Hamilton

Submitted in partial fulfillment of the requirements for
the degree of Master of Applied Science

at

Dalhousie University
Halifax, Nova Scotia
December 2020

Table of Contents

List of Figures

List of Tables

Abstract

Sampling requirements for the quality control of environmental sediment contamination characterization are not currently explicit. The effect of sample size on the accuracy of estimated volume and variability of contaminated sediments is important to quantify, as these factors potentially have major impacts on the choice of remedial action. Random field simulation has been shown to be an effective method of representing sediment thickness variation over space, and such models have been effective in the risk assessment of similar environmental studies. In this thesis, the Kriging geostatistical model, and random field simulative model, local average subdivision (LAS), have been applied to an ongoing remediation project in Boat Harbour, Nova Scotia, Canada.

The objective of this thesis is to assess the effect of sample size on the accuracy of volume estimation and its variability when comparing the more common geostatistical modeling methods versus the more novel, and promising, random field simulative methods. This thesis compares the two modeling methods at various sample sizes and discusses further implications of model effectiveness for remediation practitioners. It is found that the Kriging and LAS models produce similar results at higher sample densities (i.e. those exceeding 2.6 samples/ha), however the LAS model produces higher precision and accuracy in its estimate of the total sediment volume. Furthermore, it is concluded that, for remedial practitioners, LAS is the more effective and conservative modeling technique in comparison to Kriging for sediment volume characterization.

List of Abbreviations and Symbols

USEPA	United States Environmental Protection Agency
LAS	Local average subdivision
BH	Boat Harbour
LIF	Laser induced fluorescence
C.V.	Coefficient of variation
C.I.	Standard normal 99% confidence interval
GC	Gravity core

Acknowledgements

I would like to acknowledge the help and support of many people throughout the course of my research. I would like to express my gratitude to my co-supervisors Dr. Craig Lake and Dr. Gordon Fenton, without whose support none of this could have been possible. Without Dr. Craig Lake I would likely not have gone through with pursuing my masters and would have missed out on the opportunity for such a great experience. Furthermore, I would like to thank Hayden Tackley for his invaluable support with many different aspects of this research project.

I would like to thank Nova Scotia Lands for their support and collaboration in this project, as without their contributions none of this would be possible.

Finally, I have been blessed in many ways in life but foremost with the greatest parents, I would like to thank my parents for their unwavering support and love.

Chapter 1.0: Introduction

1.1 Preamble

This chapter will provide the problem statement and outline the rationale for the research, identify the research objectives, and frame the layout of the thesis. A discussion of the gaps in research will be presented, along with a breakdown of major milestones for the research project.

1.2 Problem Background and Statement

Environmentally impacting pollutants are an expansive issue impacting most societies globally. Many of the industrial pollutants that are released into the environment eventually settle out of the atmosphere or water and can accumulate below global waterways (United States Environmental Protection Agency, 1997). Pollutants that do not dissolve once in contact with water will eventually settle out within the waterway and can potentially adhere to the underlying sediments (United States Geological Survey, 2020). Many industrial contaminants naturally attenuate and dissipate overtime once the pollution source has halted, however, depending on the pollutant, some contaminants may persist within sediments for significant periods of time (Siegel & Bryan, 2003). The issue of contaminated sediments is a global challenge and in the United States alone it has been shown that a significant quantity of sediments have been historically contaminated by chemicals such as organics (dioxins, furans, and polychlorinated biphenyls), and heavy metals (mercury), some of which having half-lives exceeding 100 years (United States Environmental Protection Agency, 1997).

Contaminated sediments not only pose a risk to the groundwater and the adjacent surface water, but also can have adverse effects to aquatic and human health (Office of Solid Waste and Emergency Response, 2005). The adverse impacts of contaminants to aquatic and human health have societal and economic impacts as well. Depending on the contaminant and location, total destruction of aquatic life or contamination of a community's sole potable water source can have irreversible impacts on aquatic ecosystems and human health (United States Environmental Protection Agency, 1997).

In the United States it was estimated that approximately 10%, or about 917 million m^3, of sediments underlying surface waters were sufficiently contaminated with toxic pollutants that pose potential risk to aquatic and human health (United States Environmental Protection Agency, 1997). In Canada, there are over 23,663 suspected contaminated federally owned sites, of which it is estimated that the Canadian Federal Government will be liable for up to $5.7 billion in relation to the contaminant impacts and remediation (Government of Canada, 2020). When considering the cost of remediation, estimating the total volume of contaminants on a per site basis is important, as costs can vary heavily depending on the volume of contaminants that are required to be remediated (Rosengard, et al., 2010).

Estimation of contaminant sediment volumes is a challenge as developing a full understanding of the magnitude and extent of contaminant sediment volumes can prove to be difficult (Marine Environmental Support Office, 2002). Depending on the area the contamination is spread over, it could take hundreds to thousands of soil samples to accurately delineate the extent and magnitude of soil contamination across a contaminated site (Canadian Council of Minsters of the Environment, 2016). When

considering the effect of sample size on volume estimation, estimating the reliability of the volume estimate is also important, as it helps understand if greater or fewer samples would be effective (United States Environmental Protection Agency Quality Staff, 2002). Furthermore, the reliability of estimates can aid in determining how to develop a more conservative estimate of the volume to avoid issues such as project overrun costs related to volume underestimation (United States Environmental Protection Agency Quality Staff, 2002).

Most sediment remediation projects currently utilize primarily four main remediation methods, including dredging and containment, capping, monitor/natural recovery and in-situ treatment (Rosengard et al., 2010). These remediation methods have been used in many notable remediation projects, of which have been discussed at length in the 16th edition of the USEPA superfund remedy report and will not be discussed further here (Office of Land and Emergency Management, 2020). Each remediation method has its own diverse set of challenges when estimating total cost and are all dependent on total volume and extent of sediments to be remediated. Traditionally, these sediment remediation projects have high degrees of uncertainty when budgeted, and actual costs can vary up to 1,000 times the original estimate, as discussed in Rosengard et al. (2010), even after decades of industry experience and published research and reviews.

Estimating contaminant sediment volumes has not been standardized globally, but in 2003, the United States Environmental Protection Agency (USEPA) released a methodology guidance document to help support more accurate estimates (Stahl & Bromm, 2003). In essence, the USEPA suggests relatively simplistic volume calculations, using the total encapsulated 3-dimensional volume (i.e. cone or square)

based on extents of the known contamination plume. The USEPA's simplistic, basic shape, volume estimation method merely applies a 3-dimensional shape to the contaminant plume, and as such is not considering the exact variability in the extents of the contamination. Although the USEPA suggests a simplistic approach, the most potentially effective, both time and cost-wise, is parametric modeling due to its objectivity, repeatability, and speed (Rosengard, et al., 2010; Burns, et al., 1995). Parametric modeling, as a potential replacement of the simplistic USEPA approach, entails the use of statistical distribution fitting of specific parameters to predict unknown data. The use of knowledge of the mean and standard deviation of a dataset of sampled sediment thicknesses can lead to prediction of sediment thicknesses of un-sampled locations within the measured field. A major problem with the use of modeling is the apparent lack of publicly available real-world examples of model implementation and results in the estimation of contaminant sediment volumes in remediation projects (Myers & Engler, 2005).

To best utilize modeling methods, the individual models for each parameter need to be properly validated themselves, factors such as the effect of sample size on confidence and the applicability and effectiveness of individual models for the specific challenges must be considered. Globally, best practices for planning sampling regimes can be described predominantly as professional opinion, or "judgement" based, as professional judgement often leads to a more cost effective and flexible sampling regime (McBratney & Laslett, 1993; United States Environmental Protection Agency, 2002). Major drawbacks of the judgement-based sampling regime methods are that they do not allow accurate quantification of the level of confidence and allow for

unknown levels of selection bias that may lead to mischaracterization of contamination (United States Environmental Protection Agency, 2002).

Beyond the locations of the samples, the number of samples required to accurately delineate a contaminate body has not been well investigated, especially for the case of model implementation. Global guidelines and regulations, when considering sample size for contaminated sediments, stipulate a “sufficient” number of samples are necessary, however, “sufficient” is left undefined and objective (Alberta Environment and Parks, 2016; Government of New Jersey, 2018; United States Environmental Protection Agency, 2018; Association of Professional Geoscientists of Ontario, 2011; Canadian Council of Minsters of the Environment, 2016).

Furthermore, some authors have discussed required sample sizes when considering statistical modeling techniques, however, have not discussed these sample sizes in terms of sample size per unit area (sampling density) (Mitchell, et al., 2018; Webster & Oliver, 1993; Burrough & McDonnel, 1998). Some researchers have attempted to determine the potential efficiency gains resulting from model implementation in terms of percentage of fewer samples required to acquire the same level of confidence in the characterization of specific soil parameters but lack discussion of necessary sample numbers on a sample per unit area basis (Mitchell, et al., 2018). Research related to the effect of sample density on model accuracy have been limited, and mostly conclude that sample density requirements depend on parameter variability (Li & Heap, 2011; Benson, et al., 1994). The apparent lack of coverage of required sample densities leaves a gap in understanding given that 100 samples may be effective at modeling

spatial variability of soil parameters over a 10-acre plot, however, may be completely ineffective for a 100-ha plot of land.

Statistical and probabilistic modeling techniques are potentially a promising, reproduceable and effective method of accurately characterizing the extent and magnitude of sediment contamination. However, they have not been thoroughly assessed. Furthermore, challenges surrounding what is supportably a sufficient sample size and density has gone generally un-verified and left to professional judgement.

1.3 Objectives

This research will analyze the suitability of two separate geostatistical and random field simulation techniques for assessing the extent and magnitude of contaminant sediment volumes at a well-sampled study site. This thesis will address the following research questions:

- How do the total volumes of contaminated sediment at the study site compare when obtained using geostatistical modeling techniques and simulation modeling techniques?
- How does the sample size affect the confidence of the estimate of total volume of contaminated sediment for the Boat Harbour study site?

1.4 Thesis Outline

This thesis is structured into five chapters. This initial chapter has been used to identify the problem statement and the need for this research to frame the research questions.

Chapter 2 will provide a literature review of related work pertaining to geostatistical and random field simulation modeling. An overview of the relevant characteristics and background of the study site, Boat Harbour (BH), will be provided to further support model selection.

Chapter 3 details the methodology of the techniques and modeling applied to achieve the research objectives. A research plan involving the use of the ordinary Kriging model as well as a random field simulation model (i.e. 2-dimensional local average subdivision) was implemented. The research plan can be divided into four major milestones to achieve the research objectives:

1) (Milestone 1) A compilation of coordinate systems was developed for further modeling purposes.
2) (Milestone 2) The correlation structure of the sample thickness dataset, was estimated through use of an exponentially decaying correlation function, and a list of isotropic correlation lengths were generated.
3) (Milestone 3) The implementation of Kriging and 2D LAS models, in which specific setup, processing, and analysis was conducted for the individual requirements and outputs of the models.
4) (Milestone 4) The final volume estimates generated were generated from a realized grid of modeled thicknesses, which entailed developing a 3-dimensional mesh representation of BH sediment and integrating across the whole mass.

Chapter 4 presents the results obtained from the methodology presented in chapter 3 and addresses the statistical importance of the results. Further analyses and the

significance of sample size on the accuracy and confidence of volume estimates developed from each respective model will also be discussed.

Chapter 5 summarizes the findings and identify areas for further investigation.

Chapter 2.0: Background

2.1 Preamble

This chapter will provide an overview of the study location including details on the history of the site and characteristics of the contaminated sediment being examined in this study. Finally, an in-depth background on the sediment volume modeling techniques, Kriging, and 2D LAS, will be provided.

2.2 Contaminated Sediment Study Site - Boat Harbour

The study site used for investigation is a wastewater treatment facility often referred to as Boat Harbour (BH), in Pictou Landing, Nova Scotia. BH has been in operation since 1967 as a raw effluent sedimentation and stabilization pond for several industrial services, with the primary source of influent being from a nearby kraft pulp mill (Tackley, 2019). BH was originally a tidal estuary that connected to the Atlantic Ocean, however, in the 1960s was dammed as an effluent treatment pond. Boat Harbour is currently composed of primarily two separate coves (Cove A and Cove B) and is approximately 140 hectares in total size, and can be seen depicted in Figure 1.

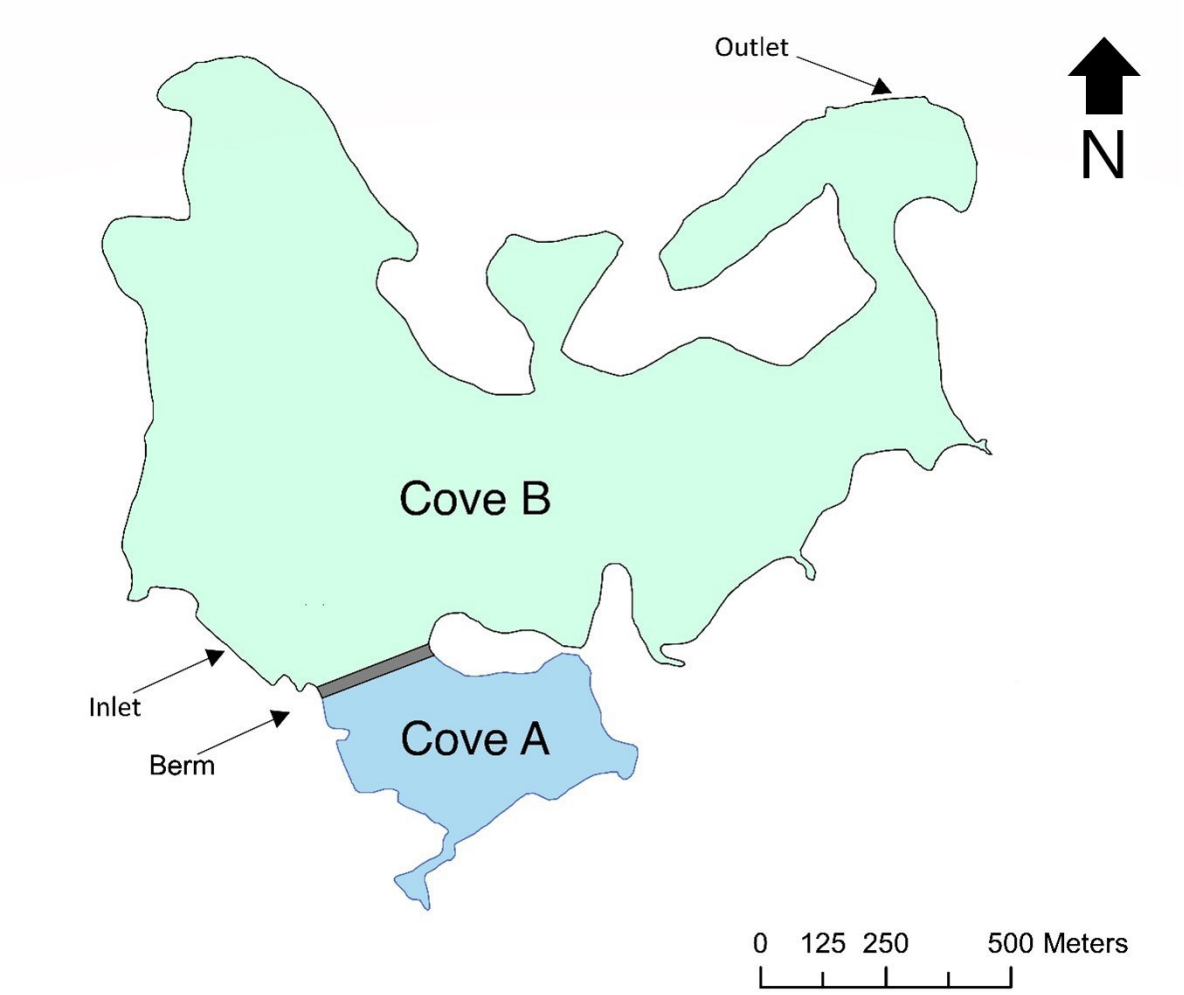

Figure 1: GIS Representation of Cove A and Cove B of Boat Harbour.

BH operated as a traditional secondary treatment facility for the raw effluent of the kraft pulp and paper mill, and as such accumulated an estimated 577,000m^3 of unconsolidated sediment in the basin (GHD, 2018). Until the beginning of 2020, the mill maintained and operated BH as a sedimentation and stabilization pond for approximately 87,000 m^3 of raw effluent per day (JWEL & Beak Consultants Limted., 1993). In January of 2020, the mill ceased operation and BH was decommissioned as a treatment facility.

Due to the sedimentation characteristics of BH, the anthropogenic sediment underlying BH varies in composition and thickness. Sample collection of the sediment underlying BH has been conducted using traditional coring techniques, which consisted of percussion coring and gravity coring, as well as recent laser induced fluorescence (LIF) techniques. The anthropogenic sediment is visually distinct, as it appears as a black sludge like layer overlying the naturally occurring grey marine silt (Spooner & Dunnington, 2016). Analysis of the sediment that underlies BH has revealed a variety of contaminants that persist above regulatory guidelines, including metals (cadmium, chromium, copper, lead, mercury and zinc), as well as organic compounds such as dioxins and furans (GHD, 2018). The sediments underlying BH have been previously extensively characterized by multiple authors (Spooner & Dunnington, 2016; Hoffman, et al., 2019; Alimohammadi, et al., 2020; Alimohammadi, et al., 2019; Tackley, et al., 2020), and as a result will not be further discussed in this paper.

2.3 Sediment Thickness Characterization

Given that the thickness of the anthropogenic sediment is variable across BH, estimation of the total volume of sediment requiring remediation is challenging without significant sample sizes (number of samples) (Tackley, 2019). Current volume estimation has been based on professional judgement and industry standard approaches. To estimate how many samples are required to achieve a sufficient confidence, modeling techniques can be implemented. The use of statistical and probabilistic modeling, although is not uncommon for subterranean estimation of many types, has not been thoroughly investigated for a wide range of environmental remediation projects.

Investigation of the varying sediment thickness underlying BH was conducted though 51 coring and 504 LIF probing measurements, or 555 measurements in total, to investigate the variability in thickness across BH. A full list of sample type (coring or LIF) as well as northing and easting data can be found in Appendix A: . The location and density of the 555 measurements were determined by the project team based on professional judgement and experience in contaminant characterization.

2.3.1 Geostatistical Modeling

Geostatistical modeling techniques have been shown to be effective in the field of soil characterization and soil contaminant volume modeling (Schrooten & Alphen, 2008). There are many available geostatistical modeling techniques, such as Inverse Distance Weighted Interpolation, Linear Regression, Gaussian decay, and Kriging (Zimmerman, et al., 1999). All of these models are relatively simplistic in implementation, with varying degrees of usefulness for different applications (Columbia Public Health, 2020). Of all the models, Kriging is the most useful for soil thickness characterization, as Kriging accounts for the spatial variability of the sampled data using an autocorrelation among sampled data points (Zimmerman, et al., 1999). In essence for this study, Kriging provides a best estimate of layer thickness which takes the spatial location of observations and their covariance structure into account (Fenton & Griffiths, 2008).

Kriging models are geostatistical interpolative methods, essentially a deterministic model that is a locally weighted moving average estimator of the conditional mean value of a point or many points (Gilbert & Simpson, 1983), conditioned on the observations. Kriging methods are implemented to produce the best estimate of a gaussian field

between known points. Simply put, common covariance models used in Kriging assume that known points closer to the point to be estimated will be weighted higher, for the purpose of estimation, rather than that of known points further away. In this research, the distance between sampled and estimated values is used to estimate their covariance, based on a specified correlation length. The specified correlation length, which in this research is assumed to be isotropic, is estimated from the site in question, as discussed later. A rough definition of correlation length is the distance beyond which two points in the field become negligibly correlated (Fenton & Griffiths, 2008).

Kriging models determine the best estimate by minimizing the estimator error, which attempts to minimize the difference between the estimate and its true (but unknown and random) value, through minimization of variation among estimated points. Kriging estimators are a best linear unbiased estimator. (Gilbert & Simpson, 1983).

The way in which kriging estimates are effected by points closer are as seen in Equation (1), where the estimate at the unobserved point $\hat{X}_{n+1}$ (Kriging best estimate thickness at the unknown point) is determined via a combination of our sampled observed thicknesses:

$$\hat{X}_{n+1} = \mu_{n+1} + \sum_{i=1}^{n} \beta_i (X_i - \mu_i) \qquad (1)$$

Where β_i is the Kriging weight, X_i is a known sampled thickness, μ_i is the mean of the sampled thicknesses and μ_{n+1} is the moving conditional mean. The Kriging weights are determined by solving the following for beta:

$$\{A\}\{\beta\} = \{b\} \qquad (2)$$

where *A* is the covariance matrix between sampled thickness points, and *b* is the covariance vector between sampled thickness points and prediction points (locations to be estimated).

The Kriging used herein (ordinary Kriging) makes some inherent assumptions about the field to be modeled, including (Fenton & Griffiths, 2008):

1) Stationarity: The probability distribution of the parameter to be estimated (the thickness) does not vary over the entire field, therefore the mean and variance of the parameters being modeled remain constant; and,
2) Isotropy: The correlation length is the same in all directions.

To develop the Kriging weights, the spatial covariance matrix must be developed and inverted. It should be highlighted that the Kriging method can suffer from numerical problems in the inversion of the covariance field if points in the field are highly correlated. Numerical singularity of the covariance matrix can occur when the sampled datapoints are too spatially close so that their correlation coefficient is very close to 1.0. Note that when the correlation coefficient is equal to 1.0, the two matrix elements become linearly dependent and the matrix becomes singular.

Due to the general simplicity and wealth of knowledge on Kriging models, it is a recommended geospatial analysis technique for the use of soil characterization in environmental site characterizations (Canadian Council of Minsters of the Environment, 2016). In the case of BH, the layer being modeled has been produced by sedimentation processes and should be expected to gradually vary, and so Kriging methods seem well suited for this application.

2.3.2 Probabilistic Modeling

When considering other modeling techniques for investigating variation in sediment thickness, probabilistic based methods are of interest. Probabilistic techniques using Monte Carlo simulations are a means of obtaining probability distribution estimates of the parameter of interest (sediment volume) and are especially useful when the cost of remedial action is high due to their ability to characterize the potential variability in the field being simulated (United States Environmental Protection Agency, 1997). Through characterizing the potential variability in the filed being simulated, practitioners implementing Monte Carlo simulations can better avoid potential risks associated with over or underestimating the variable of interest. When considering the use of Monte Carlo simulation for environmental site characterization, it has been recommended as a preferable method in order to quantitatively characterize the uncertainty and variability (Canadian Council of Minsters of the Environment, 2016). One of the most challenging aspects of this type of modeling is assessing the variability and uncertainty based on the sample data provided, especially considering quantitative assumptions are often produced from qualitative insights (United States Environmental Protection Agency, 1997). Furthermore, although Monte Carlo simulations have been implemented in the environmental field in relation to remedial activities, these projects have been primarily focused on contaminated water characterization (Canadian Council of Minsters of the Environment, 2016).

Many types of random field simulations exist, of which there is discrete Fourier transform, fast Fourier transform, turning bands method, and local average subdivision to name a few (Fenton & Griffiths, 2008). Each simulation technique has its own set of

advantages and disadvantages, which include, computation time and accuracy of the mean, variance and covariance structures (Fenton & Griffiths, 2008). The local average subdivision method is selected here because it is simple to use and provides local average values over each discrete cell similar to soil engineering parameters that tend to be measured and reported as the average or range of the property being estimated. The LAS method, like Kriging, preserves the spatial correlation, but also simulates realizations of averages which aids in reducing the variance of the random field produced (Liza, 2014). The way in which LAS simulates values in 2D can be summarized as the following (Fenton & Vanmarcke, 1990):

1) Generate a normally distributed global average (labeled Z_1^0) with mean zero and variance obtained from local averaging theory (therefore developing the parent cell of the first subdivision, to which 4 children will be generated),
2) Subdivide the field into four equal parts,
3) Generate four normally distributed values (four children), Z_1^1, Z_2^1, Z_3^1 and Z_4^1, whose means are variances are selected so as to satisfy three criteria:
    a. That they show the correct variance according to local averaging theory,
    b. That they are properly correlated with one another,
    c. That they average to the parent value, $\frac{1}{4}(Z_1^1 + Z_2^1 + Z_3^1 + Z_4^1) = Z_1^0$,

    That is, the distributions of Z_1^1, Z_2^1, Z_3^1 and Z_4^1 are conditioned on the value of Z_1^0,
4) Subdivide each cell in stage 1 into four equal parts (therefore subdividing 4 parent cells into 16 new children),

5) Generate four normally distributed values, Z_1^2, Z_2^2, Z_3^2 and Z_4^2, whose means and variances are selected to satisfy four criteria:

   a. That they show the correct variance according to local averaging theory,

   b. That they are properly correlated with one another,

   c. That they average to the parent value, $\frac{1}{4}(Z_1^2 + Z_2^2 + Z_3^2 + Z_4^2) = Z_1^1$,

   d. That they are properly correlated with Z_5^2, Z_6^2, Z_7^2, Z_8^2, Z_9^2, Z_{10}^2, Z_{11}^2, Z_{12}^2, Z_{13}^2, Z_{14}^2, Z_{15}^2 and Z_{16}^2.

To develop the normally distributed values of the children cells a mean term is added to a random component, whereas the mean term is derived from a best linear unbiased estimate, specifically (Fenton & Griffiths, 2008):

$$\underset{\sim}{Z}^{i+1} = \underset{\approx}{A}^T \underset{\sim}{Z}^i + \underset{\approx}{L}\underset{\sim}{U} \qquad (3)$$

where $\underset{\sim}{U}$ is a vector of independent N(0,1) standard normal random variables, and the covariance matrices $\underset{\approx}{A}$, and $\underset{\approx}{L}$ are defined by the following underlying covariance calculations of $\underset{\approx}{R}$ (covariances between parent cells in the neighborhood), $\underset{\approx}{S}$ (covariances between parent cells and subdivided cells) and $\underset{\approx}{B}$ (covariances between subdivided cells) (Fenton & Griffiths, 2008):

$$\underset{\approx}{R} = E\left[\underset{\sim}{Z}^i \underset{\sim}{Z}^{i^T}\right] \qquad (4)$$

$$\underset{\approx}{S} = E[\underset{\sim}{Z}^i \underset{\sim}{Z}^{i+1^T}], \text{ and} \qquad (5)$$

$$\underset{\approx}{B} = E[\underset{\sim}{Z}^{i+1} \underset{\sim}{Z}^{i+1^T}] \qquad (6)$$

and the matrix $\underset{\approx}{A}$ is determined by:

$$\underset{\approx}{A} = \underset{\approx}{R}^{-1}\underset{\approx}{S} \qquad (7)$$

The lower triangular matrix $\underset{\approx}{L}$ satisfies:

$$\underset{\approx}{L}\underset{\approx}{L}^{T} = \underset{\approx}{B} - \underset{\approx}{S}^{T}\underset{\approx}{A} \qquad (8)$$

2.4 Areas Requiring Research

Modeling techniques such as Kriging, or LAS can potentially be effective in the modeling the thickness of anthropogenic sediments for the purpose of environmental remediation. Kriging models have been significantly studied due to their past relevance in the mining industry, and have been implemented in many fields including oil exploration, ground water studies, bathymetry, acid rain reposition, air quality data, and many more (Gilbert & Simpson, 1983). Furthermore, probabilistic analyses, such as Monte Carlo simulations, have also been implemented to characterize uncertainty and variability for water characterization projects (Jiang, 2013).

An area lacking greater clarity in the literature is the effectiveness of geostatistical methods in comparison to random field simulative methods, especially when considering the effect of sample size in such a comparison. Furthermore, when comparing random field simulation modeling and Kriging, some research has been done to show that, when characterizing contaminant concentrations in soil, random field simulation methods result in smaller misclassification costs, such as underestimation of contaminant concentration levels (Goovaerts, 1996).

In terms of soil characterization modeling, simulation methods have been utilized and studied for many decades but have challenges. When considering the newer, and underutilized due to less widespread understanding in comparison to geostatistical modeling, random field simulation methods, they are potentially powerful for environmentally contaminated soil thickness characterization but lack direct examples of

implementation for such projects. The lack of directly relatable projects with the implementation of random field simulation for contaminated soil thickness characterization poses a challenge, as contaminant remediation contractors may be more ambivalent when deciding between previously proven and more novel techniques due to the speculation of potential unknown risks. Furthermore, when considering the main challenges of any remediation project, determining the extent and magnitude of contamination, both models may potentially produce useful understanding of a challenging project when project budgets may limit the number of samples. At low sample sizes, Kriging has the inherent problem of being unable to fully characterize the variability of the soil field, whereas random field simulation methods are better equipped to overcome this challenge and are recommended for characterization of the variability and confidence of its developed estimates.

Chapter 3.0: Methods

3.1 Preamble

This chapter outlines the implementation of the Kriging program, krige, and LAS program, sim2d, for the assessment of sediment thickness and overall volume of the contaminated sediments underlying BH. The required inputs and outputs of each model considered will be discussed, along with how the models use the input data.

3.2 Data Collection

The data utilized in this thesis was obtained from both traditional gravity coring (51 samples) and laser induced fluorescence probes (504 samples). The use of LIF as a novel technique for obtaining sediment thickness at the BH site has been discussed in detail by Davidson (2020) and will not be discussed any further here. In total, 555 sediment thickness values were recorded across the whole of cove A and B of BH. For this project, only data for cove B was investigated. From here on in, when referring to BH the author is only speaking about cove B. Figure 2 is a map of BH, produced using MATLAB, showing the geographic location of samples across the body of cove B.

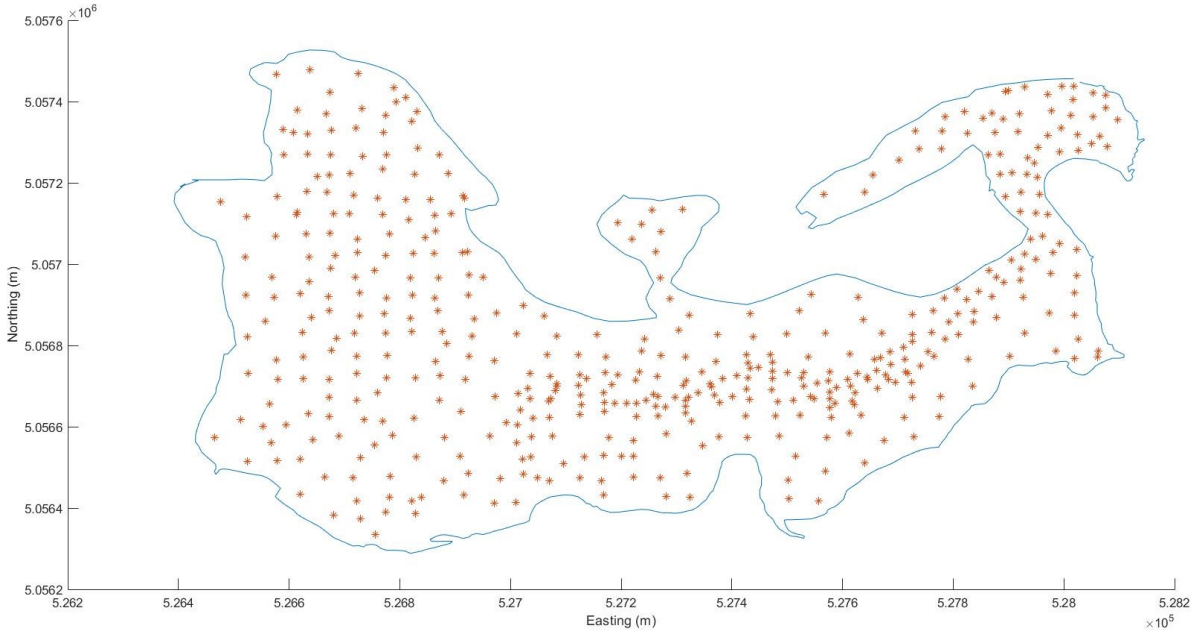

Figure 2: MATLAB representation of outline of Boat Harbour with asterisks (*) used to represent the locations of sampled sediment thicknesses.

3.3 Field Initialization and Data Filtering

To establish the extents of BH for the two model techniques employed, the shoreline of the BH sedimentation basin was determined using Google Earth Pro. Along these shoreline extents, 587 discrete pins were individually placed to produce a list of GPS points. The exact spacing between discrete pinpoints that encapsulated the cove was variable and chosen to ensure that the irregular outline of the cove was accurately represented. The 587 outline points of BH were assigned a sediment thickness of zero. A list of these 587 pin locations can be found in Appendix B: .

The discrete pinpoint outline of BH was converted from 587 discrete pin locations into a continuous polyline shape through use of the predeveloped “inpolygon” script

within Matlab_R2019b (Mathworks, Inc., 2020). The continuous polyline outline of BH was developed to filter the sampled thickness datapoints.

As the sample thickness data included both cove A and B this dataset needed to be filtered to remove cove A from the dataset. Furthermore, to assess the plan view area of cove B, the “polyarea” script within MATLAB was used, which uses the continuous polyline shape previously mentioned, and calculates the area contained within the polyline shape.

To initialize and process data for the krige and sim2d programs, a grid of 10m x 10m discrete (x,y) location points was generated for BH through use of a custom-made MATLAB script. Simulated/estimated soil thickness values were produced at each grid point. In total, a grid of 11,512 location points was generated.

To prevent potential modeling problems caused by linear dependencies in the covariance matrix for either model, the input sample data was filtered further. Filtering through removal and averaging was conducted on the LIF and cored sample data, as some locations had duplicate samples as well as clustering of sample locations. Filtering entailed considering clustered locations where a LIF and cored sample was taken, and if the measured thickness values were within 20% of each other, the average of the two values was used, otherwise the LIF reading was removed from the sample set given that the traditional thickness measurement method is coring. For this research, clusters were defined to be two or more samples within 10m of each other. Furthermore, in some locations, duplicate LIF readings were produced; in these locations an average value was used. Finally, to further avoid singularities in the covariance matrix, in locations where sample clustering occurred (i.e. 2 or more samples within a 10m radius

of each other), these samples were averaged into a singular central data point. A summary table of final 460 samples of thickness data following the data filtration can be seen in Appendix C: .

3.4 Evaluating the Correlation Structure of Contaminant Thicknesses in BH

Both the krige and sim2d programs require an understanding of the spatial correlation structure of BH to determine their covariance matrices and isotropic correlation lengths. The sampled locations within BH were irregularly spaced, as seen in Figure 2. This irregular sample regime poses a challenge for evaluating the correlation structure as classical estimators for correlation structure require equispaced data (Liza, 2014). Using the pre-initialized field of 10m x 10m spaced location grid points, the thickness values were transformed into a 10m spaced data set using the "scatteredInterpolant" linear interpolation method within MATLAB (Liza, 2014). This interpolation method uses a Delaunay triangulation of the scattered sample points to perform interpolation which provides a simplistic linearly weighted interpolated estimate of the soil thickness at predetermined location grid points (Mathworks, Inc., 2020). The interpolated equispaced field of data then allows classical correlation structure estimators to be used to estimate the correlation lengths, as the data is converted such that it is equispaced.

As BH is a non-square shape, the 2D correlation length cannot be determined for all of BH using all the samples at once. To calculate the correlation length from the grid of thickness values produced through use of scatteredInterpolant, 6 square regions were selected within BH to investigate the estimated maximum, minimum and average correlation lengths for all BH, as shown in Figure 3. These 6 regions within BH were

squares of dimension 210m, 330m, 390m, 350m, 290m, and 130m respectively (with 10m x 10m grid spacing) and were chosen to visually contain as many sampled thickness data points as possible while trying to be spaced across the entire plan area of BH. A graphical representation of the square regions used for the correlation structure estimation can be seen overlaid Figure 2 below, in Figure 3.

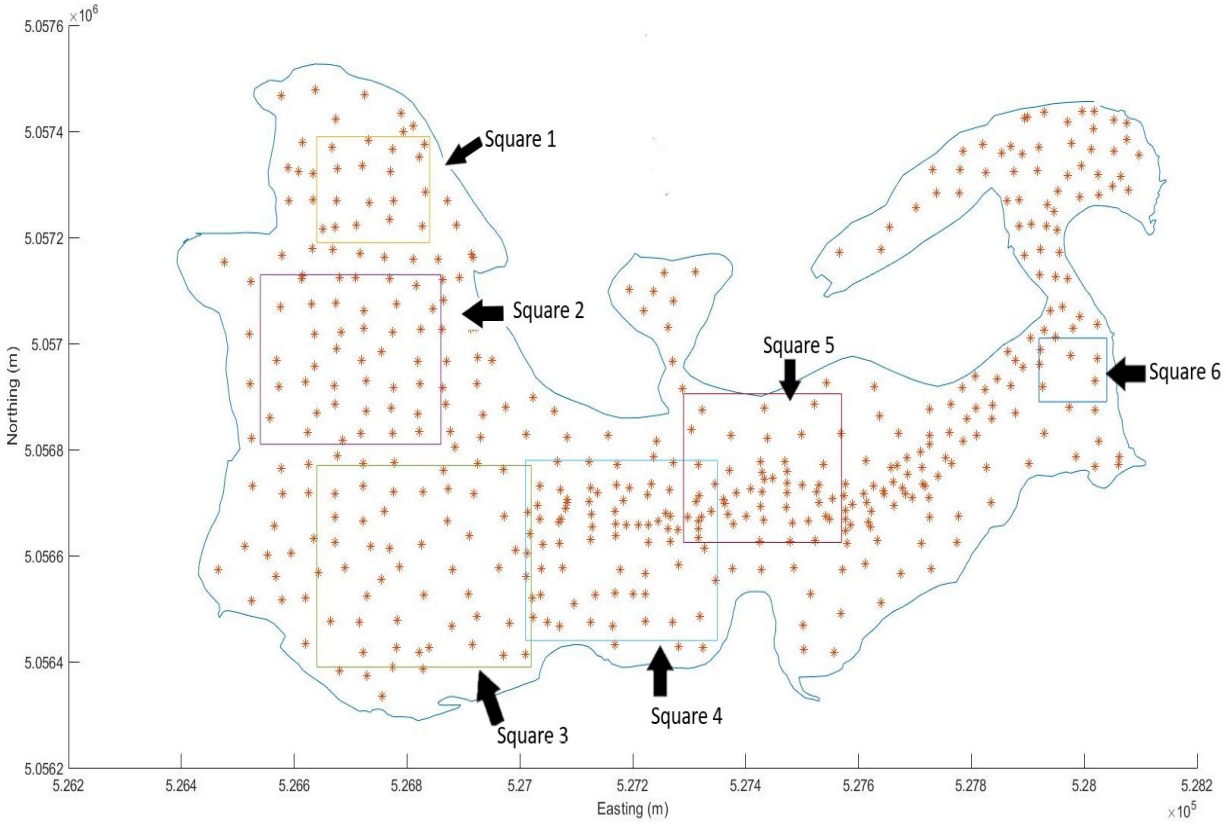

Figure 3: Graphical Representation of Square Regions used to Determine the Isotropic Correlation Length within Boat Harbour, with 460 sampled thickness locations (*).

Using a computer program called cor2d, developed by Fenton, the correlation lengths were estimated (Fenton & Griffiths, 2008). The cor2d program estimates the correlation lengths by fitting a theoretical exponentially decaying correlation model to

the thickness sample correlation function using linear regression. The fitted correlation function is Markovian in nature, having the following form

$$\rho(\tau_{ij}) = exp\left\{\frac{-2|\tau_{ij}|}{\theta}\right\} \quad (9)$$

where τ_{ij} is the distance between the *i*'th and *j*'th grid points, θ is the correlation length, and ρ is the correlation coefficient. The covariance between any pair of grid points is then calculated to be:

$$C_{ij} = \sigma_x^2 \rho(\tau_{ij}) \quad (10)$$

Where σ_x^2 is the sample point variance.

The average, maximum and minimum estimated isotropic correlation lengths from cor2d were then used for further BH modeling. Through modeling a range (maximum, average, minimum) of correlation lengths, an improved understanding of the variability in soil thickness within BH can be obtained.

To investigate the effect of sample size on the estimated correlation structure and model simulated volume and thickness, the 460 samples were randomized and split into groups. These groups were used as the "known" sampled thickness inputs to the krige and sim2d programs, as well as the inputs to scatteredinterpolant and cor2d. The groups started with 50 samples, then 100 samples and then increments of 100 until the maximum sample size (i.e. 460) was reached. In other words, six sample groups were created in total: 50, 100, 200, 300, 400, and 460 samples. The correlation lengths were estimated for each sample size group. To develop the sample size groups, a standard normal distribution random number generator was used, generating a vector of

independent N(0,1) standard normal variables, as a column within Microsoft Excel of 460 random values specified to range from 0 to 1. The column of random values was then inserted alongside a column of sampled thickness values and their locations, such that each thickness value had an assigned random value from 0 to 1. The generated random numbers were then sorted from smallest to largest to develop the groupings. The first sample size grouping of 0-50 encapsulated the thickness data with the smallest 50 random number values, the next grouping of 0-100 had the smallest 100 random number values and so on until all 6 groupings were generated. The use of the random number generator and associated sorting of thickness values was done to avoid any bias. The sample thickness groupings and their related (x,y) location data can be found in Appendix C: .

3.5 Kriging

3.5.1 Thickness Data Setup

An ordinary Kriging program written by Fenton (krige), was used to determine the Kriging weights, best estimate, and estimator error at each of series of unknown locations. The program requires the following input parameters:

1) Number of samples, number of unknown points to be estimated, space dimension (i.e. 2 dimensional);
2) Sample thickness point variance, correlation length;
3) Coordinates of each known thickness sample point (x,y);
4) Coordinates of each unknown (to be estimated) point (x,y); and,
5) Known thickness values.

Using the pre-initialized 10m x 10m field of location points as described in section 3.3, the program krige was used to provide best estimates of the contaminant thickness

at 11,512 unknown points in BH (11,512 points generated by the 10m x 10m grid). The thickness estimates were determined at all unknown points for differing numbers of sample thickness known locations (sample size groups), as well as differing point variances and correlation lengths, as described in section 3.4. For each of the 6 sample groups, three Kriging models were developed using the max, min and average correlation lengths, leading to 18 models in total. The input parameters for each Kriging model are summarized in Table 1:

Table 1: Summary of kriging model input parameters.

Group - Type	***Correlation Length (m)***	***Number of Unknown Points***	***Number of Known Points***	***Sample Point Variance (cm)***
50 - Kavg	106.6	11,512	637	1245.1
50 - Kmax	154.9	11,512	637	1245.1
50 - Kmin	78.7	11,512	637	1245.1
100 - Kavg	107.1	11,512	687	827.0
100 - Kmax	143.0	11,512	687	827.0
100 - Kmin	64.6	11,512	687	827.0
200 - Kavg	110.5	11,512	787	600.7
200 - Kmax	147.2	11,512	787	600.7
200 - Kmin	46.8	11,512	787	600.7
300 - Kavg	101.3	11,512	887	554.7
300 - Kmax	134.4	11,512	887	554.7
300 - Kmin	66.5	11,512	887	554.7
400 - Kavg	99.1	11,512	987	524.6
400 - Kmax	146.8	11,512	987	524.6
400 - Kmin	59.5	11,512	987	524.6
460 - Kavg	92.5	11,512	1,087	485.7
460 - Kmax	135.8	11,512	1,087	485.7
460 - Kmin	61.0	11,512	1,087	485.7

It should be noted that the number of known points for the krige program included the discrete boundary data, and as such, each grouping of known points in Table 1 is the number of sampled sediment thickness values plus the number of 0 thickness boundary points.

Once the krige program input file was prepared and processed with the following outputs:

1) Vector of Kriging weights + Lagrange parameter (used to develop the best estimate thickness value in the matrix functions by minimizing the estimator error);
2) Best estimate of thickness at the unknown point; and
3) Estimator error standard deviation at the estimated location.

3.5.2 Processing of Krige Output Data

Using the output from the krige program, all subsequent data analyses were performed using Microsoft Excel (Excel) in conjunction with MATLAB. As all 11,512 estimated points had in the order of 1,000 related known points within the field, the output text files were very large and required further data analysis. Furthermore, due to the size of the output krige program files, data handling programs such as Excel have difficulty due to data management constraints. For example, Excel worksheets are limited to 1,048,576 rows (Microsoft, n.d.), whereas the Kriging output files were an order of magnitude larger. Excel's 'Power Query', which allows for data manipulation of files prior to importation into Excel and therefore is able to handle more than 1,048,576 rows of data, was used to transform the krige output file into a file consisting of 11,512 estimated point lines, each containing 3 values: the best estimate, the Lagrange parameter, and the error standard deviation.

3.6 Sim2d

3.6.1 Sim2d Model Setup

To investigate the effectiveness of random field simulation for the estimation of BH contaminant thickness, a 2-dimensional conditioned random field that uses the LAS

technique was used. This program was written by Fenton and is entitled “sim2d’. The program generates a series of two dimensional local average random fields using the LAS algorithm, and is setup to allow for conditioning of the covariance matrices using a set of known points (known thicknesses and locations) within the field. The program requires the following input parameters:

1) The desired field resolution (N1 x N2);
2) X and Y field sizes;
3) Sample Point variance of the process;
4) X direction correlation length;
5) Y direction correlation length;
6) Number of realizations;
7) Field mean;
8) Number of known thicknesses; and,
9) Coordinates and values of known thicknesses (X, Y, and Z {thickness in cm} value).

The field resolution given by N1 x N2 determines the number of points in the x and y directions, and the X and Y field sizes determine the length, in meters, for which the sim2d program must compute values. In this thesis, a 10m x 10m spaced grid was required, of 1760m x 1760m in total. Combining the N1 x N2 and X and Y field sizes together, there are 176 locations for the sim2d program to estimate thicknesses in the x direction (which is 1760m long) and 176 locations in the y direction (which is 1760m long), or 176 locations in each direction with 10m spacing.

Using the same sample data as used in the krige program setup (see Appendix C:), the random field was conditioned so that it assumes the known (sampled) thickness values at the known locations. The conditioning of the field entails setting sampled

locations to a fixed (known) thickness value (fixed as a known value within the field). Using the same sample groups as described in section 3.4, the sim2d input parameters were adjusted to investigate the effect of the sample size on the uncertainty in the contaminant volume estimate. The point variance, x and y correlation lengths, field mean, number of known sampled thicknesses, and coordinates and values for the known thicknesses were adjusted to represent the different sample groups and correlation lengths. It should be noted that the estimated correlation lengths used in both krige and sim2d are considered “isotropic”, such that they are the same in both the x and y direction. The number of realizations was determined through trials of computation time, determining 1,000 realizations was the optimal count, as more realizations led to computation and processing times that would delay the project unnecessarily. The determination of 1,000 realizations was done by comparing volume estimate changes for 1, 100, 1,000, and 10,000 realizations, finding that 1,000 realizations produced nearly identical results to 10,000 realizations for the investigated case at a fraction of the computation time. Furthermore, for each sample number group (e.g. 50, 100, 200, etc.), the minimum, average and maximum correlation lengths were input into the sim2d program, producing 18 individual LAS models with 1,000 realizations each (18,000 simulations of BH in total).

For sim2d to construct a random field realization, it requires a rectangular region to simulate. A 176 by 176 points field, with 10m by 10m spacing, was constructed to ensure that the resulting field fully covered the bounds of BH. As such, 176^2 = 30,976 data points were simulated for each realization of BH. A summary table of all sim2d input parameters can be seen below in Table 2.

Table 2: Summary table of sim2d program input parameters.

Group - Type	Correlation Length (m)	Sample Field Mean (cm)	Sample Point Variance (cm)	N1 x N2	X and Y Field Sizes (m)	Number of Known Points
50 - Savg	106.6	37.3	1245.1	176 176	1760 1760	637
50 - Smax	154.9	37.3	1245.1	176 176	1760 1760	637
50 - Smin	78.7	37.3	1245.1	176 176	1760 1760	637
100 - Savg	107.1	31.4	827.0	176 176	1760 1760	687
100 - Smax	143.0	31.4	827.0	176 176	1760 1760	687
100 - Smin	64.6	31.4	827.0	176 176	1760 1760	687
200 - Savg	110.5	29.3	600.7	176 176	1760 1760	787
200 - Smax	147.2	29.3	600.7	176 176	1760 1760	787
200 - Smin	46.8	29.3	600.7	176 176	1760 1760	787
300 - Savg	101.3	28.7	554.7	176 176	1760 1760	887
300 - Smax	134.4	28.7	554.7	176 176	1760 1760	887
300 - Smin	66.5	28.7	554.7	176 176	1760 1760	887
400 - Savg	99.1	28.4	524.6	176 176	1760 1760	987
400 - Smax	146.8	28.4	524.6	176 176	1760 1760	987
400 - Smin	59.5	28.4	524.6	176 176	1760 1760	987
460 - Savg	92.5	27.7	485.7	176 176	1760 1760	1,087
460 - Smax	135.8	27.7	485.7	176 176	1760 1760	1,087
460 - Smin	61.0	27.7	485.7	176 176	1760 1760	1,087

Once the input file was prepared, it could be processed by the sim2d program with the following outputs in the form of a text file for each realization:

1) The input parameters echoed; and,
2) 30,978 contaminant thickness realizations for each point in the field.

3.6.2 Sim2d Output Data Processing

Using the output text file from the sim2d program, all further analysis was done using Microsoft Excel in conjunction with MATLAB. As each sample group had over (30,978 thickness realizations x 1,000 simulations/correlation length x 3 correlation lengths/sample group) 15,489,000 output thickness values to process. As sim2d generates a rectangular grid of simulated thickness, not all simulated data points are within BH, as in the case of estimated thickness locations in krige, only 11,512 simulated thicknesses were needed of the 30,978. In essence, sim2d simulated thicknesses outside of the bounds of BH, and all simulated values outside of the bounds of BH were removed. A MATLAB script was employed to determine the locations within and outside of BH using MATLAB's inpolygon function (as described in section 3.3).

3.7 Volume Estimation and Visual 3-D Model Development

3.7.1 Volume and 3-D Model Setup

MATLAB was used for all volume estimation and 3-D modeling. Two scripts were produced to calculate the volume for each set of output data points for kriging and sim2d, and then produce and save individual 3-D renderings of thickness variation within the BH outline.

Volume calculation was done by inputting each realization (for both krige and sim2d) of BH individually into MATLAB and setting the bounds of BH to zero thickness. The use of the MATLAB function "griddata" was used to convert the discrete scattered thickness data produced through the krige best estimate and sim2d individual simulations into 3-D

continuous surface plots. The volume was then calculated through numerically evaluating the griddata function as a double integral by the MATLAB function “quad2d”.

To produce the individual 3-D thickness variation renderings, for the purpose of visual inspection, the MATLAB “Delaunay” function was used to develop a 3-D Delaunay triangulation plot of the discrete gridded data. The actual 3-D renderings were then produced through the MATLAB function “trisurf” which uses the Delaunay triangulation to plot the varying surface of the sediment thickness. The 3-D renderings were produced to inspect the model output thickness variation to ensure model stability and allow for improved understanding of thickness variation.

3.7.2 Processing of Sim2d Realizations

As sim2d produced 1,000 realizations for each correlation length, an extra layer of processing was required. A MATLAB script was used to automate the processing of each 1,000 realizations, such that each realization had an individual volume calculation and 3-D rendering.

3.8 Statistics and Probability

Through use of preloaded statistical packages within MATLAB, all necessary post processing statistical and probabilistic analyses were conducted.

As sim2d produces 1,000 realizations for each simulation it was possible to conduct statistical analyses of the data. The following statistics were conducted on the LAS results:

1) 99% confidence intervals about the mean;

2) Probability plots of volume compared to a normal distribution;

3) Boxplots of the volumes;

4) Bar graphs of the volumes with the 99% confidence interval as error bars; and,

5) Histograms of the volumes with a fitted normal distribution overlaid.

As kriging only produces a singular best estimate for each simulation the following analysis was conducted:

1) 3-D renderings of the variance (or standard deviation) of the Kriging estimate at each grid point;

2) Computation of the total volume estimator error; and,

3) Bar graphs of the volumes with the 99% confidence interval, based on the estimator error, shown as error bars.

Finally, comparison between the Kriging and LAS results was conducted through use of bar-graphs with both LAS and Kriging results depicted along with their error bars. In terms of error bars, the 99% confidence interval is depicted for the LAS volume distribution, as well as the 99% confidence interval for Kriging based on best estimate estimator error standard deviation.

Chapter 4.0: Results and Discussion

4.1 Preamble

This section presents the results obtained from the Kriging and LAS models and provides analysis of these results. The effect of sample size is investigated on a per model basis, as well as a comparison of volume estimates between models. Finally, the accuracy and efficiency of both models is discussed in the context of increasing sample sizes, as well as how the discussed details may affect practitioners that may use either model.

4.2 Correlation Lengths

The correlation lengths were assessed as anisotropic and isotropic, with the assumption that the results for the anisotropic correlation structure would differ minimally from the isotropic structure. It was found that the average anisotropic correlation length differed minimally in the x and y directions from the average isotropic correlation lengths for the 6 squares defined in Figure 3, and as such the isotropic assumption was shown to be valid. A summary table of the correlation length results can be found in Appendix D:

The isotropic correlation lengths obtained from the different squares shown on Figure 3 via cor2d is shown in Table 3. A summary of the average, maximum, and minimum isotropic correlation lengths in meters from the 6 squares, using increasing amounts of sample sizes are provided as well in the table. These correlation lengths were used in both the LAS and Krige models discussed later in this section.

Table 3: Cor2d estimated isotropic correlation lengths given in meters.

	Sample Size (#)					
Square (#)	**50**	**100**	**200**	**300**	**400**	**460**
1	115	114	134	102	77	80
2	93	119	135	116	132	97
3	106	142	115	134	146	135
4	154	121	147	115	105	104
5	90	80	84	66	59	61
6	78	64	46	73	72	75
Max	154	142	147	134	146	135
Avg	106	107	110	101	99	92
Min	78	64	46	66	59	61

When considering the correlation lengths in Table 3, it can be seen that at the minimum number of samples considered in the study (i.e. 50), the average, maximum, and minimum correlation lengths are generally in good comparison to that calculated from the 460 sample size. Although there is an 820% increase in sample size from the smallest count to the largest count, the difference in correlation length is only about 20m when the number of samples is varied from 50 to 460 for all three (max, avg, min) scenarios (or 29% difference in the case of the minimum correlation length).

4.3 Kriging Volume Estimates

Krige best estimate values are determined by producing the best linear unbiased estimate, and as such, only one best estimates model is produced per set of input parameters. As per the steps outlined previously in section 3.5, the Krige models produced 18 sets of output data, and these results can be summarized in the table below.

Table 4: Summary table of Kriging model results.

Sample Number Group – Type	***Correlation Length (m)***	***Sample Point Variance (cm)***	***Best Estimate Volume (m^3)***	***Avg. Sample Thickness (cm)***	***Avg. Estimated Thickness (cm)***	***Standard Deviation of the Volume (m^3)***
50 - Kavg	106.6	1245.1	147,219	37.3	13.02	38,095
50 - Kmax	154.9	1245.1	172,680	37.3	15.26	48,245
50 - Kmin	78.7	1245.1	124,824	37.3	11.09	30,460
100 - Kavg	107.1	827.0	172,147	31.4	15.34	29,499
100 - Kmax	143.0	827.0	186,738	31.4	16.61	34,882
100 - Kmin	64.6	827.0	141,330	31.4	12.65	20,593
200 - Kavg	110.5	600.7	209,147	29.3	18.80	23,337
200 - Kmax	147.2	600.7	217,366	29.3	19.49	26,949
200 - Kmin	46.8	600.7	169,850	29.3	15.32	12,997
300 - Kavg	101.3	554.7	218,498	28.7	19.67	19,906
300 - Kmax	134.4	554.7	223,568	28.7	20.12	22,849
300 - Kmin	66.5	554.7	206,380	28.7	18.61	12,050
400 - Kavg	99.1	524.6	220,411	28.4	19.94	17,980
400 - Kmax	146.8	524.6	224,443	28.4	20.32	21,502
400 - Kmin	59.5	524.6	210,272	28.4	19.05	13,453
460 - Kavg	92.5	485.7	221,182	27.7	20.02	16,128
460 - Kmax	135.8	485.7	224,609	27.7	20.34	19,225
460 - Kmin	61.0	485.7	214,351	27.7	19.43	12,823

As seen in Table 4, the Krige best estimate volume increases as the sample size increases. This is also true of the average estimated thickness. When considering the variability about the mean, the standard deviation values decrease as sample size increases, and this is to be expected as, the sample point variance to overall model variance can be depicted below for the ordinary kriging (i.e. ok) model in Equation (11).

$$\sigma_{OK}^2 = \sigma^2 - w'D \qquad (11)$$

Where σ_{OK}^2 is the overall estimator variance, σ^2 is the sample point variance, w' represents a transposed vector of kriging weights, and D is a vector of kriging covariances between the sample locations and location being estimated. Hence, overall, as the correlation between observations and prediction points increases due to

increased sample size, the sample point variance decreases, and the overall estimator standard deviation σ_{OK} decreases. This decrease in estimator standard deviation as sample size increases is well documented, and what is to be expected (Altman & Bland, 1996).

When considering the gradual decrease in standard deviation of the volume estimate, the coefficient of uncertainty (C.V.) can be a useful comparative variable, as calculated in Equation (12).

$$C.V.(\%) = \frac{Volume\ Standard\ Deviation}{Mean\ Volume} \qquad (12)$$

The C.V. value makes it possible to compare the variability about the estimated volume between multiple sample sizes and both model types. In essence, higher C.V. percentages represent increased uncertainty and less precision. Furthermore, when considering the variability about the mean, the standard normal 99% confidence interval (C.I.) can be calculated. A summary of C.V. and C.I. values for Kriging estimated volumes can be found in Table 5.

Table 5: Summary table of Kriging estimated volume model 99% confidence intervals and coefficients of variation.

Sample Number Group – Type	***Best Estimate Volume (m^3)***	***99% C.I. (+/-) (m^3)***	***C.V. (%)***
50 - Kavg	147,219	88,610	25.9
50 - Kmax	172,680	112,219	27.9
50 - Kmin	124,824	70,851	24.4
100 - Kavg	172,147	68,615	17.1
100 - Kmax	186,738	81,136	18.7
100 - Kmin	141,330	47,900	14.6
200 - Kavg	209,147	54,282	11.2
200 - Kmax	217,366	62,684	12.4
200 - Kmin	169,850	30,230	7.7
300 - Kavg	218,498	46,301	9.1
300 - Kmax	223,568	53,147	10.2
300 - Kmin	206,380	28,027	5.8
400 - Kavg	220,411	41,822	8.2
400 - Kmax	224,443	50,015	9.6
400 - Kmin	210,272	31,291	6.4
460 - Kavg	221,182	37,515	7.3
460 - Kmax	224,609	44,717	8.6
460 - Kmin	214,351	29,826	6.0

The gradual decline of C.V. is to be expected traditionally as sample number increases, as there is an expected gradual decline of sample point variance and therefore estimator standard deviation.

When considering the Kriging estimate volume for BH, for a given sample size, the maximum correlation length produced the largest volume estimate while the minimum correlation the smallest volume estimate. The trend of larger correlation lengths causing larger best estimate volumes is likely caused by the increased effect of the sampled thicknesses on the estimated values that surround them. The relationship between larger correlation lengths and larger volume is potentially because of increased

correlation with nearby (sampled) points, in comparison to the farther boundary (0 thickness) points.

Due to the gradual trends in the estimated volume results, the sample size groupings of 50, 300 and 460 at the average correlation lengths will be selected for further illustration of the effect of sample size.

4.3.1 50 Samples

At a sample size of 50, the Krige model produces the lowest confidence in its volume estimate, with large variability among the estimated points and large C.V. The average correlation length of 154.9 m has a volume 99% C.I. of 88,610 m^3 and C.V. of 25.9% with an estimated volume of 147,219m^3. Furthermore, when considering the average sampled thickness to average estimated thickness, there is a disparity of approximately 2.85 sampled thickness:1 estimated thickness, which, is likely caused by the prevalence of 587 BH boundary 0 cm thickness values in comparison to only 50 interior sampled thicknesses. The 2-D predicted contaminant thickness map for the best estimate thickness can be seen below for the average correlation length. It should be noted that 2-D predicted contaminant thickness maps were produced for both the Krige model, and an averaged thickness simulation case of the LAS model, at the average correlation length and remaining sample sizes, and can be found in Appendix E: .

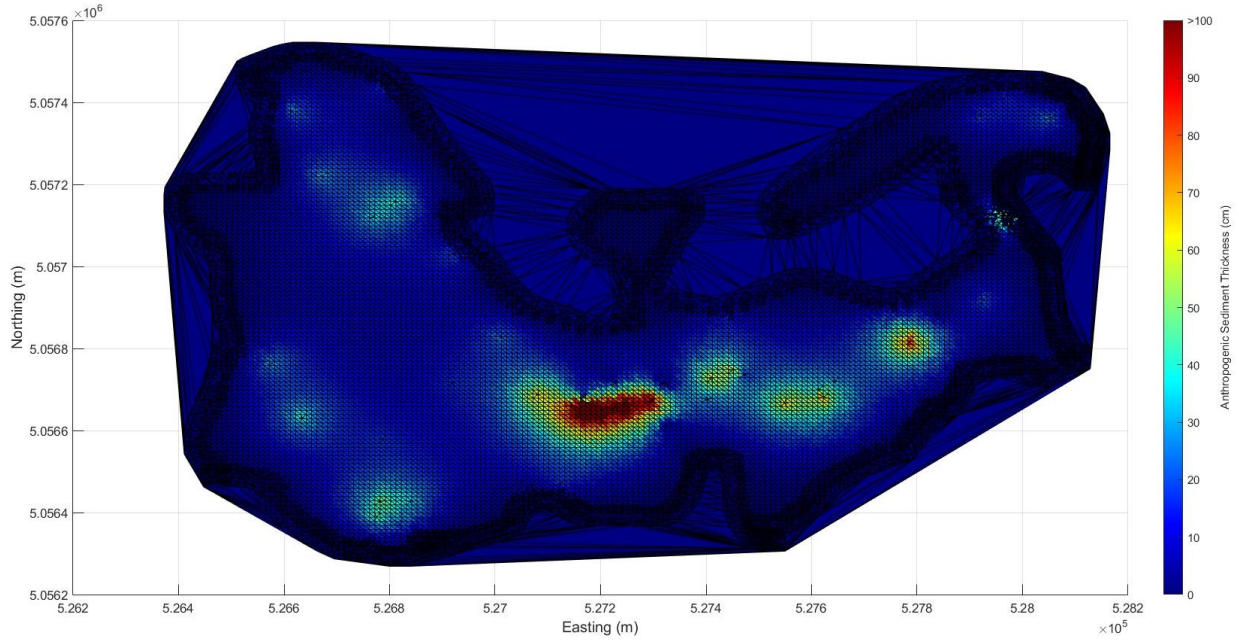

Figure 4: Krige best estimate of BH at the average correlation length and sample size of 50.

As seen in Figure 4, the regions of increased sediment thickness (red on the RGB colour scale) are at locations where a number of actual sample locations occur within BH, as shown in Figure 5. Furthermore, it should be noted that in all consequent thickness variation figures, the upper bound of the sediment thickness colour bar has been set to >100cm to improve comparison of thickness variation between parameter sets. This decision of setting the maximum colour bar colour is to standardize the colour scale between model variations, as well as account for the fact that some thicknesses exceed 150cm, and as such make it difficult to visualize the variation in thickness due to scaling issues. It should be noted that the main features of Figure 4 are that it shows signs of increased thickness around the center of Figure 4, as well as small pockets of increased thickness throughout.

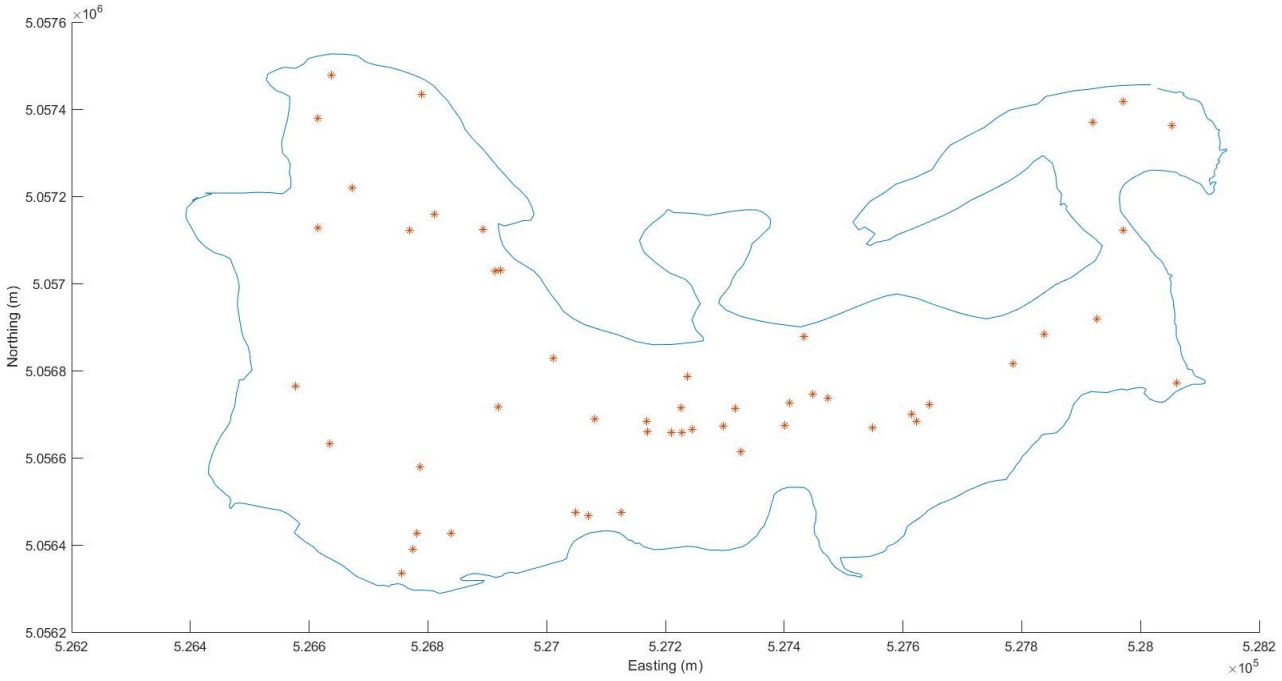

Figure 5: Outline of BH sampled locations for a sample size of 50.

As clear when comparing Figure 4 and Figure 5, areas which contain greater numbers of samples are generally regions of increased thickness. The effect of sample thickness locations is further demonstrated on the variability plot, in which the standard deviation value for each estimated thickness location is plotted, as seen in Figure 6. Where the thickness has been sampled, the thickness is assumed to be known, and so the estimator standard deviation (standard deviation) at the sample points is zero. The standard deviation increases with distance from sample points. The largest standard deviation found was 35 cm.

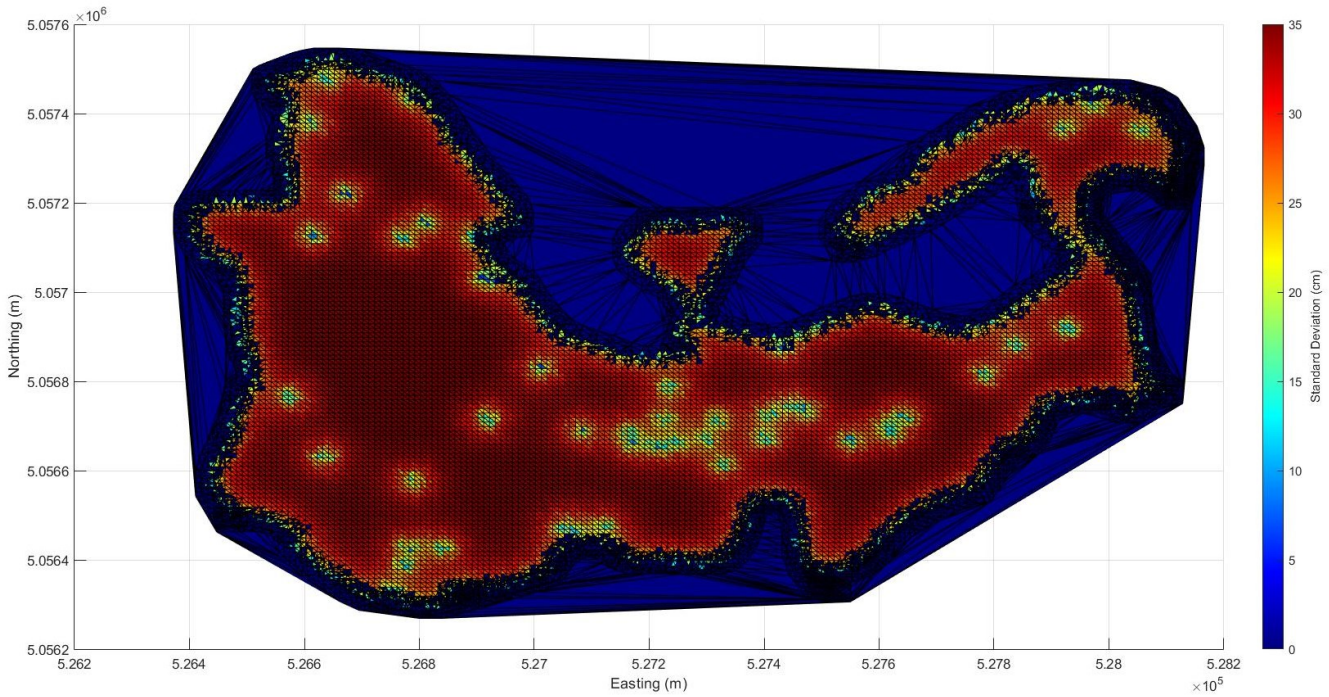

Figure 6: Standard deviation plot using the average correlation length and sample size of 50.

4.3.2 300 Samples

At a sample size of 300, the Kriging model produces improved confidence in its best estimates, with improved standard deviation between sample points compared to a sample size of 50. The average correlation length of 101.3 m has a volume 99% C.I. of 46,301 m^3 and has a C.V. of 9.1% with total volume estimate of 218,498m^3. This C.V of 9.1% is a noticeable improvement in comparison to the 50-sample coefficient of variation of 25.9% and supports the improvement (reduction) in variance as sample size increases. Furthermore, when considering the average sampled thickness compared to the average estimated thickness, the disparity is approximately 1.46:1, which shows a noticeable improvement when compared to a sample size of 50. This improvement in the ratio of average sampled thickness to average estimated thickness goes to support

the effect of increased sample size improving the volume estimate due to a lesser effect of the BH bounds. When considering the change in best estimate volume from the 50-sample size grouping to 300-sample size grouping, there is a notable increase in estimated volume of 48.4%. The 2-D colour map model for the best estimate thickness can be seen in Figure 7 for the average correlation length.

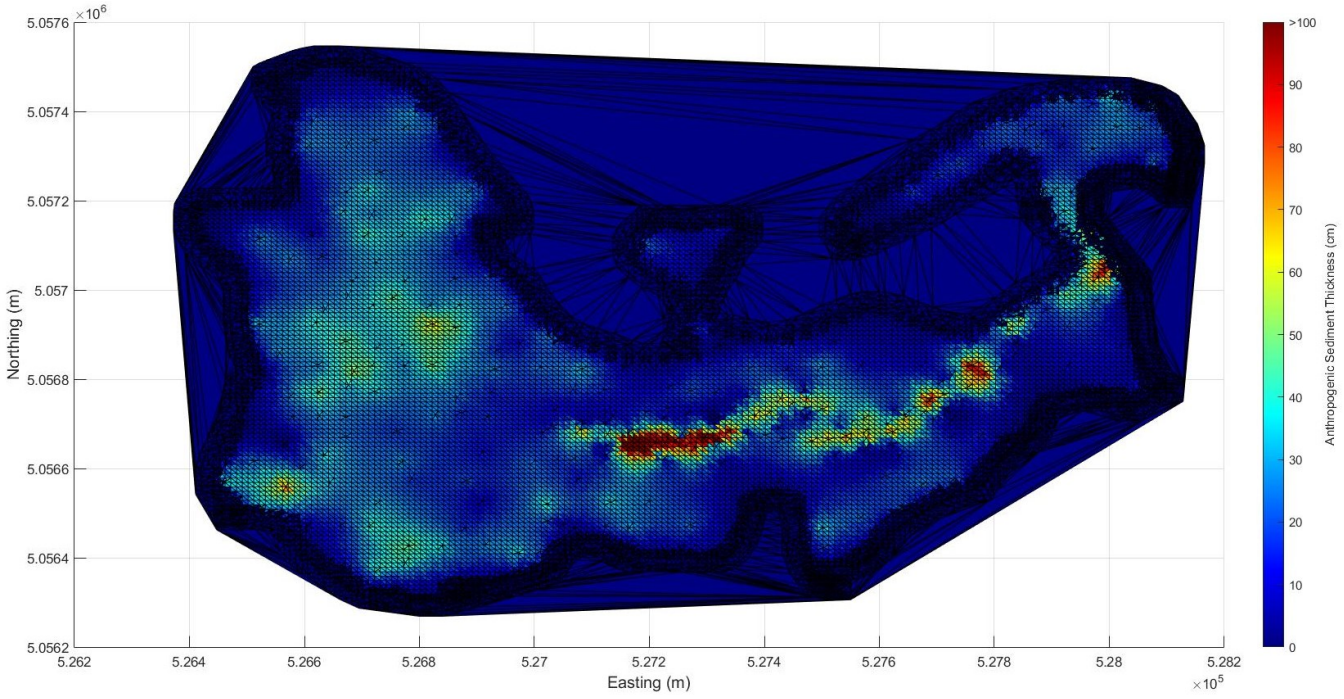

Figure 7: Krige best estimate of thickness within BH at the average correlation length and sample size of 300.

As previously mentioned in Section 4.4.1, and as seen in Figure 7, the regions of increased thickness are regions at which actual samples have been taken within BH, when compared to Figure 8. It should be noted that there is a clear structure forming within Figure 7, with the majority of thicker values within a main body, also to the left-hand side of Figure 7, and along a seemingly continuous increased thickness channel

from inlet to outlet of BH. Furthermore, there are signs of thicker contaminant layers at the outlet of BH, which is in the upper right-hand of Figure 7.

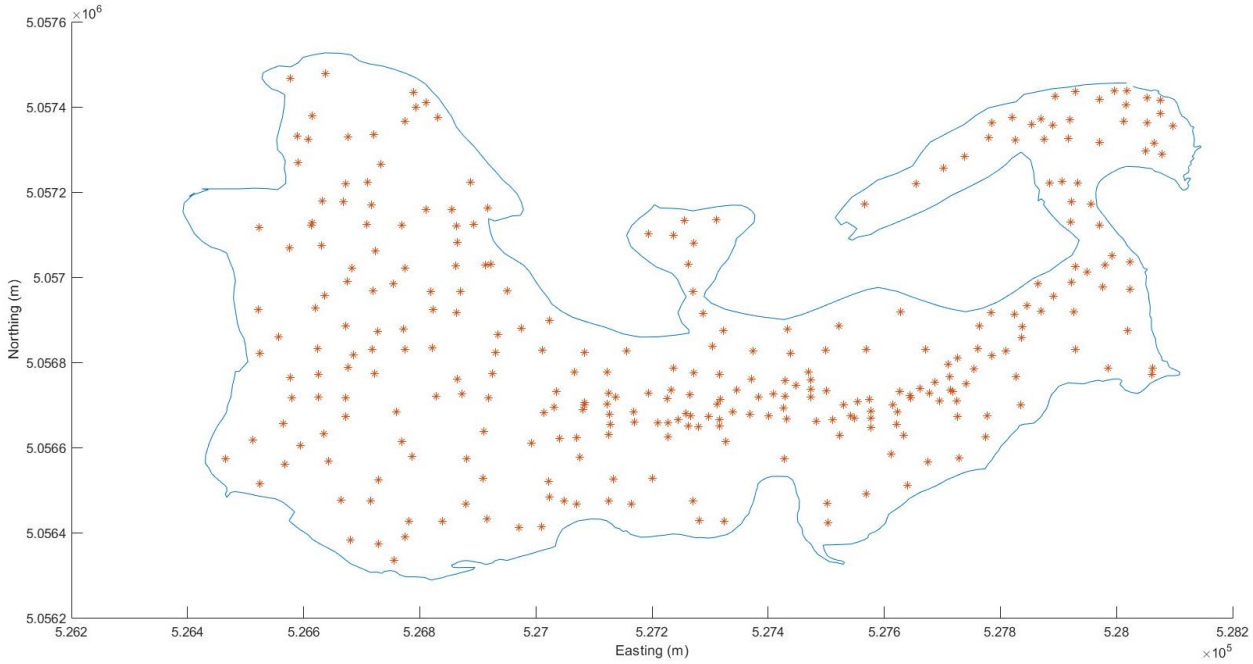

Figure 8: Outline of BH sampled locations for sample size of 300.

As is clear once again, when comparing Figure 7 and Figure 8, areas with greater numbers of samples are generally regions of increased thickness. The observed increase in estimated thickness is caused by the correlation of estimated thickness to sampled thickness, through the best linear unbiased estimate which Kriging uses. This best linear unbiased estimate is in essence linearly interpolating between known thickness values, and therefore regions with fewer sampled thicknesses will be further affected by the 0-thickness boundary condition and estimate values trending to 0.The effect of sample thickness locations is also demonstrated in the variability plot, in which the standard deviation of each estimated thickness location is plotted in Figure 9.

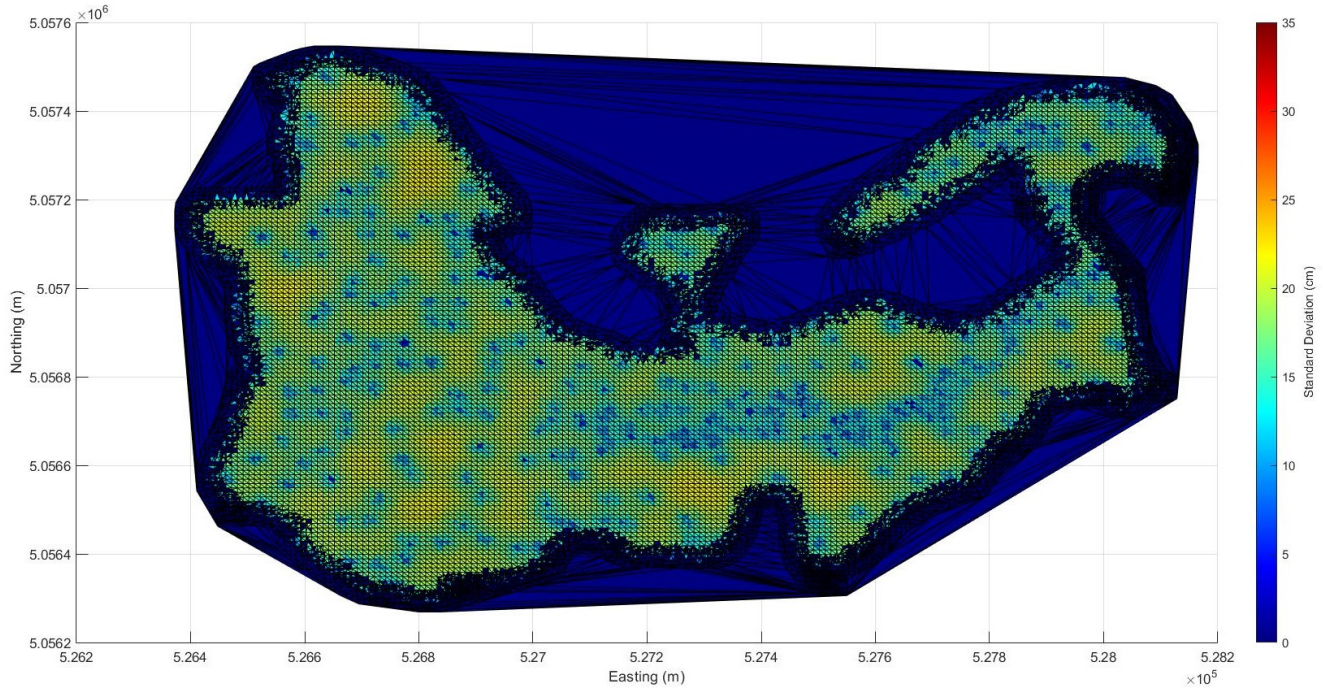

Figure 9: Standard deviation plot using the average correlation length and sample size of 300.

As seen in Figure 9, regions in which sample thickness values have been measured have (assumed) zero variance. Regions further away from the sampled data show higher variability, peaking at a standard deviation value of 22.5 cm. When considering the maximum standard deviation found for the 50-sample group (35 cm), the 300-sample group provides over a 35% decrease in maximum estimator standard deviation.

4.3.3 460 Samples

At an input sample size of 460, the Krige model produces its highest confidence in its best estimates, with minimized variability among the estimated points. The average correlation length of 92.5 m has a 99% C.I. of 37,515 m^3 and C.V. of 7.3% at an estimated volume of 221,182 m^3. This C.V. of 7.3% is a smaller improvement in comparison to the 300-sample grouping error of 9.1%, however, further supports the

improvement in variability as sample size increases. Furthermore, when compared to the best estimate produced from the 300-sample grouping, the best estimate volume only resulted a 1.2% increase.

When considering the average sampled thickness compared to the average estimated thickness, the disparity is approximately 1.43:1, which shows a minimal change when compared to the 300-sample grouping. The minimal change in sampled to estimated average thickness appears to support that at 300 samples the effects of the BH 0 thickness bounds have been minimized. The 2-D colour map model for the best estimate volume can be seen below for the average correlation length.

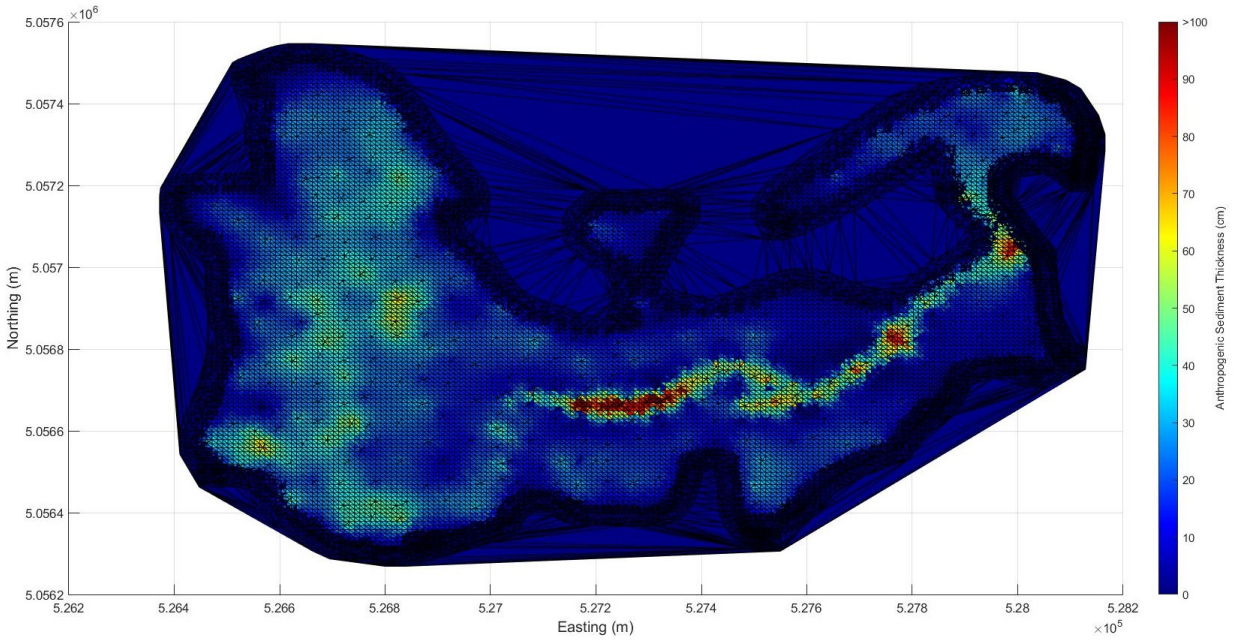

Figure 10: Krige best estimate of thicknesses within BH at the average correlation length and sample size of 460.

As seen previously mentioned, as seen above in Figure 10, the regions of increased thickness are regions at which actual samples have been taken within BH, when

compared to Figure 11 below. Furthermore, the thickness structures mentioned in Section 4.4.2 have become more prevalent and clear at the increased sample number. It should be noted that the channel from inlet to outlet has further increased in granularity.

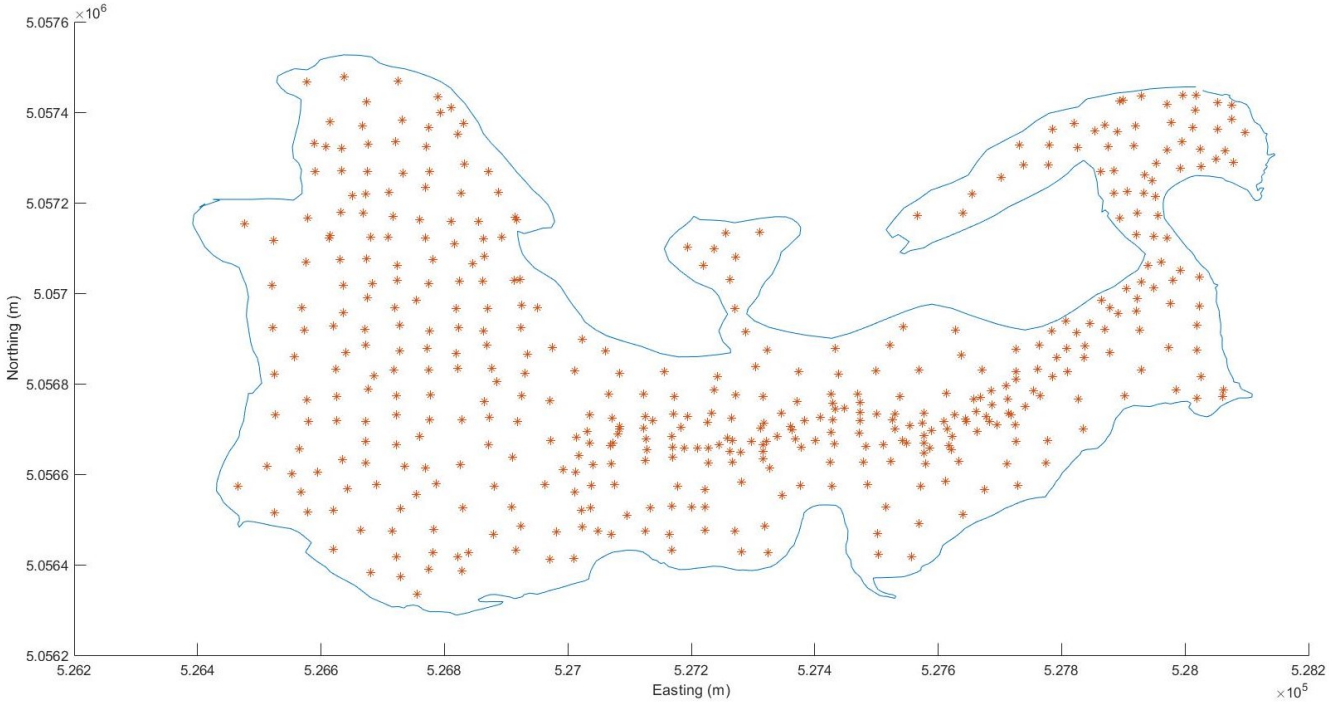

Figure 11: Outline of BH sampled locations for sample size of 460.

At the sample size of 460 the effect of sample location and count is less clear on the regions of increased thickness in comparison to a sample size of 300. However, the effect of sample thickness locations is clearly demonstrated on the variability plot, in which the standard deviation value for each estimated thickness location is plotted, as seen below in Figure 12.

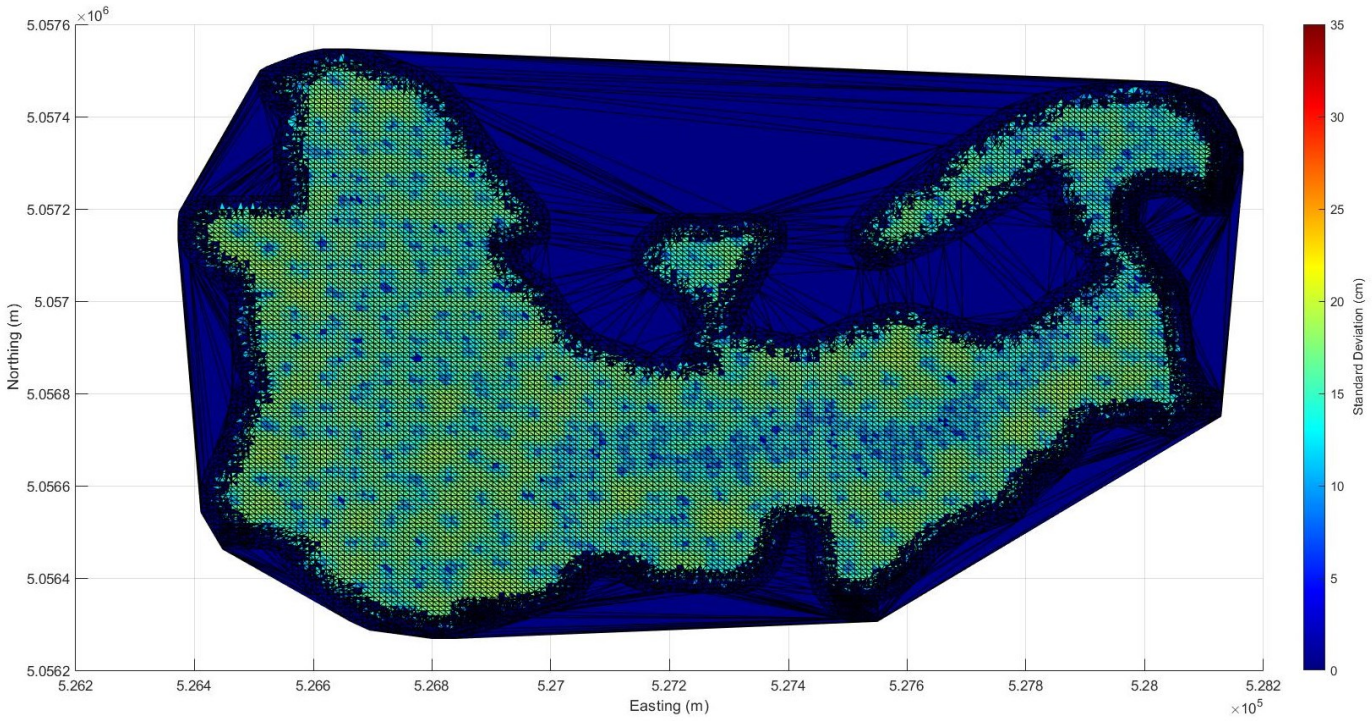

Figure 12: Standard deviation plot using the average correlation length and sample size of 460.

As seen in Figure 12, regions in which actual samples have been included have the highest confidence, as the standard deviation values in these regions are reduced. The estimated point standard deviation peaks at approximately 22.5 cm. When considering the variability peaks of the 300-sample size, the 460-sample size shows minimal improvement in maximum point standard deviation. However, it should be noted that via visual comparison of Figure 9 and Figure 12, the clustering of increased estimated point standard deviation has been mitigated, and a greater prevalence of lower estimated point standard deviation is clear.

4.3.4 Comparison of Results Across Sample Sizes

When considering the effect of sample size from 50 to 460 samples, the effect of sample size on Kriging estimates are clear. A summary table of kriging estimated volumes, along with their upper and lower 99% C.I. bounds and C.V. can be seen in Table 6.

Table 6: Kriging volume estimates with 99% confidence bounds and C.V.

Group – Type	***Best Estimate Volume (m^3)***	***99% C.I. (m^3)***	***99% C.I. Upper Bound (m^3)***	***99% C.I. Lower Bound (m^3)***	***C.V. (%)***
50 - Kavg	147,219	88,610	235,829	58,609	25.9
50 - Kmax	172,680	112,219	284,898	60,461	27.9
50 - Kmin	124,824	70,851	195,675	53,973	24.4
100 - Kavg	172,147	68,615	240,762	103,532	17.1
100 - Kmax	186,738	81,136	267,874	105,602	18.7
100 - Kmin	141,330	47,900	189,230	93,430	14.6
200 - Kavg	209,147	54,282	263,429	154,864	11.2
200 - Kmax	217,366	62,684	280,049	154,682	12.4
200 - Kmin	169,850	30,230	200,080	139,620	7.7
300 - Kavg	218,498	46,301	264,800	172,197	9.1
300 - Kmax	223,568	53,147	276,715	170,421	10.2
300 - Kmin	206,380	28,027	234,407	178,352	5.8
400 - Kavg	220,411	41,822	262,233	178,588	8.2
400 - Kmax	224,443	50,015	274,458	174,429	9.6
400 - Kmin	210,272	31,291	241,563	178,981	6.4
460 - Kavg	221,182	37,515	258,697	183,667	7.3
460 - Kmax	224,609	44,717	269,326	179,892	8.6
460 - Kmin	214,351	29,826	244,177	184,526	6.0

At a sample size of 50, the C.V. varied from 24.4-27.9%; as sample size increases the C.V. improves considerably to 5.8-10.2% at sample size of 300 and to 6.0-8.6% at sample size of 460. The general trend in sample volume estimates and 99% C.I. is depicted below in the bar chart below.

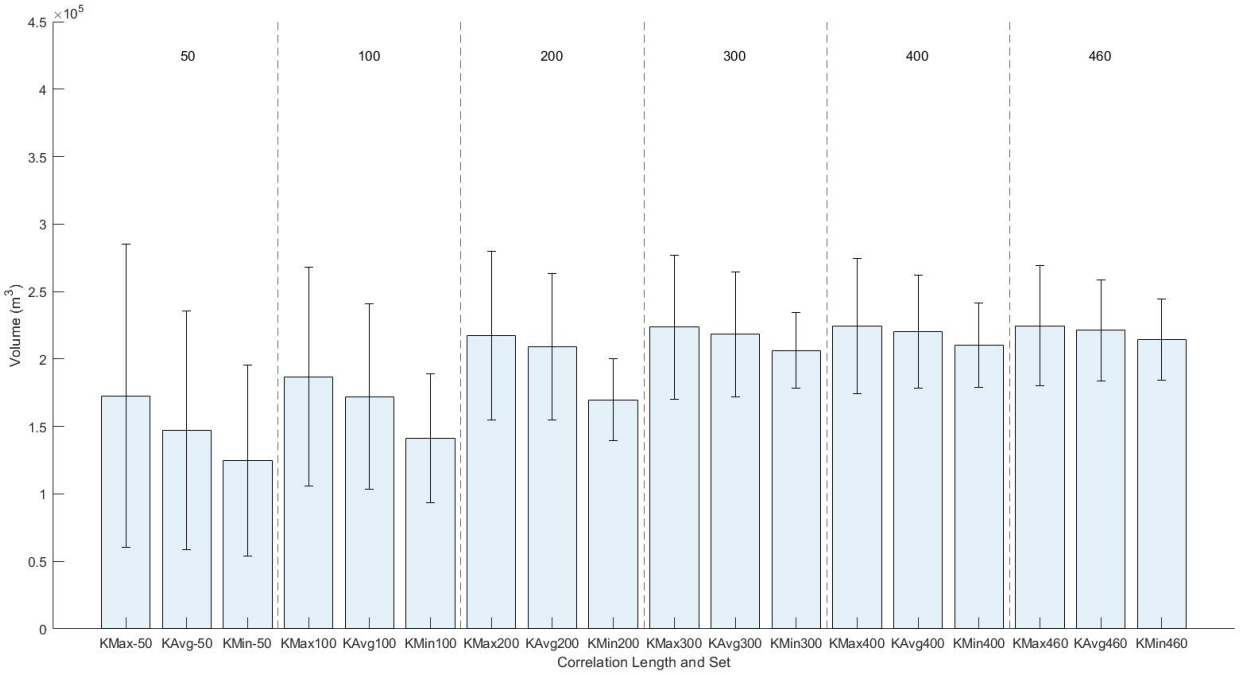

Figure 13: Bar graph of all Krige best estimate volumes with 99% confidence bounds as error bars.

As depicted in Figure 13, the Krige best estimate volumes gradually increase until they center around a best estimate volume of about 221,000 m^3 at the average correlation length for a sample size of 460. Furthermore, the bar graphs illustrate the effect of sample size on the confidence in the volume estimate, as at 50 samples the maximum, average and minimum correlation length 99% confidence bounds all vary considerably. When considering the total range of the C.I. for the 50-sample size grouping (range from slower to upper 99% confidence bound), the average total range of 181,120m^3 represents a low confidence in the Krige estimate of volume in comparison to the average estimated volume of 148,241m^3. As sample size increases, the C.I. bounds considerably decrease. At the 300-sample size grouping, the average

total C.I. range is 84,984m^3 representing a 53% reduction in C.I. range, with an average volume of 216,149m^3 or 45.8% increase in average volume. In comparison sample grouping 460, the average final total C.I. range of 74,705 or 12% reduction in total C.I. range in comparison to sample size grouping 300 with an average estimated volume of 220,047m^3 or 1.8% increase in total volume compared to sample size grouping 300.

If it is assumed that the final sample size of 460, at the average correlation length, accurately estimates the volume of contaminated sediment in BH, it should be noted that that volume of sediment in BH is within the 99% confidence bounds of nearly every volume best estimate from the Krige model. The only confidence intervals that do not include the best estimate volumes resulting from the 460-sample size are the minimum correlation length for sample sizes of 50 to 200. The fact that the minimum correlation length produces a confidence interval that does not include the, potentially, most accurate Krige volume is likely because of the zero thickness bounds. As mentioned previously, it appears that when the correlation length is larger the effect of internal sampled points is greater than the effect of the boundary. Therefore, at a smaller sample size, there are fewer internal samples to influence the volume estimate, and as such the volume estimate is biased to an overall lower volume because of the boundary points.

4.4 Sim2D Volume Estimates

The LAS random field simulations entailed producing 1,000 simulations per parameter setup (per sample grouping per correlation length) and entailed 18,000 simulations in total from the sim2d program. The results of these 18,000 simulations are summarized in Table 7. It should be noted that, as per Chapter 3.0:, the outputs from

the LAS model differ from the outputs of the Krige model, and as such the presentation of results will differ to reflect this.

Table 7: Summary of LAS simulation results.

Grouping - Type	***Correlation Length (m)***	***Sample Field Mean (cm)***	***Sample Point Variance (cm)***	***Avg. Vol. (m^3)***	***Max Vol. (m^3)***	***Min Vol. (m^3)***
50 - Savg	106.6	37.3	1245.1	288,488	365,634	217,936
50 - Smax	154.9	37.3	1245.1	268,093	357,590	196,141
50 - Smin	78.7	37.3	1245.1	308,681	368,179	250,437
100 - Savg	107.1	31.4	827.0	250,256	313,244	202,664
100 - Smax	143.0	31.4	827.0	241,642	296,052	200,323
100 - Smin	64.6	31.4	827.0	273,001	317,324	235,127
200 - Savg	110.5	29.3	600.7	245,016	277,266	212,509
200 - Smax	147.2	29.3	600.7	240,116	278,722	211,084
200 - Smin	46.8	29.3	600.7	268,796	298,276	229,493
300 - Savg	101.3	28.7	554.7	244,681	270,795	221,800
300 - Smax	134.4	28.7	554.7	240,825	263,447	218,546
300 - Smin	66.5	28.7	554.7	252,478	279,551	224,195
400 - Savg	99.1	28.4	524.6	239,685	264,927	218,649
400 - Smax	146.8	28.4	524.6	235,873	261,445	218,874
400 - Smin	59.5	28.4	524.6	248,885	274,708	229,142
460 - Savg	92.5	27.7	485.7	237,039	255,304	209,080
460 - Smax	135.8	27.7	485.7	233,543	251,141	197,524
460 - Smin	61.0	27.7	485.7	244,008	261,047	227,242

As shown in Table 7, there is a clear trend between correlation length and volume, in which the largest volume per sample size grouping is obtained when simulating the smallest (min) correlation length; conversely as correlation length increases, volume decreases. This relationship between correlation length and simulated volume is likely once again caused by the effect of the BH outline 587, 0 thickness data points. The effect of these outline points is greater at a low sample size and diminished as sample size increases. This relationship is opposite to the Krige model, as the random field simulation is not in essence linearly interpolating, but rather attempting to keep the

overall field mean constant. Therefore, as the sim2d program uses and inputted sample average thickness opposed to the krige programs internally calculated average sample thickness (which is biased trending towards 0 thickness due to the ratio of sampled thicknesses to boundary points), the sim2d program is simulating with an increased field mean in comparison to the krige program. It should be noted that for the sim2d program, the BH outline thickness data was not included in calculating the sample field mean, and as such is greater than what the krige program would internally calculate. Furthermore, the diminishing effect of the BH outline is supported by the minimal range from maximum to minimum observed on the volumes between sample groupings when considering their correlation length. As previously mentioned, it appears the volume estimate produced is greater effected by the sample field mean, which slowly decreases as sample size increases, producing a reciprocal gradual decrease in volume. The gradual reduction in sample thickness mean is likely caused by outliers and a large spread in sample thickness values at a lower sample sizes, which this spread gradually tightens as sample size increases, although with many outliers, as seen in the boxplot in Figure 14.

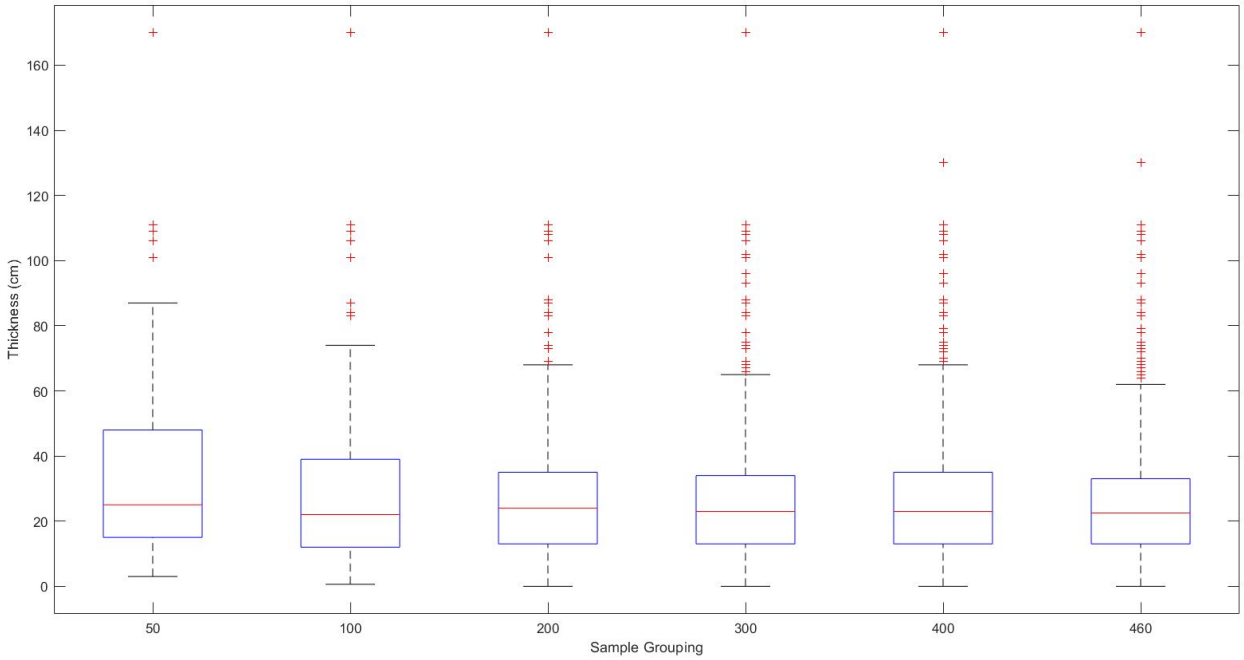

Figure 14: Summary boxplot of sample thickness distribution on a sample grouping basis.

As seen Figure 14, the distribution of sample thickness values does “tighten” in terms of smaller range between the 3rd and 1st quartiles (interquartile range) as sample sizes increase, however the number of outliers (shown as +) remains high. Furthermore, when considering the sample thickness distributions in Figure 14, the effect of the large >160 cm outliers at lower sample sizes would be notable on the sample thickness mean, considering the sample median is slightly above 20 cm. When considering the LAS volume results, the normal distribution tendencies can be summarized in Table 8:

Table 8: Summary table of standard normal distribution parameters for LAS results.

Grouping - Type	***Sample Field Mean (cm)***	***Volume Standard Deviation***	***Avg. Vol. (m^3)***	***99% Confidence Interval (+/-) (m^3)***	***Coefficient of Variation (%)***
50 - Savg	37.3	23,315	288,488	54,378	8.1
50 - Smax	37.3	25,491	268,093	62,212	9.5
50 - Smin	37.3	20,798	308,681	49,656	6.7
100 - Savg	31.4	15,085	250,256	34,358	6.0
100 - Smax	31.4	15,374	241,642	37,570	6.4
100 - Smin	31.4	13,657	273,001	32,240	5.0
200 - Savg	29.3	9,545	245,016	24,495	3.9
200 - Smax	29.3	9,824	240,116	23,355	4.1
200 - Smin	29.3	9,055	268,796	19,733	3.4
300 - Savg	28.7	7,706	244,681	17,238	3.1
300 - Smax	28.7	7,326	240,825	17,803	3.0
300 - Smin	28.7	7,944	252,478	17,699	3.1
400 - Savg	28.4	6,091	239,685	15,252	2.5
400 - Smax	28.4	5,625	235,873	12,791	2.4
400 - Smin	28.4	6,272	248,885	14,100	2.5
460 - Savg	27.7	5,380	237,039	14,286	2.3
460 - Smax	27.7	4,889	233,543	11,056	2.1
460 - Smin	27.7	5,526	244,008	12,736	2.3

As seen in Table 8, as the sample size increases, the standard deviation about the mean volume for each grouping and type generally decreases. At the lower end of sample sizes (0-200), the maximum correlation length produces the highest standard deviation, but as sample size increases to greater than 300 samples, the maximum correlation length results in the lowest standard deviation about the mean volume. This switch in relationship is likely caused by the tightening of the sample thickness distribution, resulting in higher correlation among sample points, and therefore less variation among the mean. This reduction in variation among the mean has a higher effect at larger correlation lengths, due to the field being more correlated at farther

distances. Like the Krige results for C.V., as the number of samples increases, the LAS model variability decreases.

Due to the gradual trends within the output results, the sample groupings of 50, 300 and 460 at the average correlation length will be further investigated for the purpose of illustrating the effect of sample size. As sim2d produces 1,000 simulations per set of model input parameters (18 models in total), it is not feasible to insert each model of the average correlation length for the chosen sample groupings. Hence, an averaged simulation case is presented. The averaged simulation model entailed averaging of each simulated location thickness across 1,000 simulations and 11,512 data points.

4.4.1 50 Samples

At a sample size of 50, the LAS model produces the most widely variable confidence interval about its mean. At the average correlation length of 154.9 m, the 99% confidence interval was 54,231 m^3 and a C.V. of 8.1% when compared to the average volume of 288,488 m^3. The average thickness variation 2-D rendering can be seen in Figure 15.

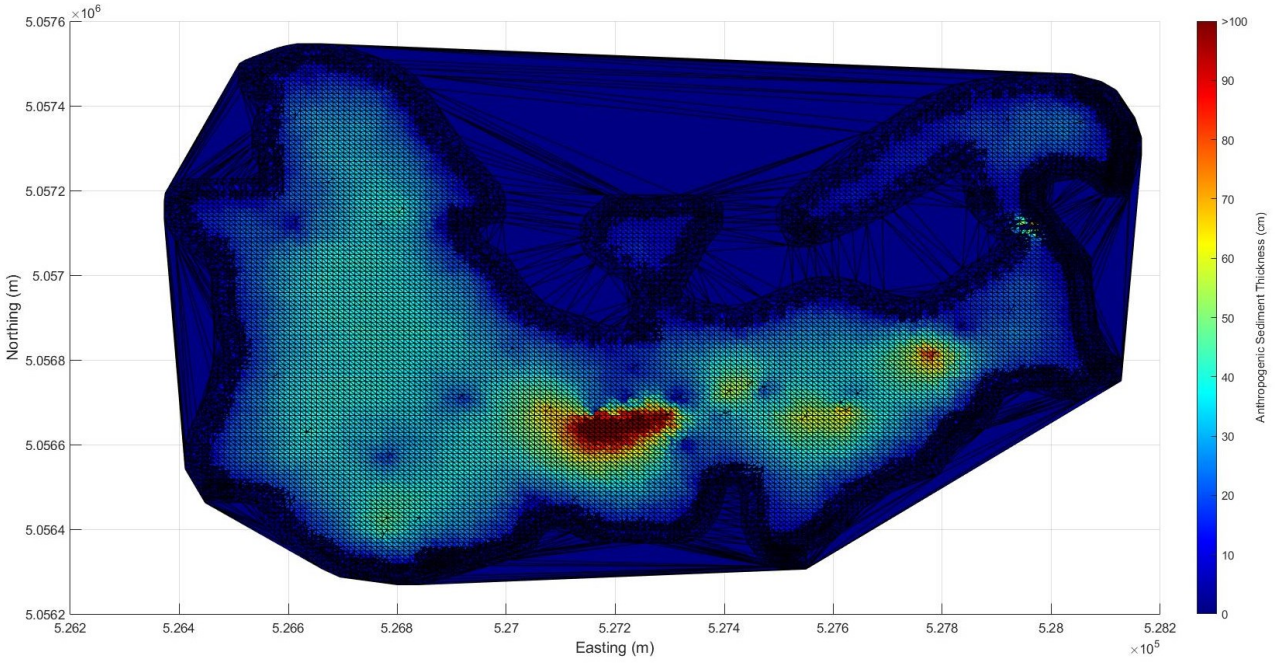

Figure 15: Sim2d averaged simulation thickness at the average correlation length and a sample size of 50.

As seen in Figure 15, the regions of increased thickness (red on the RGB colour scale) are regions at which sample thicknesses have been taken within BH, when compared to Figure 5. When considering Figure 15, there seems to be large deposits of sediment thickness on the left-hand side, that continues from the inlet towards the outlet on the top right right-hand side of Figure 15. For this model, it appears the 0 cm thickness bounds of BH have minimal influence on the simulated thickness.

4.4.2 300 Samples

At a sample size of 300, the LAS model produces improved confidence in its volume estimates, with high precision in comparison to a sample size of 50. The average correlation length of 101.3m has a 99% confidence interval of 17,238 m^3 and C.V. of 3.1% with average volume of 244,681 m^3. This C.V. of 3.1% is a noticeable

improvement in comparison to the 50-sample size C.V. of 8.1%. The 2-D model for the average simulated thickness volume can be seen below for the average correlation length.

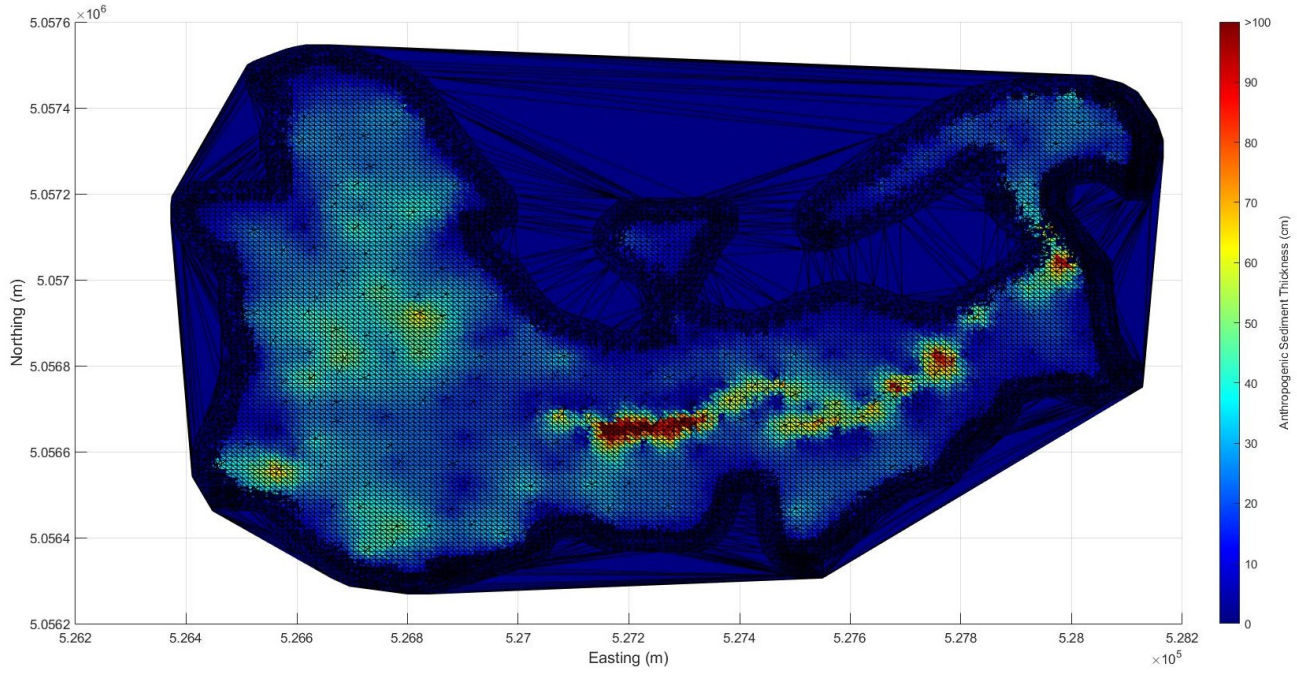

Figure 16: Sim2d averaged simulation thickness at the average correlation length and sample size of 300.

As previously mentioned in Section 4.4.1, the regions of increased thickness in Figure 16, are regions where actual samples have been taken within BH, when compared to Figure 8. Furthermore, it should be noted that there is a clear structure forming within Figure 16, with the majority of major thickness values within a main body to the left-hand side of Figure 16, and along a highly correlated thicker sediment channel from inlet to outlet of BH. When considering the change from the sample size of 50, the increase in sample size has resulted with greater thickness variation granularity,

with the left-hand side of Figure 16 not being one seemingly continuous body of constant thickness, rather a varying field of thicknesses.

4.4.3 460 Samples

At an input sample size of 460, the LAS model produces its highest confidence in its volume estimates, with high precision. The average correlation length of 92.5m has a 99% confidence interval of 14,286 m^3 and C.V. of 2.3% with average volume of 237,039 m^3. This C.V. of 2.3% is a minor improvement in comparison to the 300-sample grouping uncertainty of 3.1%. The 2-D colour map model for the average simulated thickness volume can be seen below for the average correlation length.

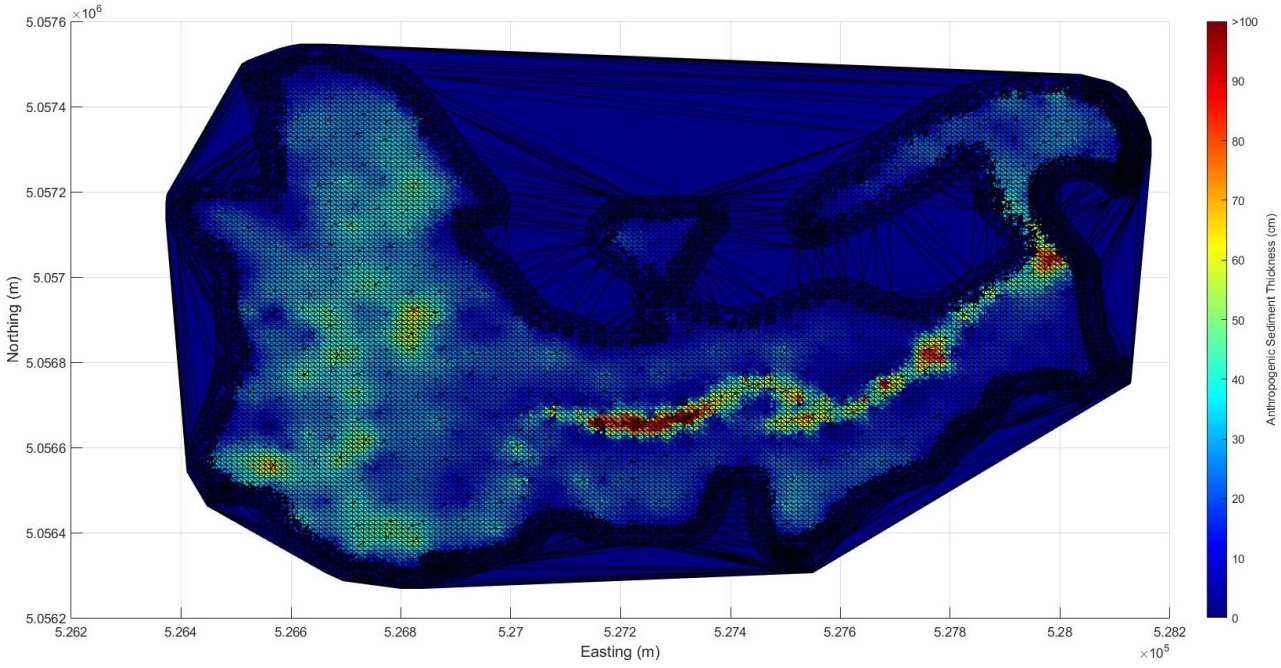

Figure 17: Sim2d averaged simulation thickness at the average correlation length and sample size of 460.

As seen in Figure 17 regions of increased thickness are regions where actual samples have been taken within BH, when compared to Figure 11. Furthermore, it

should be noted that there is a clear structure forming within Figure 16, with the majority of major thickness values within a main body to the left-hand side of Figure 16, and along a highly correlated thickness channel from inlet to outlet of BH. When considering the change from the sample size of 300, the increase in sample size has resulted with greater thickness variation granularity, with the left-hand side of Figure 16 being multiple pockets of increased thickness that are interconnected.

4.4.4 Comparison of Results Across Sample Sizes

When considering the changes from the sample size of 50 to 460, the effect of sample size on the LAS simulation volume and precision is clear. A summary table of LAS average volumes with normally distributed 99% confidence intervals can be seen in Table 9:

Table 9: LAS average volume with normally distributed 99% C.I and C.V.

Grouping - Type	***Correlation Length (m)***	***Avg. Vol. (m^3)***	***99% C.I. Upper Bound (m^3)***	***99% C.I. Lower Bound (m^3)***	***Coefficient of Variation (%)***
50 - Savg	106.6	288,488	342,866	234,110	8.1
50 - Smax	154.9	268,093	330,305	205,881	9.5
50 - Smin	78.7	308,681	358,338	259,025	6.7
100 - Savg	107.1	250,256	284,614	215,898	6.0
100 - Smax	143.0	241,642	279,212	204,072	6.4
100 - Smin	64.6	273,001	305,241	240,761	5.0
200 - Savg	110.5	245,016	269,511	220,521	3.9
200 - Smax	147.2	240,116	263,471	216,761	4.1
200 - Smin	46.8	268,796	288,529	249,063	3.4
300 - Savg	101.3	244,681	261,920	227,443	3.1
300 - Smax	134.4	240,825	258,628	223,022	3.0
300 - Smin	66.5	252,478	270,177	234,779	3.1
400 - Savg	99.1	239,685	254,937	224,432	2.5
400 - Smax	146.8	235,873	248,664	223,081	2.4
400 - Smin	59.5	248,885	262,985	234,785	2.5
460 - Savg	92.5	237,039	251,325	222,753	2.3
460 - Smax	135.8	233,543	244,599	222,486	2.1
460 - Smin	61.0	244,008	256,744	231,272	2.3

At a sample size of 50, the C.V. varies from 6.7-9.5%, and as the sample sizes increase the variability about the mean improves considerably to 3.0-3.1% at 300 samples and as low as 2.1-2.3% at 460 samples. This general trend in volume and confidence intervals is depicted in Figure 18.

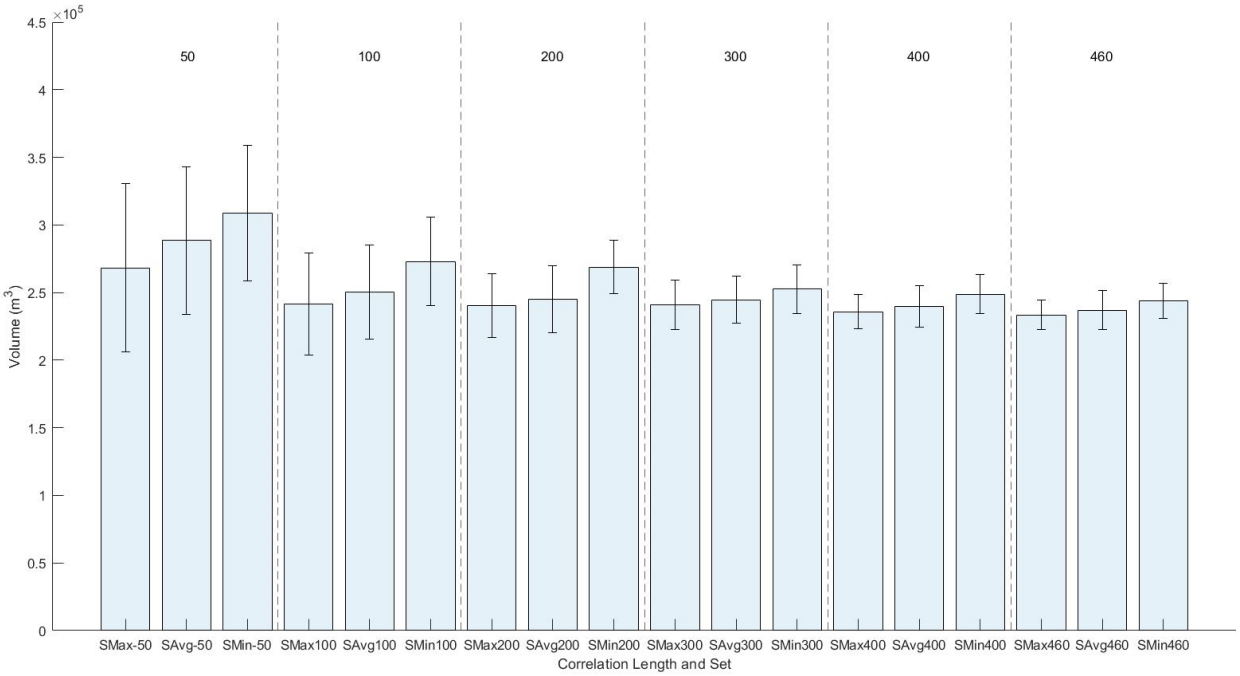

Figure 18: Bar graph of LAS average volumes for each correlation length and sample grouping with 99% confidence bounds as error bars.

As clearly depicted above in Figure 18, the LAS average volumes gradually decrease and "tighten" until they center around the average of the average correlation length volume of 237,039 m^3 for a sample size of 460. Furthermore, the bar graph illustrates the effect of sample size on the confidence in the volume estimate, as the confidence bounds incrementally decrease in range as the sample size increases. At a sample size of 50, the average total confidence interval range is 107,934m^3 with an average volume of 288,421m^3. As sample size increases to 300 samples, the total confidence interval range reduces to 35,629m^3 with an average volume of 245,995m^3. The improvement in confidence interval range represents a large increase in confidence of the volume with a 67% reduction in total C.I. range, however only a 14.7% decrease in volume. Furthermore, when considering the change from a sample size of 300 to 460,

the total average interval range reduces to 24,493 m^3 representing a further 31.3% reduction in total C.I. range, and an average volume of 238,197m^3 or 3.2% reduction in volume.

If assuming the final sample grouping of 460 accurately estimates the volume of sediment in BH, it should be noted that the volume of sediment in BH is within the confidence bounds for every simulation set, except for a sample size of 50 at the minimum correlation length, likely for the same reasons as discussed for the Kriging model at the minimum correlation length and smaller sample sizes.

As LAS produces sets of simulations for each set of input parameters, it is possible to conduct further statistical testing on the sample set. A boxplot of the results can be seen below in Figure 19.

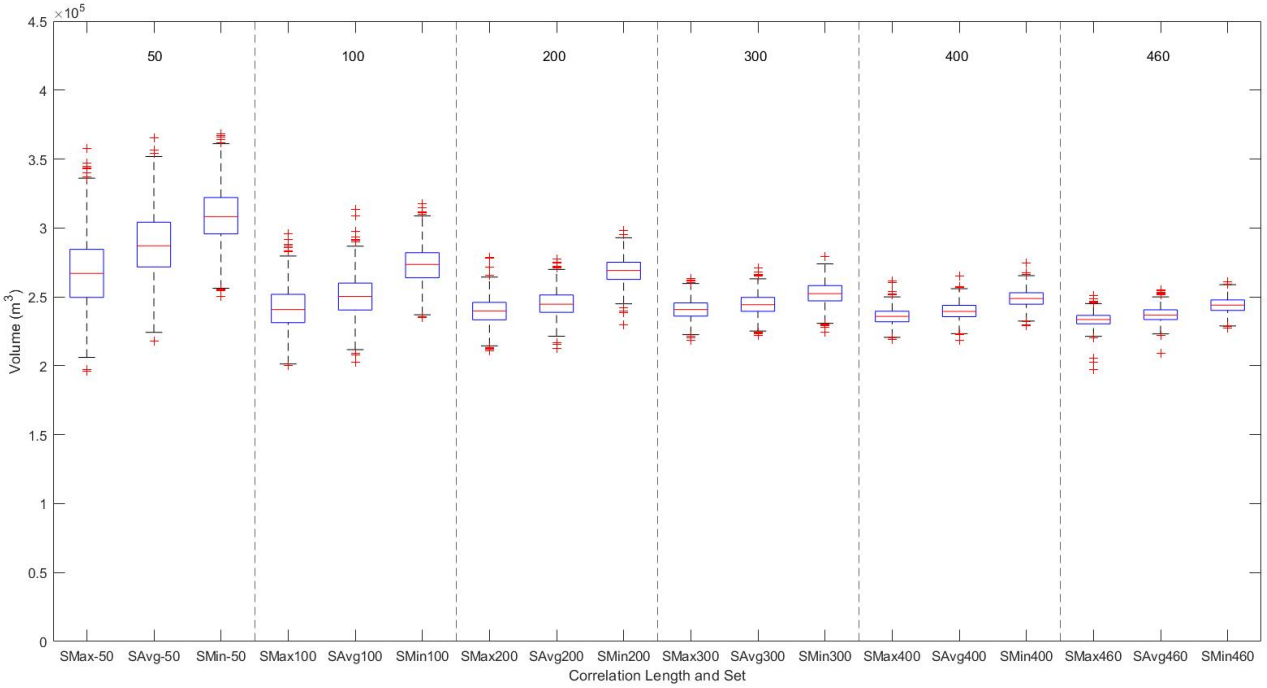

Figure 19: Boxplots of LAS volume results.

When considering the results, as seen in Figure 19, it is clear how the distribution of simulated volumes quickly improves as sample size increases. At a sample size of 50, the maximum and minimum (excluding outliers) of the boxplot are of a range of approximately 1.5 x 10^5 m^3, whereas this range quickly tightens as at 200 sample size the range is approximately half of the range at sample grouping 50. Once the sample size increases to about 300 samples, it becomes evident that the median and range does not considerably change in comparison to the final sample size of 460.

4.5 Comparison of Models

The results of both the LAS and Krige models both converge around an expectation of BH volume to be in the range of 220,000 – 240,000 m^3, with differing levels of variance about the average estimate. The results of the Krige best estimate and LAS models can be seen directly compared in Table 10.

Table 10: Comparison table of Krige and LAS model results with respective 99% confidence interval bounds.

Grouping - Type	***LAS Average Vol. (m^3)***	***Krige Volume (m^3)***	***LAS Upper Bound (m^3)***	***LAS Lower Bound (m^3)***	***Krige Upper Bound (m^3)***	***Krige Lower Bound (m^3)***
50 - Avg	288,488	147,219	342,866	234,110	235,829	58,609
50 - Max	268,093	172,680	330,305	205,881	284,898	60,461
50 - Min	308,681	124,824	358,338	259,025	195,675	53,973
100 - Avg	250,256	172,147	284,614	215,898	240,762	103,532
100 - Max	241,642	186,738	279,212	204,072	267,874	105,602
100 - Min	273,001	141,330	305,241	240,761	189,230	93,430
200 - Avg	245,016	209,147	269,511	220,521	263,429	154,864
200 - Max	240,116	217,366	263,471	216,761	280,049	154,682
200 - Min	268,796	169,850	288,529	249,063	200,080	139,620
300 - Avg	244,681	218,498	261,920	227,443	264,800	172,197
300 - Max	240,825	223,568	258,628	223,022	276,715	170,421
300 - Min	252,478	206,380	270,177	234,779	234,407	178,352
400 - Avg	239,685	220,411	254,937	224,432	262,233	178,588
400 - Max	235,873	224,443	248,664	223,081	274,458	174,429
400 - Min	248,885	210,272	262,985	234,785	241,563	178,981
460 - Avg	237,039	221,182	251,325	222,753	258,697	183,667
460 - Max	233,543	224,609	244,599	222,486	269,326	179,892
460 - Min	244,008	214,351	256,744	231,272	244,177	184,526

For Table 10, the upper and lower bounds for Krige and LAS are referring to the standard normal 99% confidence bounds.

The comparative results of the Krige and LAS models can be visually depicted in a comparative bar graph, as seen in Figure 20 where the blue bars are LAS results and green are Krige results.

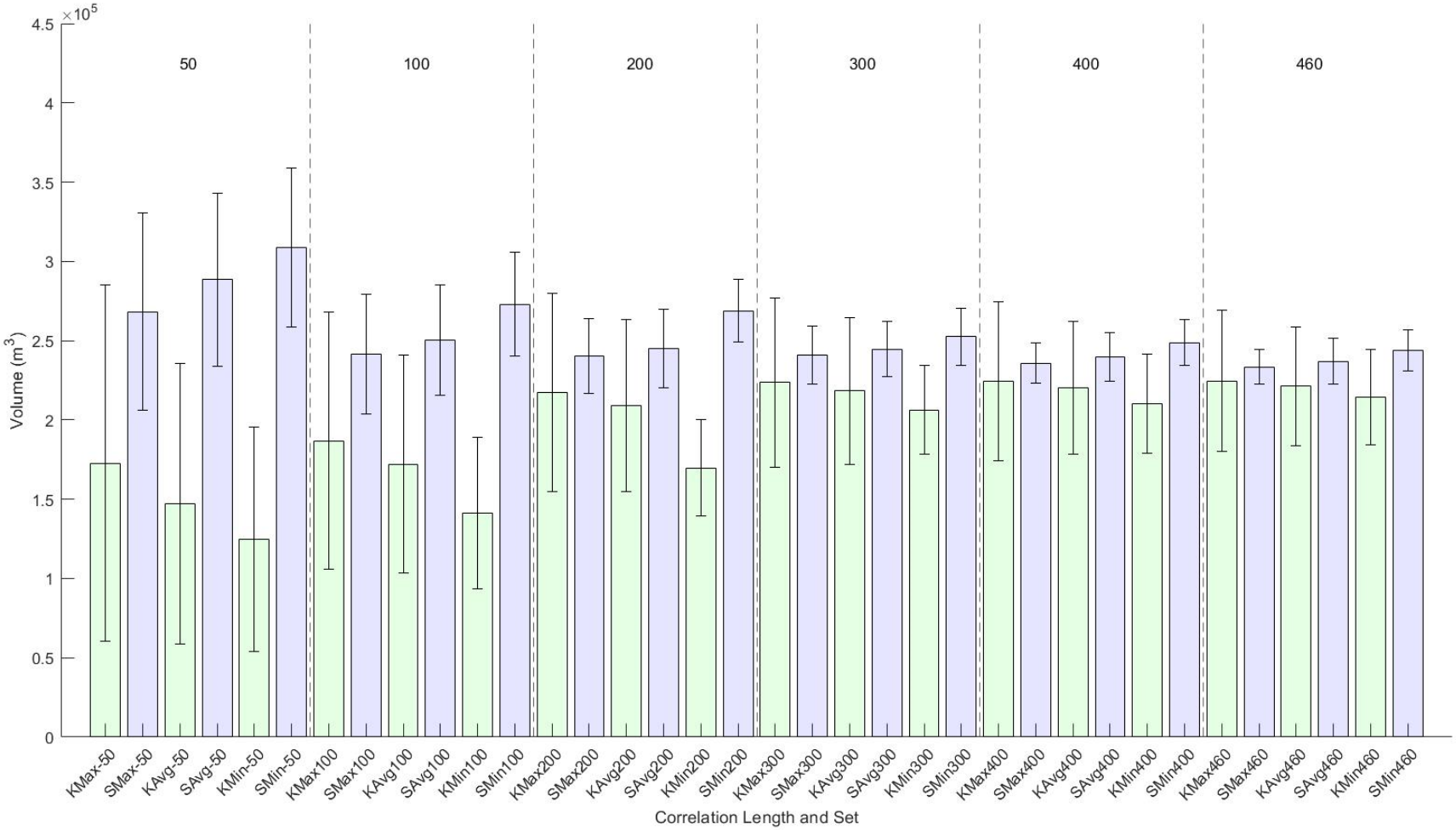

Figure 20: Comparison bar graph of LAS and Krige volume results with 99% confidence intervals as error bars.

As seen in Figure 20, the LAS results are quicker to approach the final volume (of the 460 sample size) in comparison to the Krige results. When considering the confidence intervals as depicted above, the LAS results produce a higher confidence estimate of the BH volume, and more rapidly approach that value than the Krige model. Taking for example the sample groupings 50 and 100, the LAS volumes are within ±30,000 - 65,000 m^3 of the final estimate of BH volume, and their 99% confidence intervals are within range of the final BH volume estimate. Furthermore, the range of the 99% confidence interval for the LAS results is approximately ±50,000 – 62,000 m^3 and contains the final expected mean at the 460-sample size. This variability about the mean LAS volume represents a C.V. of only 5.0 - 9.5%.

When comparing the results of Krige for sample groupings 50 and 100 to LAS, the 99% confidence interval produced does contain the final volume estimate, and the variability represents a C.V. of 14.6-25.9%. Furthermore, the Krige best estimate volumes are ±50,000 – 90,000 m^3 away from the final estimate for a sample size of 50 and ±49,000 – 73,000 m^3 off the final estimate for a samples size of 100.

When considering the differences between the two models considered, the LAS model is more capable of accurately and precisely estimating the volume of BH at lower and higher sample sizes. LAS was able to quickly characterize the expected BH sediment volume, producing an estimate at a sample size of only 50 which included the final estimate within its 99% confidence bounds. Furthermore, at a sample size of 50, LAS produced a comparable C.V. (6.7 – 9.5%) of that of the Krige model at a sample size of 460 (6.0 – 8.6%).

Another consideration at the lower samples sizes is the comparison between 2-D thickness variation maps, as the 2-D renderings depict understanding of the granularity of BH sediment thickness and are important in the context of remediation. At 50 samples, both models produced imprecise details of the BH sediment thickness variation, however, LAS clearly displayed a better understanding of how the sediment thickness was thicker on the left-hand side of the model. Furthermore, at 50 samples, LAS produced a better understanding of how the thickness is thicker along a channel running from the inlet to outlet, although minimal understanding of the granularity of the main significant thickness channel.

When considering the models at 100 samples, LAS produced a far higher understanding of the granularity and variation in the increased thickness region in the left-hand side of BH, as well as showed signs of a continuous increased thickness channel running from inlet to outlet. When considering the Krige model, it produced minimal to no understanding of the large, increased thickness region in the left-hand side of BH, although it did show signs of discrete increased thickness regions from inlet to outlet.

At 200 samples, both models began to converge in appearance, with the Krige model beginning to show a larger region of increased thickness on the left-hand side of BH. Furthermore, both models began to show clear signs of a significant increased thickness channel running from inlet to outlet.

At 300 samples, and upwards of 460 samples, both models become visually almost indistinguishable. Both models clearly show a region of increased thickness on the left-hand of BH, as well as a clearly continuous channel of increased thickness running from

inlet to outlet of BH. Furthermore, both models showed clear signs of generally increased thickness around the outlet region.

When considering the differences between the two models at a higher sample size (300 - 460 samples), there was minimal difference between the Krige best estimate to the LAS average estimate on a per correlation length basis. The main difference between the two models at the higher sample size was primarily the C.V., which LAS still produced a lower C.V. of (2.1– 3.1%) in comparison to the Krige model (6.0 – 10.2%).

Furthermore, to consider the results of this project and their broader implications for other thickness/volume estimation projects, it is important to consider the effect of sample density on the confidence of either model. Table 11 summarizes the effect of sample density on the average correlation length for each model type with a BH calculated plan area of 115.16 ha.

Table 11: Effect of sample density on model confidence.

Sample # (n)	***Sample Density (n/ha)***	***Krige C.V. (%)***	***LAS C.V. (%)***	***LAS Volume (m^3)***	***Krige Volume (m^3)***
50	0.43	25.9	8.1	288,488	147,219
100	0.87	17.1	6.0	250,256	172,147
200	1.74	11.2	3.9	245,016	209,147
300	2.60	9.1	3.1	244,681	218,498
400	3.47	8.2	2.5	239,685	220,411
460	3.99	7.3	2.3	237,039	221,182

It should be noted that for the LAS volume, the average volume of the average correlation length was used, and for the Krige volume, the Krige best estimate volume at the average correlation was used.

As seen in Table 11, the effect of sample density is clear, as previously stated the LAS model has clear advantages in comparison to the Krige model, especially at low sample densities. Furthermore, the effect of sample density on the Krige model precision is greater, with sample densities greater than 2.6 samples/ha producing a C.V. of 9.1% and below. When considering the LAS model, the effect of sample density is lesser, with 0.43 samples/ha producing a C.V. of 8.1%, and C.V. of 3.1% at 2.6 samples/ha compared to the Krige C.V. of 9.1% at the same sample density.

It is important to consider the effect of sample density on the volume estimates of both Krige and LAS. At a sample density of less than 1 sample/ha LAS produces an estimate within about 13,000 m^3 of the final estimate, whereas kriging is about 49,000 m^3 off its final estimate, or over 3.75x further away from the final estimate volume in comparison to the LAS model.

Furthermore, it is important to consider the context of these results compared to the literature on effective sample sizes for statistical modeling techniques. Although previous research on effective sample sizes to produce accurate statistical models are primarily based on a sample size, as opposed to sample density, the results of this study generally align. Webster & Oliver (1993) found that minimum sample sizes of 150 to 225 samples are required for reliable spatial interpolations of the Kriging method, while Mitchell, et. al. (2018) found that sample sizes exceeding 184 samples produced accurate spatial interpolations of the Kriging method. In terms of this research, it was found that Kriging required more than 200 samples to accurately depict the spatial variability in sediment thickness, as well as be within 5.8% of the final estimated sediment thickness volume calculated by Kriging at the 460-sample size.

4.6 Implications on Practical Implementation

When considering the differences between the Krige and LAS model outputs and the effect these differences can have in a practical implementation situation, one model clearly has many advantages over the other. Both the Krige and LAS models require understanding of similar parameters, but LAS produces a far more robust, accurate and precise output at lower sample sizes, and remains more confident with lower variability in the final estimate at higher sample sizes.

At lower sample sizes (50 – 200), both models lack advanced understanding of the granularity of sediment thickness variation, however, LAS produces a better concept of overall volume and regions to expect increased thickness. Furthermore, at lower sample sizes LAS allows a remediation operator to feel more confident that the estimate is within reason of what an estimate would be with higher sample sizes, with an C.V. range of only upward of 9.5%. When considering Krige, although the model does show some variation in the thickness field at low sample sizes, it produces a highly uncertain estimate with C.V. values of upwards of 27.9%, and less understanding of overall thickness regions. At lower sample sizes the LAS model is more effective and useful for practitioners in the field, as the Krige model has been shown to produce minimal understanding of the volume and thickness variation in comparison.

At higher sample sizes (300 – 460+), both models produce similar, if not nearly identical results. LAS and Krige both show good understanding of the variation of thickness within BH and main thickness features. When directly comparing models, LAS still has the advantage of improved C.V. values.

For practitioners in the industry, the highest confidence volume estimates for remediation projects are important and sought after. LAS at lower and higher sample sizes produces better estimates of sediment volumes, as well as improved coefficients of variation for these estimates.

Although high confidence in volume estimates for remediation projects are important to practitioners, the overall cost of the remediation project is exceedingly important as well to maintain profits and competitive advantages in comparison to competing firms bidding for remediation work. When considering the cost of remediation projects, the number of samples collected can have a large effect, especially for smaller remediation projects, and so keeping sample sizes as low as reasonably possible can be preferable. When considering the importance of sample size for practitioners, LAS once again produces the better results, with better understanding of overall volume and thickness variation at lower sample sizes and sample densities in comparison to the Krige model.

When considering the comparison in C.V. of the sample densities, LAS in theory can be more effectively scaled up and down for smaller to larger projects. LAS can achieve C.V. levels of 8.1% at a sample density of less than 1 sample / 2 ha, whereas Krige requires sample densities of almost 7x that of LAS to achieve comparable results. When comparing the effect of sample density on the confidence in volume estimate of either model, LAS has greater advantages for practitioners, both in cost and effectiveness. When further considering the difference in final estimate volumes at 4.6 samples/ha to estimated volumes at less than 1 sample/ha, LAS is within 13,000 m^3 (or within 6% of final volume), whereas Kriging is over 45,000 m^3 (or about 22.2% of final volume) away from its final estimate. This difference in estimate volume at lower sample densities

compared to the estimate volume at the final sample density is large, as depending on the project the final volume may be the most important factor for the practitioner due to project constraints.

Another major consideration of this difference in volume estimate for the practitioner is, Kriging consistently underestimated the volume in comparison to its final estimated volume, whereas LAS consistently overestimated in comparison to its final volume. When considering the goals of remediation practitioners, when the estimation of volume is of great importance, it is likely that the volume estimate is guiding the decisions on the remediation pathway. For example, if the practitioner determines landfilling is the best remediation pathway, then the final volume may affect the size of landfill site required and the final cost of the project. Furthermore, if the volume estimate results in underestimating the total volume of contaminants to dispose of, and the landfill site is unable to handle the final volume, this can result in major project overrun costs and potentially stall projects indefinitely depending on funding.

Chapter 5.0: Summary: Conclusions and Recommendations

After comparison of the Krige and LAS models it was shown that LAS can produce better understanding of thickness variability spatially, as well as high confidence and high accuracy volume estimates at lower and higher sample sizes. LAS produced an average initial (50 sample size) volume across the three correlation lengths of 288,421 m^3 at an average C.V. of 8.1%, and a final (460 sample size) average volume of 238,197 m^3 and an average C.V. of 2.2%. The LAS results can be starkly compared to the Krige initial average best estimate volume of 148,241 m^3 at an average C.V. of 26.1%, although Krige improves considerably at the final sample size producing and average sample size of 220,047 m^3 at an average C.V. of 7.3%.

5.1 Conclusions

To compare the Krige and LAS models effectively, a maximum, average and minimum correlation length was considered at multiple sample sizes ranging from 50 to 460 samples. These sample sizes were shown to be effective at investigating the differences between the models at different sample sizes and highlighted the effectiveness of the LAS model in comparison to Kriging.

To properly assess the differences in outputs from both models, the models were thoroughly investigated at 50 samples, 300 samples and 460 samples for the average correlation length. Furthermore, visual assessment of both models' abilities to depict granularity of the thickness variation within BH was assessed. It was found that LAS was more capable of assessing the thickness variation within BH at lower sample sizes in comparison to Kriging, but minimal difference was found at higher sample sizes (300 or more samples or sample densities of 2.6 samples/ha or more). It was shown that

LAS could produce comparable precision and volume estimates at sample densities 7x lesser than that of Kriging, as well as accurately characterize the range of final expected volume at low sample sizes.

With the implementation of LAS, it was shown that a sample size of 300, or 2.6 samples/ha, properly characterizes the total volume of sediment with high confidence, as well as the variation in sediment thickness across BH. When considering only the total volume of sediment, LAS was capable of accurately and precisely characterizing the total volume of sediment at a sample size of 200, or sample density of 1.74 samples/ha. In terms of sample thickness variation at 1.74 samples/ha, it was shown that a large improvement in understanding of thickness variation still occurred from 1.74 samples/ha to 2.6 samples/ha, but improvements in thickness variation became minimal at sample densities in excess of 2.6 samples/ha.

In consideration of the BH remediation project, it should be noted that the model findings are important, as it has been shown that far fewer samples than of that which were taken could produce an accurate depiction of BH sediment thickness variation and total volume with the use of the LAS model. It was shown that 34.8% fewer samples, or 300 samples instead of 460, could have been taken to accurately determine the sediment thickness variation in BH. Furthermore, the total volume of sediment to be remediated could have been determined at 56.4% fewer samples, or a sample size of 200 instead of 460.

Furthermore, when considering the broader implications of this research, it was found that LAS is more capable of being a useful tool for remediation practitioners, as it can be used to minimize sample sizes required to properly characterize thickness

variations and overall sediment volumes for projects, in comparison to the more traditional Krige models. LAS was further shown to produce higher confidence estimates at lower sample densities and more conservative overall volume estimates at lower sample densities in comparison to the Krige model. It was shown that the LAS model is capable of producing an accurate thickness variation map representation of BH at sample densities exceeding 1.74 samples/ha, as well as an accurate total volume estimate at sample densities of 0.87 samples/ha.

5.2 Recommendations

- As the variation in sediment thickness and overall volume was assessed originates from a real-world contaminated site, the research conducted may be expanded upon through monitoring and comparison of the thickness variation and overall final volume during the physical remediation work on site; and,
- Additional research into implementation and comparison of probabilistic and geostatistical models for differing sample sizes for other remediation sites may be helpful in further understanding the required number of samples and effectiveness of these methods for a broader scope of projects.

References

Alberta Environment and Parks, 2016. *Alberta Environmental Site Assessment Standard,* Edmonton: Alberta Government.

Alimohammadi, M. et al., 2020. Characterising sediment physical property variability for bench-scale dewatering purposes. *Environmental Geotechnics.*

Alimohammadi, M. et al., 2019. Effect of different sediment dewatering techniques on subsequent particle sizes in industrial derived effluent. *Canadian Journal of Civil Engineering,* Issue 47, pp. 1145-1153.

Altman, D. & Bland, J., 1996. Standard deviations and standard errors. *BMJ.*

Association of Professional Geoscientists of Ontario, 2011. *Guidance for Environmental Site Assessments under Ontario Regulation 153/04 (as amended),* s.l.: Association of Professional Geoscientists of Ontario.

Benson, C., Zhai, H. & Rashad, S., 1994. STATISTICAL SAMPLE SIZE FOR CONSTRUCTION OF SOIL LINERS. *Geotechnical Engineering,* 120(10), pp. 1704-1724.

Burns, T., Thurston, M. & Edgar, M., 1995. Case study: Using a parametric model for environmental remediation cost estimating. *Federal Facilities Environmental Journal,* 6(2), pp. 51-61.

Burrough, P. & McDonnel, R., 1998. *Principles of Geographical Information Systems.* Oxford: Oxford University Press.

Canadian Council of Minsters of the Environment, 2016. *GUIDANCE MANUAL FOR ENVIRONMENTAL SITE CHARACTERIZATION IN SUPPORT OF ENVIRONMENTAL*

AND HUMAN HEALTH RISK ASSESSMENT, s.l.: Canadian Council of Minsters of the Environment.

Columbia Public Health, 2020. *Population Health Methods.* [Online] Available at: https://www.publichealth.columbia.edu/research/population-health-methods/kriging

Fenton, G. & Griffiths, D., 2008. *Risk Assessment in Geotechincal Engineering.* s.l.:Wiley.

Fenton, G. & Vanmarcke, E., 1990. Simulation of Random Fields via Local Average Subdivision. *Journal of Engineering Mechanics,* 116(8), pp. 1733-1749.

GHD, 2018. *Remedial Option Decision Document,* Pictou County: s.n.

Gilbert, R. & Simpson, J., 1983. *KRIGING FOR ESTIMATING SPATIAL PATTERN OF CONTAMINANTS: POTENTIAL AND PROBLEMS,* Richland: Pacific Northwest Laboratory.

Goovaerts, P., 1996. *Kriging vs Stochastics Simulation for Risk Analysis in Soil Contamination.* Libson, Springer, Dordrecht, pp. 247-258.

Government of Canada, 2020. *Action plan for contaminated sites.* [Online] Available at: https://www.canada.ca/en/environment-climate-change/services/federal-contaminated-sites/action-plan.html
[Accessed 3 December 2020].

Government of New Jersey, 2018. *TECHNICAL REQUIREMENTS FOR SITE REMEDIATION,* New Jersey: Government of New Jersey.

Hoffman, E. et al., 2019. Characterization and spatial distribution of organic-contaminated sediment derived from historical industrial effluents. *Environmental Monitoring and Assessment.*

Jiang, Y., 2013. Risk assessment of water qualtiy using Monte Carlo simulatio nand artificial neural network method. *Journal of Environmental Management,* pp. 130-136.

JWEL & Beak Consultants Limted., 1993. *Remediation Alternatives - Phase 2 Boat Harbour Treatment Facility,* Dartmouth: Nova Scotia Department of Supply and Services.

Li, J. & Heap, A., 2011. A review of comparative studies of spatial interpolation methods in environmetal sciences: Performance and impact factors. *Ecologoical Informatics,* Volume 6, pp. 228-241.

Liza, R., 2014. *STATISTICAL SAMPLE SIZE FOR QUALITY CONTROL PROGRAMS OF CEMENT-BASED SOLIDIFICATION/STABILIZATION,* Halifax: Dalhousie University.

Maloney, A., 2016. *Federal Contaminated Sites Inventory,* Ottawa: Treasury Board of Canada Secretariat.

Marine Environmental Support Office, 2002. *Critical Issues for Contaminated Sediment Management,* s.l.: United States Navy.

Mathworks, Inc., 2020. *Matlab R2019b,* s.l.: s.n.

McBratney, A. & Laslett, G., 1993. Sampling Schemes for Contaminated Soil. *Soil & Environment,* Volume 1.

Microsoft, n.d. *Excel specifications and limits.* [Online]
Available at: https://support.microsoft.com/en-us/office/excel-specifications-and-limits-1672b34d-7043-467e-8e27-269d656771c3
[Accessed 26 October 2020].

Mitchell, D., Forsythe, K., Marvin, C. & Burniston, D., 2018. Assessing statistical and spatial validity of sediment survey design and sampling densities - examples from Lake Erie. *Water Quality Research Journal,* 53(3), pp. 118-132.

Mitchell, D., Forsythe, K., Marvin, C. & Burniston, D., 2018. Assessing statistical and spatial validity of sediment survey design and sampling densities: exmaples from Lake Erie. *Water Quality Research Journal,* 53(3), pp. 118-132.

Myers, T. & Engler, R., 2005. *Cost Estimating for Contaminated Sediment Treatment - A Summary of the State of the Practice,* Omaha Ne: Engineer Research Development Center.

Office of Land and Emergency Management, 2020. *Superfund Remedy Report,* s.l.: United States Environmental Protection Agency.

Office of Solid Waste and Emergency Response, 2005. *Contaminated Sediment Remediation Guidance for Hazardous Waste Sites,* s.l.: United States Environmental Protection Agency.

Office Of The Parliamentary Budget Officer, 2014. *Contaminated Sites Cost,* Ottawa: Office Of The Parliamentary Budget Officer.

Rosengard, J. et al., 2010. A Parametric Model For Estimating Costs For Remediating Contaminated Sediment Sites Using A Dredging Method - A Budgetary &

Planning Tool For Decision-Makers. *Proceedings of the Annual International Conference on Soils, Sediments, Water and Energy,* 14(1), p. Article 21.

Schrooten, P. & Alphen, A., 2008. GEMS: GIS and geo-statistics integrated in Brownfield remediation and redevelopment, applied in the Vilvoorde region. *Ecology and the Environment,* Volume 107, pp. 55-64.

Siegel, M. & Bryan, C., 2003. *Environmental Geochemistry.* 1st ed. s.l.:Elsevier Ltd..

Spooner, I. & Dunnington, D., 2016. *Boat Harbour graviry core sediment survey,* s.l.: s.n.

Spooner, L. & Dunnington, D., 2016. *Boat Harbour Gravity Core Sediment Survey,* Halifax: Nova Scotia Lands Inc..

Stahl, M. & Bromm, S., 2003. *Measure and Calculations for Volume of Contaminated Medium Addressed With Respect to the Superfund And RCRA Corrective Action Programs,* s.l.: United States Environmental Protection Agency.

Tackley, H., 2019. *THE BEHAVIOR AND MIGRATORY FATE OF SELECT HEAVY METALS DURING THE DEWATERMENT OF AN EFFLUENT DERIVED SEDIMENT ,* Halifax: Dalhousie University.

Tackley, H., Lake, C. & Alimohammadi, M., 2020. Examining metal migration through geotextiles during dewatering. *Geotextiles and Geomembranes.*

United States Environmental Protection Agency Quality Staff, 2002. *Guidance on Choosing a Sampling Design for Environmental Data Collection,* Washington: Office of Environmental Information.

United States Environmental Protection Agency, 1997. *Guiding Principles for Monte Carlo Analysis,* Washington: Risk Assessment Forum.

United States Environmental Protection Agency, 1997. *The Incidence And Severity Of Sediment Contamination In Surface Waters Of The United States,* Washington: United States Environmental Proteciton Agency.

United States Environmental Protection Agency, 2002. *Guideance on Choosing a Sampling Design for Environmental Data Colleciton,* Washington: Office of Environmental Information.

United States Environmental Protection Agency, 2018. *STRATEGIC SAMPLING APPROACHES TECHNICAL GUIDE ,* s.l.: United States Environmental Protection Agency.

United States Geological Survey, 2020. [Online]
Available at: https://www.usgs.gov/mission-areas/water-resources/science/sediment-associated-contaminants?qt-science_center_objects=0#qt-science_center_objects

Webster, R. & Oliver, M., 1993. How large a sample is needed to estimate the regional variogram adequately?. In: *Quantitative Geology and Geostatistics.* s.l.:Springer, pp. 155-166.

Zimmerman, D., Pavlik, C., Ruggles, A. & Armstrong, M., 1999. An Experimental Comparison of Ordinary and. *Mathematical Geology,* 31(4).

Appendix A: List of Sample Type with GPS Coordinates and Sample Thicknesses

Type	Co-ordinates (UTM Nad83 CSRS 2010 Zone 20 N)		Top of Competent Sludge (masl)	Bottom of Sludge (masl)	Thickness (cm)
	Northing (m)	Easting (m)			
GC	526822.236	5056832.945	-2.738	-3.238	50.0
GC	527383.742	5056718.853	-2.78	-3.37	59.0
GC	527713.226	5056766.379	-2.773	-3.378	60.5
GC	527500.544	5056733.622	-2.569	-3.189	62.0
GC	527824.46	5056912.739	-2.074	-2.714	64.0
GC	527980.32	5057028.727	-0.957	-1.737	78.0
GC	526782.227	5056476.939	-1.7	-1.89	19.0
GC	526613.976	5057127.934	-1.664	-1.749	8.5
GC	526613.634	5057121.993	-1.654	-1.794	14.0
GC	526769.433	5057232.855	-2.525	-2.775	25.0
GC	527835.692	5056700.524	-1.092	-1.139	4.7
GC	527503.547	5056423.076	-0.864	-1.064	20.0
GC	526755.745	5056335.079	-1.241	-1.301	6.0
GC	526924.085	5056923.26	-1.905	-2.005	10.0
GC	527061.006	5056872.105	-1.559	-1.659	10.0
GC	527323.448	5056874.93	-0.954	-0.979	2.5
GC	527269.916	5056966.159	-0.77	-0.858	8.8
GC	527193.767	5057101.183	-0.692	-0.929	23.7
GC	527939.452	5057062.218	-1.152	-1.182	3.0
GC	527427.435	5056572.583	-1.341	-1.416	7.5
GC	527322.361	5056527.637	-1.494	-1.504	1.0
GC	527069.961	5056466.178	-1.353	-1.425	7.2
GC	526924.232	5056176.222	-0.905	-1.2	29.5
GC	526979.58	5056274.082	-1.888	-1.913	2.5
GC	527023.806	5056325.447	-0.971	-1.179	20.8
GC	527063.295	5056276.522	-1.558	-1.708	15.0
GC	527100.142	5056292.922	-0.439	-0.694	25.5
GC	527091.073	5056188.03	-1.757	-1.907	15.0
GC	527274.564	5056167.42	-1.148	-1.348	20.0
GC	527275.431	5056218.798	-1.026	-1.286	26.0

Type	Northing (m)	Easting (m)	Top of Competent Sludge (masl)	Bottom of Sludge (masl)	Thickness (cm)
GC	527272.1	5057081	-1.153	-1.253	10.0
GC	527256.4	5057134	-0.407	-0.407	0.0
GC	526865.1	5057081	-2.12	-2.29	17.0
GC	526917.1	5057162	-0.459	-0.465	0.6
GC	526780.9	5057074	-2.625	-2.86	23.5
GC	527323.9	5056426	-0.894	-0.974	8.0
GC	527281.1	5056429	-1.243	-1.34	9.7
GC	526759.9	5056684	-1.981	-2.166	18.5
GC	528025.6	5056816	-0.95	-1	5.0
GC	527875.7	5057323	-1.963	-2.198	23.5
GC	527952.5	5057214	-1.224	-1.414	19.0
GC	527900	5057425	-1.953	-2.238	28.5
GC	527893.6	5057425	-1.267	-1.482	21.5
GC	528062.5	5056787	-0.747	-0.897	15.0
GC	527639.9	5057177	-0.176	-0.286	11.0
GC	526918.7	5056128	-1.753	-1.943	19.0
GC	527076.1	5056119	-1.446	-1.536	9.0
GC	527381.1	5056138	-0.311	-0.313	0.2
GC	527225.3	5056124	-1.19	-1.363	17.3
LIF	526588.5	5057430	-1.039	-1.149	11
LIF	526576.4	5057466	-0.088	-0.128	4
LIF	527628.4	5056919	-1.078	-1.148	7
LIF	527637	5056862	-1.13	-1.24	11
LIF	527785.1	5056817	-2.665	-3.535	87
LIF	527761	5056832	-2.674	-3.604	93
LIF	527671.6	5056830	-0.967	-1.067	10
LIF	527726.3	5056876	-1.136	-1.256	12
LIF	527763.9	5056885	-1.447	-1.537	9
LIF	527784.1	5056917	-1.092	-1.132	4
LIF	527791.5	5056857	-2.398	-2.988	59
LIF	527725.8	5056826	-1.248	-1.268	2
LIF	527726.5	5056810	-1.882	-2.072	19
LIF	527973.5	5056880	-0.883	-0.973	9
LIF	527928.6	5056830	-0.936	-1.046	11
LIF	527878	5056870	-0.995	-1.125	13
LIF	527864.2	5056984	-1.112	-1.312	20
LIF	527807.2	5056938	-0.99	-1.16	17
LIF	527824.5	5056913	-2.187	-2.737	55
LIF	527845.3	5056932	-2.119	-2.619	50

Type	Northing (m)	Easting (m)	Top of Competent Sludge (masl)	Bottom of Sludge (masl)	Thickness (cm)
LIF	527877.7	5056967	-2.419	-3.019	60
LIF	527922.5	5056988	-2.183	-2.693	51
LIF	527976.1	5056976	-1.492	-1.762	27
LIF	527807.5	5056877	-2.186	-2.546	36
LIF	527836.5	5056858	-1.006	-1.116	11
LIF	527838.2	5056883	-1.363	-1.403	4
LIF	527870.6	5056919	-1.211	-1.371	16
LIF	527891	5056955	-1.47	-1.63	16
LIF	527921.6	5056960	-1.506	-1.726	22
LIF	527926.6	5056918	-1.338	-1.538	20
LIF	527808.9	5056827	-1.069	-1.169	10
LIF	528025.6	5056816	-0.944	-1.004	6
LIF	528018.8	5056874	-0.871	-1.001	13
LIF	528018.9	5056929	-0.829	-0.949	12
LIF	528023.2	5056971	-0.802	-0.892	9
LIF	526512.9	5056617	-1.661	-1.911	25
LIF	526525.7	5056732	-1.74	-2.06	32
LIF	526576.7	5056764	-2.076	-2.366	29
LIF	526564.4	5056656	-0.977	-0.977	0
LIF	526552.5	5056600	-1.813	-2.213	40
LIF	526579.2	5056716	-1.804	-1.994	19
LIF	526634.3	5056632	-1.418	-1.808	39
LIF	526736.2	5056618	-1.984	-2.564	58
LIF	526625.5	5056719	-1.695	-1.985	29
LIF	526672.2	5056672	-1.768	-2.018	25
LIF	526759.9	5056684	-2.04	-2.27	23
LIF	526777.7	5056776	-2.069	-2.299	23
LIF	526721.7	5056730	-2.447	-2.917	47
LIF	526676.4	5056787	-2.939	-3.269	33
LIF	526769.1	5056614	-1.722	-2.012	29
LIF	526671.8	5056624	-1.907	-2.167	26
LIF	526721.6	5056772	-2.552	-2.912	36
LIF	526722.7	5056665	-2.169	-2.539	37
LIF	526775.5	5056720	-2.283	-2.543	26
LIF	526672.3	5056715	-1.919	-2.179	26
LIF	526624.8	5056772	-2.317	-2.787	47
LIF	526870.7	5056665	-1.525	-1.855	33
LIF	526910.8	5056637	-1.334	-1.464	13

Type	Northing (m)	Easting (m)	Top of Competent Sludge (masl)	Bottom of Sludge (masl)	Thickness (cm)
LIF	526828.3	5056721	-1.758	-2.028	27
LIF	526825.6	5056621	-1.547	-1.817	27
LIF	526972.7	5056675	-1.295	-1.445	15
LIF	526918.7	5056716	-1.459	-1.629	17
LIF	526970.2	5056763	-1.408	-1.608	20
LIF	526865.1	5056760	-1.673	-1.923	25
LIF	526992	5056609	-1.635	-1.885	25
LIF	526873.4	5056726	-1.641	-1.811	17
LIF	526925.7	5056773	-1.564	-1.714	15
LIF	526815.5	5056776	-2.64	-2.227	-41.3
LIF	527066.8	5056778	-1.423	-1.623	20
LIF	527173	5056771	-1.577	-1.837	26
LIF	527013	5056605	-2.666	-3.166	50
LIF	527069.7	5056622	-1.48	-1.72	24
LIF	527040.9	5056620	-1.612	-1.792	18
LIF	527069.3	5056663	-1.34	-1.48	14
LIF	527073.1	5056668	-1.354	-1.474	12
LIF	527076.8	5056677	-2.455	-2.905	45
LIF	527079.4	5056682	-2.614	-3.164	55
LIF	527080.9	5056688	-3.222	-3.902	68
LIF	527083.3	5056700	-1.187	-1.327	14
LIF	527083.1	5056706	-1.179	-1.289	11
LIF	527035.9	5056731	-1.204	-1.314	11
LIF	527014	5056681	-1.216	-1.376	16
LIF	527072.1	5056724	-1.162	-1.292	13
LIF	527031.7	5056695	-1.181	-1.311	13
LIF	527035.5	5056670	-2.378	-2.768	39
LIF	527127.1	5056677	-3.129	-3.689	56
LIF	527018.1	5056641	-1.687	-1.877	19
LIF	527128.4	5056653	-1.284	-1.354	7
LIF	527167.8	5056684	-1.42	-1.61	19
LIF	527189.1	5056657	-3.244	-3.994	75
LIF	527170.3	5056638	-1.346	-1.416	7
LIF	527125	5056630	-1.243	-1.353	11
LIF	527125.8	5056728	-1.342	-1.462	12
LIF	527193.5	5056727	-1.447	-1.627	18
LIF	527122.2	5056702	-1.28	-1.36	8
LIF	527170.4	5056660	-2.459	-4.159	170

Type	Northing (m)	Easting (m)	Top of Competent Sludge (masl)	Bottom of Sludge (masl)	Thickness (cm)
LIF	527137	5056719	-1.357	-1.467	11
LIF	527171.1	5056733	-1.466	-1.646	18
LIF	527183.7	5056703	-1.364	-1.514	15
LIF	527122.8	5056777	-1.569	-1.739	17
LIF	527371.7	5056761	-1.352	-1.472	12
LIF	527383.7	5056719	-3.408	-4.098	69
LIF	527346.1	5056735	-1.302	-1.422	12
LIF	527315.6	5056772	-1.293	-1.463	17
LIF	527318	5056713	-1.317	-1.347	3
LIF	527265.7	5056723	-1.464	-1.564	10
LIF	527272.1	5056775	-1.395	-1.635	24
LIF	527237.1	5056786	-1.483	-1.623	14
LIF	527232.3	5056735	-1.438	-1.588	15
LIF	527226.5	5056715	-1.347	-1.447	10
LIF	527227.1	5056625	-1.314	-1.404	9
LIF	527266.8	5056626	-1.349	-1.519	17
LIF	527262.2	5056650	-2.883	-3.763	88
LIF	527257.9	5056680	-1.266	-1.446	18
LIF	527210.7	5056657	-3.202	-4.212	101
LIF	527227.5	5056657	-3.126	-4.216	109
LIF	527244.9	5056665	-3.598	-4.708	111
LIF	527266.4	5056674	-3.349	-4.179	83
LIF	527279.5	5056648	-2.516	-3.396	88
LIF	527297.3	5056672	-3.564	-4.624	106
LIF	527322.2	5056673	-3.507	-4.807	130
LIF	527316.6	5056664	-3.354	-4.434	108
LIF	527339.3	5056684	-3.881	-4.841	96
LIF	527360.9	5056706	-3.441	-4.161	72
LIF	527362.7	5056698	-3.869	-4.829	96
LIF	527369.3	5056677	-1.491	-1.631	14
LIF	527378.6	5056659	-1.193	-1.283	9
LIF	527327.1	5056613	-1.335	-1.425	9
LIF	527316	5056634	-1.343	-1.403	6
LIF	527315.8	5056650	-1.913	-2.193	28
LIF	527312.8	5056701	-1.262	-1.312	5
LIF	527580	5056623	-1.22	-1.34	12
LIF	527523.1	5056629	-1.266	-1.366	10
LIF	527478.5	5056626	-1.363	-1.423	6

Type	Northing (m)	Easting (m)	Top of Competent Sludge (masl)	Bottom of Sludge (masl)	Thickness (cm)
LIF	527425.6	5056626	-1.213	-1.353	14
LIF	527585.8	5056658	-1.259	-1.309	5
LIF	527577.5	5056669	-2.604	-3.294	69
LIF	527577.4	5056648	-1.134	-1.214	8
LIF	527577.3	5056686	-2.68	-3.2	52
LIF	527574.5	5056713	-2.576	-3.166	59
LIF	527576.5	5056735	-1.215	-1.295	8
LIF	527589	5056696	-2.667	-3.117	45
LIF	527553.7	5056707	-2.378	-2.688	31
LIF	527542.1	5056674	-2.924	-3.704	78
LIF	527511.7	5056666	-2.758	-3.418	66
LIF	527537.9	5056771	-1.332	-1.392	6
LIF	527529.8	5056733	-2.529	-3.119	59
LIF	527530.5	5056700	-1.379	-1.489	11
LIF	527473	5056737	-1.833	-2.033	20
LIF	527473.1	5056719	-1.324	-1.384	6
LIF	527473.8	5056758	-3.421	-4.151	73
LIF	527469.1	5056778	-1.436	-1.526	9
LIF	527447.5	5056745	-2.903	-3.463	56
LIF	527428.5	5056757	-3.139	-3.789	65
LIF	527426.9	5056777	-1.399	-1.489	9
LIF	527526.2	5056719	-2.479	-3.269	79
LIF	527500.5	5056734	-2.604	-3.174	57
LIF	527549	5056668	-2.834	-3.474	64
LIF	527471.7	5056690	-1.29	-1.4	11
LIF	527482.2	5056662	-2.328	-2.928	60
LIF	527432.1	5056667	-1.819	-2.029	21
LIF	527425.8	5056692	-1.43	-1.56	13
LIF	527428.6	5056720	-2.096	-2.356	26
LIF	527433.7	5056744	-2.773	-3.153	38
LIF	527409	5056726	-3.12	-3.7	58
LIF	527774.8	5056624	-1.065	-1.185	12
LIF	527711.5	5056622	-1.208	-1.358	15
LIF	527634.1	5056629	-1.203	-1.323	12
LIF	527671.9	5056678	-1.12	-1.24	12
LIF	527726	5056673	-1.134	-1.264	13
LIF	527777.2	5056674	-1.081	-1.241	16
LIF	527668	5056769	-1.006	-1.046	4

Type	Northing (m)	Easting (m)	Top of Competent Sludge (masl)	Bottom of Sludge (masl)	Thickness (cm)
LIF	527425.6	5056626	-1.213	-1.353	14
LIF	527585.8	5056658	-1.259	-1.309	5
LIF	527627.2	5056731	-1.041	-1.151	11
LIF	527609.8	5056717	-1.297	-1.377	8
LIF	527657.8	5056765	-1.02	-1.11	9
LIF	527765	5056774	-1.151	-1.231	8
LIF	527754.9	5056784	-2.79	-3.46	67
LIF	527740.5	5056750	-1.102	-1.172	7
LIF	527713.2	5056766	-3.581	-4.451	87
LIF	527709.5	5056795	-1.119	-1.249	13
LIF	527685.9	5056784	-1.056	-1.146	9
LIF	527687.6	5056752	-3.107	-4.067	96
LIF	527714.2	5056735	-1.097	-1.217	12
LIF	527724.8	5056709	-1.251	-1.301	5
LIF	527717.5	5056730	-1.072	-1.172	10
LIF	527694.6	5056710	-1.038	-1.228	19
LIF	527683.2	5056717	-2.899	-3.379	48
LIF	527677.4	5056727	-3.244	-3.684	44
LIF	527662	5056738	-2.127	-2.467	34
LIF	527613.6	5056778	-1.129	-1.189	6
LIF	527644.4	5056722	-2.227	-2.517	29
LIF	527645.7	5056716	-2.596	-3.346	75
LIF	527663.5	5056694	-1.429	-1.549	12
LIF	527671.7	5056680	-1.175	-1.245	7
LIF	527621.2	5056653	-1.208	-1.288	8
LIF	527617.1	5056664	-1.169	-1.229	6
LIF	527622.8	5056683	-2.876	-3.566	69
LIF	527614	5056700	-2.465	-2.835	37
LIF	527835.7	5056701	-0.97	-1.09	12
LIF	527826.7	5056766	-0.987	-1.087	10
LIF	527902.1	5056774	-1.002	-1.112	11
LIF	527985.3	5056787	-0.992	-1.082	9
LIF	528019	5056768	-0.118	-0.148	3
LIF	528061.1	5056772	-0.513	-0.633	12
LIF	526525.2	5056515	-1.205	-1.555	35
LIF	526465.8	5056574	-1.247	-1.647	40
LIF	526568.2	5056560	-2.365	-3.105	74
LIF	526578.1	5056516	-1.714	-1.974	26

Type	Northing (m)	Easting (m)	Top of Competent Sludge (masl)	Bottom of Sludge (masl)	Thickness (cm)
LIF	526664.7	5056476	-1.813	-1.973	16
LIF	526620.2	5056521	-1.926	-2.296	37
LIF	526728.6	5056524	-1.755	-2.075	32
LIF	526787	5056578	-1.713	-1.893	18
LIF	526689.5	5056577	-2.142	-2.642	50
LIF	526782.2	5056477	-1.763	-2.233	47
LIF	526595	5056605	-1.812	-1.992	18
LIF	526643.3	5056568	-1.928	-2.258	33
LIF	526714.9	5056474	-2.145	-2.555	41
LIF	526754.4	5056555	-1.859	-1.999	14
LIF	526781.9	5056427	-1.539	-2.019	48
LIF	526839.1	5056426	-1.588	-1.968	38
LIF	526878.9	5056467	-1.727	-1.887	16
LIF	526881.4	5056573	-1.435	-1.645	21
LIF	526963.1	5056577	-1.237	-1.367	13
LIF	526981.2	5056473	-1.469	-1.749	28
LIF	526916.2	5056432	-1.548	-1.838	29
LIF	526829.5	5056525	-1.615	-1.865	25
LIF	526909.2	5056528	-1.502	-1.582	8
LIF	526923.4	5056485	-1.567	-1.677	11
LIF	526821.6	5056416	-1.576	-1.996	42
LIF	526971.1	5056412	-1.861	-2.221	36
LIF	527009.4	5056413	-1.431	-1.651	22
LIF	527070	5056466	-1.411	-1.581	17
LIF	527133.3	5056525	-1.449	-1.799	35
LIF	527164.5	5056467	-1.42	-1.71	29
LIF	527036.5	5056526	-1.451	-1.591	14
LIF	527075.7	5056576	-1.485	-1.615	13
LIF	527177.7	5056573	-1.39	-1.56	17
LIF	527168.4	5056432	-1.334	-1.534	20
LIF	527038.2	5056575	-1.661	-1.971	31
LIF	527011	5056561	-1.259	-1.439	18
LIF	527049.3	5056474	-1.862	-1.952	9
LIF	527169.1	5056529	-1.542	-1.672	13
LIF	527125.4	5056474	-1.605	-1.795	19
LIF	527096.4	5056508	-1.649	-1.769	12
LIF	527021.9	5056520	-2.303	-2.693	39
LIF	527023.2	5056483	-2.108	-2.328	22

Type	Northing (m)	Easting (m)	Top of Competent Sludge (masl)	Bottom of Sludge (masl)	Thickness (cm)
LIF	527281.1	5056429	-1.23	-1.34	11
LIF	527323.9	5056426	-0.86	-1.01	15
LIF	527319.5	5056486	-1.296	-1.496	20
LIF	527270.9	5056474	-1.362	-1.612	25
LIF	527221.5	5056526	-1.497	-1.717	22
LIF	527281.7	5056581	-1.393	-1.563	17
LIF	527318.8	5056529	-1.394	-1.544	15
LIF	527376.7	5056576	-1.942	-2.152	21
LIF	527222	5056566	-1.535	-1.705	17
LIF	527222.2	5056477	-1.45	-1.6	15
LIF	527427.4	5056573	-1.999	-2.299	30
LIF	527486.1	5056577	-1.641	-1.891	25
LIF	527571.4	5056574	-1.394	-1.534	14
LIF	527515	5056527	-1.08	-1.4	32
LIF	527501.6	5056468	-0.964	-1.314	35
LIF	527503.5	5056423	-0.971	-1.261	29
LIF	527556.7	5056417	-0.897	-1.137	24
LIF	527568.6	5056491	-1.062	-1.312	25
LIF	527639.8	5056511	-0.947	-1.157	21
LIF	527611.3	5056584	-1.233	-1.423	19
LIF	527675.2	5056566	-1.128	-1.398	27
LIF	527729	5056575	-0.936	-1.176	24
LIF	526755.7	5056335	-0.475	-0.585	11
LIF	526680.1	5056384	-1.093	-1.313	22
LIF	526679.8	5056379	-0.389	-0.459	7
LIF	526728.4	5056374	-1.723	-2.153	43
LIF	526775.1	5056390	-1.67	-2.08	41
LIF	526827.9	5056386	-1.486	-2.006	52
LIF	526982.5	5056308	-1.255	-1.825	57
LIF	526876.9	5056275	-1.341	-1.871	53
LIF	526886.6	5056224	-1.487	-1.487	0
LIF	526979.6	5056274	-1.684	-1.694	1
LIF	526924.4	5056239	-1.081	-1.881	80
LIF	526913.7	5056278	-0.993	-1.823	83
LIF	526994.3	5056240	-1.738	-1.958	22
LIF	527176.8	5056275	-0.468	-0.678	21
LIF	527158.1	5056224	-1.645	-1.755	11
LIF	527100.1	5056293	-0.406	-0.416	1

Type	Northing (m)	Easting (m)	Top of Competent Sludge (masl)	Bottom of Sludge (masl)	Thickness (cm)
LIF	527088	5056240	-1.731	-1.941	21
LIF	527063.3	5056277	-1.646	-1.856	21
LIF	527023.8	5056325	-1.202	-1.592	39
LIF	527010.3	5056261	-1.696	-1.906	21
LIF	527330.7	5056271	0.069	-0.021	9
LIF	527326	5056221	-0.962	-1.352	39
LIF	527267.6	5056270	-0.902	-1.172	27
LIF	527275.4	5056219	-1.277	-1.497	22
LIF	527226.8	5056221	-1.119	-1.469	35
LIF	527232.7	5056268	-0.744	-1.084	34
LIF	526971.3	5056128	-1.887	-1.887	0
LIF	526981.2	5056169	-1.465	-2.005	54
LIF	527173.8	5056171	-1.263	-1.723	46
LIF	527177.7	5056122	-1.274	-1.664	39
LIF	527161.5	5056082	-1.151	-1.371	22
LIF	527127	5056050	-0.845	-1.115	27
LIF	527064.6	5056065	-0.781	-0.891	11
LIF	527083.9	5056018	-0.592	-0.652	6
LIF	527126.6	5056119	-1.298	-1.638	34
LIF	527128.3	5056166	-1.532	-1.802	27
LIF	527076.1	5056119	-1.522	-1.792	27
LIF	527025.5	5056127	-1.393	-1.813	42
LIF	527021.5	5056169	-1.627	-1.997	37
LIF	527091.1	5056188	-1.692	-1.882	19
LIF	527381.1	5056138	-0.301	-0.301	0
LIF	527373.2	5056179	-0.408	-0.408	0
LIF	527325.2	5056166	-1.06	-1.45	39
LIF	527325.8	5056122	-0.996	-1.266	27
LIF	527274.6	5056167	-1.16	-1.38	22
LIF	527227.7	5056176	-1.133	-1.623	49
LIF	527225.3	5056124	-1.166	-1.346	18
LIF	527276.2	5056123	-0.941	-1.211	27
LIF	526637.4	5057478	-0.774	-0.824	5
LIF	526724.9	5057469	-1.042	-1.162	12
LIF	526789.4	5057433	-1.476	-1.646	17
LIF	526673.4	5057422	-1.929	-2.139	21
LIF	526793.3	5057400	-1.951	-2.261	31
LIF	526810.8	5057410	-1.529	-1.549	2

Type	Northing (m)	Easting (m)	Top of Competent Sludge (masl)	Bottom of Sludge (masl)	Thickness (cm)
LIF	527900	5057425	-2.108	-2.408	30
LIF	527929.5	5057436	-2.154	-2.444	29
LIF	527971.2	5057417	-0.582	-0.742	16
LIF	527995.9	5057437	-2.244	-2.624	38
LIF	528018.2	5057438	-1.137	-1.457	32
LIF	528075.7	5057415	-1.881	-2.181	30
LIF	528052.5	5057421	-3.245	-3.245	0
LIF	528016.9	5057404	-1.031	-1.311	28
LIF	526588.5	5057332	-1.543	-1.713	17
LIF	526589.8	5057268	-1.034	-1.144	11
LIF	526614.2	5057378	-1.783	-2.043	26
LIF	526732.2	5057382	-2.024	-2.294	27
LIF	526769.9	5057324	-2.154	-2.504	35
LIF	526677	5057330	-2.242	-2.512	27
LIF	526633.2	5057269	-2.071	-2.251	18
LIF	526732.4	5057264	-2.488	-2.728	24
LIF	526769.4	5057233	-2.429	-2.809	38
LIF	526651.3	5057215	-2.139	-2.449	31
LIF	526775.3	5057366	-2.123	-2.413	29
LIF	526667.6	5057369	-2.068	-2.368	30
LIF	526633.6	5057320	-2.193	-2.453	26
LIF	526675.5	5057268	-2.392	-2.652	26
LIF	526776.2	5057269	-2.389	-2.739	35
LIF	526721.1	5057336	-2.198	-2.458	26
LIF	526709.7	5057224	-2.591	-2.981	39
LIF	526672.4	5057220	-2.421	-2.701	28
LIF	526608.2	5057324	-1.801	-2.091	29
LIF	526831.4	5057375	-1.18	-1.41	23
LIF	526832.9	5057286	-2.123	-2.453	33
LIF	526887.7	5057222	-1.738	-2.048	31
LIF	526826.9	5057220	-2.539	-3.029	49
LIF	526871.7	5057268	-1.911	-2.111	20
LIF	526822.2	5057351	-1.946	-2.276	33
LIF	527655.2	5057219	-0.96	-1.17	21
LIF	527701.5	5057256	-1.201	-1.381	18
LIF	527731.3	5057327	-0.985	-1.225	24
LIF	527778.7	5057284	-1.047	-1.307	26
LIF	527780	5057328	-1.168	-1.358	19

Type	Northing (m)	Easting (m)	Top of Competent Sludge (masl)	Bottom of Sludge (masl)	Thickness (cm)
LIF	527738.5	5057283	-1.464	-1.684	22
LIF	527785.8	5057362	-0.951	-1.131	18
LIF	527825.1	5057321	-0.872	-1.082	21
LIF	527820.3	5057374	-0.838	-1.078	24
LIF	527917	5057325	-0.551	-0.681	13
LIF	527919.7	5057370	-0.662	-0.842	18
LIF	527977.7	5057377	-0.792	-1.042	25
LIF	527952.5	5057214	-1.445	-1.705	26
LIF	527869.9	5057372	-1.264	-1.474	21
LIF	527875.7	5057323	-2.246	-2.506	26
LIF	527885.2	5057271	-2.844	-3.154	31
LIF	527862.9	5057269	-0.802	-0.992	19
LIF	527934	5057262	-1.825	-2.075	25
LIF	527992.4	5057276	-1.827	-2.047	22
LIF	527971	5057317	-1.915	-2.195	28
LIF	527933.7	5057220	-1.438	-1.778	34
LIF	527905.7	5057225	-2.744	-3.044	30
LIF	527884.4	5057221	-1.477	-1.777	30
LIF	527853.7	5057359	-2.956	-3.136	18
LIF	527890.3	5057357	-0.946	-1.086	14
LIF	527995.1	5057335	-1.657	-1.947	29
LIF	527953.9	5057287	-2.048	-2.258	21
LIF	527947.1	5057248	-1.901	-2.211	31
LIF	528065.3	5057315	-0.657	-0.807	15
LIF	528078.5	5057288	-0.716	-0.976	26
LIF	528096.7	5057355	-0.779	-1.009	23
LIF	528075.3	5057385	-1.228	-1.398	17
LIF	528013.1	5057366	-2.241	-2.541	30
LIF	528053.3	5057363	-2.381	-2.631	25
LIF	528025.8	5057281	-0.789	-0.949	16
LIF	528024.7	5057318	-2.041	-2.341	30
LIF	528050.2	5057295	-0.574	-0.704	13
LIF	526520.4	5057017	-1.773	-1.873	10
LIF	526523.1	5057115	-1.785	-2.065	28
LIF	526476.4	5057154	-1.248	-1.478	23
LIF	526577.7	5057166	-1.103	-1.103	0
LIF	526575.1	5057068	-2.04	-2.33	29
LIF	526668.1	5057177	-2.193	-2.523	33

Type	Northing (m)	Easting (m)	Top of Competent Sludge (masl)	Bottom of Sludge (masl)	Thickness (cm)
LIF	526759.4	5057162	-2.554	-2.904	35
LIF	526708.8	5057124	-2.182	-2.612	43
LIF	526614	5057128	-1.679	-1.829	15
LIF	526636	5057017	-2.094	-2.454	36
LIF	526673.5	5057076	-2.288	-2.568	28
LIF	526780.9	5057074	-2.652	-3.162	51
LIF	526724	5057028	-2.35	-2.74	39
LIF	526631.8	5057179	-1.672	-1.822	15
LIF	526717.2	5057170	-2.46	-2.74	28
LIF	526769.6	5057122	-2.618	-2.968	35
LIF	526723.9	5057062	-2.449	-2.759	31
LIF	526775.2	5057021	-2.574	-2.904	33
LIF	526680.8	5057124	-2.211	-2.541	33
LIF	526630.5	5057075	-2.127	-2.307	18
LIF	526682.6	5057021	-2.321	-2.611	29
LIF	526914.6	5057168	-0.561	-0.681	12
LIF	526922.2	5057030	-1.863	-2.083	22
LIF	526865.1	5057081	-2.068	-2.168	10
LIF	526855.9	5057158	-2.208	-2.558	35
LIF	526816	5057110	-2.585	-2.965	38
LIF	526824.7	5057027	-2.41	-2.74	33
LIF	526862.5	5057025	-2.184	-2.404	22
LIF	526863.1	5057120	-2.234	-2.404	17
LIF	526893.3	5057124	-1.32	-1.36	4
LIF	526810.8	5057159	-2.873	-3.293	42
LIF	526846.4	5057066	-2.258	-2.508	25
LIF	526912.6	5057028	-1.967	-2.147	18
LIF	527193.8	5057101	-0.919	-1.149	23
LIF	527310.8	5057134	-0.78	-0.92	14
LIF	527256.4	5057134	-0.35	-0.45	10
LIF	527272.1	5057081	-1.135	-1.265	13
LIF	527262.5	5057030	-0.892	-1.052	16
LIF	527219.7	5057062	-0.997	-1.157	16
LIF	527236.9	5057099	-0.96	-1.13	17
LIF	527565.8	5057170	0.007	-0.033	4
LIF	527639.9	5057177	-0.085	-0.175	9
LIF	527893.9	5057167	-1.094	-1.794	70
LIF	527922.5	5057176	-2.727	-3.127	40

Type	Northing (m)	Easting (m)	Top of Competent Sludge (masl)	Bottom of Sludge (masl)	Thickness (cm)
LIF	527955.6	5057171	-1.452	-1.692	24
LIF	527921	5057129	-1.758	-2.068	31
LIF	527949.2	5057126	-3.029	-3.499	47
LIF	527971	5057121	-2.449	-3.289	84
LIF	527992.9	5057049	-2.21	-3.23	102
LIF	527961.9	5057068	-2.158	-2.838	68
LIF	527939.5	5057062	-1.128	-1.128	0
LIF	527928.6	5057024	-1.578	-1.788	21
LIF	527949.2	5057012	-1.932	-2.372	44
LIF	527980.3	5057029	-2.132	-3.082	95
LIF	527904.7	5057011	-1.03	-1.21	18
LIF	528023	5057036	-0.746	-0.966	22
LIF	526524.5	5056822	-0.884	-0.884	0
LIF	526522.1	5056924	-1.835	-2.155	32
LIF	526569.1	5056968	-2.254	-2.574	32
LIF	526557.2	5056860	-1.926	-2.226	30
LIF	526572.4	5056917	-2.329	-2.349	2
LIF	526620.7	5056928	-2.357	-2.767	41
LIF	526623.6	5056833	-2.231	-2.511	28
LIF	526718.6	5056831	-2.344	-2.784	44
LIF	526672.3	5056885	-2.242	-2.702	46
LIF	526727.3	5056928	-2.245	-2.505	26
LIF	526675.8	5056989	-2.25	-2.56	31
LIF	526754.2	5056984	-2.588	-3.068	48
LIF	526771.3	5056878	-2.199	-2.559	36
LIF	526774.3	5056831	-2.059	-2.339	28
LIF	526727.1	5056871	-2.246	-2.586	34
LIF	526776	5056916	-2.214	-2.484	27
LIF	526719.9	5056967	-2.169	-2.539	37
LIF	526635.7	5056957	-2.238	-2.538	30
LIF	526640.1	5056868	-2.187	-2.337	15
LIF	526685.6	5056818	-2.683	-3.213	53
LIF	526671.4	5056920	-2.035	-2.515	48
LIF	526924.1	5056923	-1.89	-2.18	29
LIF	526930.9	5056822	-1.695	-1.975	28
LIF	526974.4	5056879	-1.823	-1.943	12
LIF	526951.1	5056967	-1.821	-2.081	26
LIF	526869.5	5056967	-2.2	-2.55	35

Type	Northing (m)	Easting (m)	Top of Competent Sludge (masl)	Bottom of Sludge (masl)	Thickness (cm)
LIF	526823	5056924	-2.754	-3.424	67
LIF	526868.7	5056885	-2.226	-2.526	30
LIF	526822.2	5056833	-3.079	-3.739	66
LIF	526884.6	5056804	-1.883	-2.213	33
LIF	526934.2	5056866	-1.797	-1.947	15
LIF	526863.1	5056916	-2.873	-3.343	47
LIF	526819.5	5056866	-2.555	-3.175	62
LIF	526818.9	5056965	-2.736	-3.026	29
LIF	526924.6	5056973	-1.932	-2.162	23
LIF	526876.5	5056834	-1.87	-2.09	22
LIF	527011.3	5056828	-1.575	-1.825	25
LIF	527022.6	5056898	-1.518	-1.798	28
LIF	527061	5056872	-1.444	-1.614	17
LIF	527083.8	5056824	-1.525	-1.865	34
LIF	527156.6	5056826	-1.652	-1.742	9
LIF	527269.9	5056966	-0.809	-0.979	17
LIF	527287.4	5056914	-0.86	-1.06	20
LIF	527323.4	5056875	-1.052	-1.052	0
LIF	527304.6	5056837	-1.257	-1.397	14
LIF	527242.8	5056816	-1.448	-1.618	17
LIF	527374.4	5056826	-1.486	-1.726	24
LIF	527439.1	5056822	-1.542	-1.682	14
LIF	527432.7	5056877	-1.314	-1.464	15
LIF	527499.2	5056827	-1.566	-1.866	30
LIF	527568.4	5056831	-1.373	-1.493	12
LIF	527521.4	5056885	-1.477	-1.577	10
LIF	527543.8	5056925	-1.231	-1.331	10
GC	527262.475	5057029.953	-0.926	-1.026	10.0
GC	527226.762	5056221.219	-1.121	-1.411	29.0

Appendix B: List of BH Boundary Locations

Easting (m)	Northing (m)	Thickness (cm)	Easting (m)	Northing (m)	Thickness (cm)
528118.9906	5057242.563	0	527979.1541	5057143.275	0
528115.4556	5057238.803	0	527982.9413	5057136.004	0
528117.6054	5057226.725	0	527987.3701	5057128.113	0
528121.7532	5057232.787	0	527991.5789	5057120.633	0
528127.604	5057232.602	0	527995.7964	5057112.952	0
528124.7121	5057226.134	0	528003.1582	5057100.697	0
528122.2293	5057220.501	0	528009.8858	5057092.606	0
528124.5543	5057214.479	0	528014.7254	5057083.462	0
528122.4893	5057209.47	0	528017.4786	5057075.764	0
528118.7448	5057205.498	0	528022.9531	5057067.467	0
528113.9416	5057204.843	0	528027.5798	5057060.61	0
528108.8895	5057212.742	0	528033.0401	5057053.757	0
528105.7273	5057219.594	0	528038.505	5057045.871	0
528100.8818	5057228.316	0	528040.6378	5057037.548	0
528093.7591	5057232.45	0	528044.6402	5057029.245	0
528087.4689	5057236.799	0	528046.7634	5057021.333	0
528078.8794	5057243.216	0	528053.6781	5057018.453	0
528072.8052	5057246.31	0	528048.9009	5057011.976	0
528065.6891	5057248.989	0	528051.4467	5057003.655	0
528060.9264	5057254.912	0	528050.8625	5056993.242	0
528049.8396	5057257.15	0	528050.4177	5056981.274	0
528038.7635	5057258.767	0	528052.5544	5056972.118	0
528029.5683	5057259.559	0	528055.1113	5056961.308	0
528017.4424	5057260.749	0	528056.2366	5056943.192	0
528006.8053	5057256.535	0	528055.3495	5056953.377	0
527997.4316	5057250.249	0	528057.743	5056932.144	0
527989.4823	5057244.169	0	528057.7955	5056920.479	0
527984.4846	5057239.992	0	528057.0041	5056911.098	0
527978.66	5057234.344	0	528060.1759	5056902.158	0
527972.4213	5057227.227	0	528060.0317	5056889.18	0
527968.3608	5057219.032	0	528060.2907	5056878.349	0
527965.9033	5057209.444	0	528064.112	5056863.578	0
527964.6856	5057201.317	0	528067.2906	5056854.849	0
527964.5108	5057193.395	0	528067.9215	5056844.475	0
527964.7575	5057185.274	0	528069.215	5056835.737	0
527965.8451	5057175.491	0	528072.8197	5056824.087	0
527966.2962	5057166.96	0	528077.2532	5056813.486	0
527969.8837	5057159.066	0	528078.9233	5056804.161	0
527974.7281	5057150.544	0	527969.8283	5057454.643	0

Easting (m)	Northing (m)	Thickness (cm)	Easting (m)	Northing (m)	Thickness (cm)
528089.0026	5056794.007	0	527832.6509	5056651.458	0
528091.5391	5056787.763	0	527829.5555	5056643.323	0
528103.2696	5056781.161	0	527823.1094	5056635.384	0
528108.9719	5056777.709	0	527816.2535	5056626.743	0
528108.1712	5056770.417	0	527812.1036	5056619.225	0
528100.6517	5056769.139	0	527806.0827	5056610.243	0
528087.698	5056768.87	0	527800.8948	5056603.143	0
528076.3426	5056763.097	0	527796.5563	5056592.502	0
528066.7637	5056757.221	0	527790.7458	5056583.51	0
528057.8041	5056750.514	0	527786.1977	5056572.669	0
528050.126	5056739.447	0	527779.6472	5056561.907	0
528042.6392	5056730.87	0	527773.4357	5056550.225	0
528035.7628	5056726.884	0	527760.6974	5056548.712	0
528024.7268	5056729.767	0	527745.4626	5056544.478	0
528015.0895	5056735.146	0	527731.0012	5056538.003	0
528005.8366	5056748.637	0	527720.7935	5056531.503	0
528009.5618	5056756.986	0	527708.4892	5056525.204	0
528003.4806	5056761.536	0	527697.4599	5056515.99	0
527993.6699	5056760.459	0	527686.6248	5056508.653	0
527984.4793	5056758.329	0	527675.1627	5056502.147	0
527976.343	5056755.593	0	527662.4492	5056495.014	0
527968.1845	5056757.845	0	527652.0297	5056487.046	0
527955.6653	5056754.456	0	527642.8675	5056480.139	0
527943.3007	5056749.612	0	527635.122	5056469.972	0
527927.6216	5056750.786	0	527625.9709	5056460.555	0
527916.9584	5056752.194	0	527616.6048	5056452.181	0
527900.4877	5056743.998	0	527607.2452	5056442.351	0
527894.4044	5056733.361	0	527604.362	5056431.928	0
527887.7575	5056723.332	0	527602.0214	5056422.152	0
527883.9206	5056710.305	0	527596.203	5056414.838	0
527882.699	5056703.011	0	527591.8428	5056408.986	0
527879.4101	5056691.119	0	527584.7646	5056402.91	0
527874.1242	5056681.574	0	527576.8455	5056398.498	0
527869.9887	5056672.601	0	527572.6777	5056394.947	0
527864.1727	5056664.876	0	527571.6641	5056388.065	0
527857.7249	5056657.347	0	527565.002	5056383.036	0
527848.3296	5056655.639	0	527554.7806	5056377.78	0
527840.3952	5056654.77	0	527543.7296	5056373.365	0
527999.0708	5057456.029	0	527532.444	5056372.693	0

Easting (m)	Northing (m)	Thickness (cm)	Easting (m)	Northing (m)	Thickness (cm)
527519.4903	5056372.214	0	527378.6544	5056495.862	0
527508.1495	5056371.675	0	527377.0261	5056485.234	0
527499.7913	5056371.438	0	527374.16	5056470.844	0
527494.3659	5056370.37	0	527369.747	5056457.459	0
527496.2847	5056361.001	0	527366.2548	5056443.701	0
527498.8254	5056353.724	0	527360.6456	5056436.599	0
527502.2014	5056346.039	0	527353.6868	5056421.036	0
527506.818	5056341.471	0	527345.3687	5056411.634	0
527513.105	5056337.966	0	527337.6799	5056402.645	0
527519.7994	5056335.696	0	527328.5095	5056395.728	0
527526.9144	5056333.438	0	527319.3286	5056392.977	0
527531.3152	5056330.125	0	527308.2757	5056388.973	0
527529.8758	5056326.163	0	527297.205	5056387.258	0
527523.1746	5056328.211	0	527285.0767	5056388.661	0
527515.8578	5056330.268	0	527274.8428	5056387.994	0
527511.2518	5056330.658	0	527260.7463	5056392.321	0
527504.7706	5056332.296	0	527248.4063	5056395.811	0
527499.3204	5056336.861	0	527235.2351	5056396.998	0
527493.0242	5056342.455	0	527220.4139	5056394.233	0
527485.4702	5056348.877	0	527207.2562	5056392.298	0
527478.9468	5056360.091	0	527194.5201	5056390.165	0
527474.085	5056372.569	0	527180.9372	5056389.273	0
527464.3563	5056384.57	0	527163.0207	5056396.005	0
527459.5001	5056395.792	0	527155.8787	5056404.518	0
527458.1817	5056410.374	0	527150.0335	5056403.248	0
527451.0087	5056425.83	0	527143.3116	5056410.085	0
527450.1967	5056442.169	0	527137.2512	5056411.725	0
527453.2652	5056456.56	0	527130.1083	5056420.449	0
527453.8011	5056476.405	0	527121.2932	5056428.532	0
527448.9626	5056492.493	0	527109.3655	5056432.225	0
527446.5939	5056508.526	0	527097.0401	5056432.382	0
527442.5577	5056522.874	0	527085.202	5056429.787	0
527433.9508	5056531.38	0	527073.0874	5056428.068	0
527419.1136	5056532.348	0	527063.2986	5056421.781	0
527405.9499	5056531.879	0	527054.1261	5056415.286	0
527396.7729	5056528.295	0	527045.5969	5056407.75	0
527388.5636	5056522.559	0	527040.6295	5056396.274	0
527382.3281	5056514.41	0	527036.7032	5056385.447	0
527381.5329	5056505.663	0	527034.8618	5056377.106	0

Easting (m)	Northing (m)	Thickness (cm)	Easting (m)	Northing (m)	Thickness (cm)
527033.6446	5056368.557	0	526748.9889	5056310.946	0
527025.7251	5056364.145	0	526738.3481	5056308.823	0
527015.2933	5056360.567	0	526734.6031	5056304.64	0
527004.654	5056356.355	0	526726.0211	5056307.515	0
526992.9734	5056351.516	0	526714.9447	5056307.056	0
526984.4183	5056348.145	0	526704.0954	5056313.609	0
526973.3573	5056344.142	0	526691.9508	5056320.634	0
526962.44	5056339.34	0	526680.4226	5056327.462	0
526950.3359	5056335.121	0	526671.8217	5056336.58	0
526938.4212	5056337.57	0	526663.5576	5056345.278	0
526928.6127	5056333.983	0	526654.5361	5056354.394	0
526926.366	5056329.263	0	526643.0077	5056363.1	0
526913.6282	5056325.664	0	526625.1361	5056375.867	0
526905.464	5056329.173	0	526615.0725	5056384.579	0
526892.7071	5056331.829	0	526607.9223	5056395.169	0
526881.8045	5056334.426	0	526593.8723	5056406.975	0
526874.7014	5056333.984	0	526584.4258	5056417.145	0
526866.3625	5056331.026	0	526574.7663	5056427.937	0
526854.4858	5056322.854	0	526584.5013	5056448.799	0
526857.6373	5056318.29	0	526572.9529	5056462.293	0
526866.8319	5056317.907	0	526563.2953	5056472.662	0
526877.2772	5056318.374	0	526550.5022	5056480.24	0
526886.2675	5056318.413	0	526533.9795	5056483.703	0
526895.2491	5056318.652	0	526518.9231	5056486.772	0
526891.2975	5056313.635	0	526504.6941	5056491.289	0
526882.9534	5056310.066	0	526491.0997	5056494.976	0
526869.6037	5056305.631	0	526481.0596	5056496.399	0
526859.5536	5056302.044	0	526474.3844	5056494.282	0
526848.9095	5056298.876	0	526471.0653	5056488.858	0
526837.2278	5056294.248	0	526467.3264	5056483.22	0
526826.5837	5056291.081	0	526464.9956	5056490.91	0
526819.2861	5056288.75	0	526467.7954	5056497.532	0
526808.6044	5056294.336	0	526467.0419	5056508.039	0
526801.0734	5056295.548	0	526461.3735	5056514.681	0
526793.5519	5056296.349	0	526451.9256	5056525.262	0
526785.1926	5056296.314	0	526441.8448	5056538.13	0
526775.7894	5056296.273	0	526436.885	5056552.208	0
526765.7347	5056301.019	0	526430.575	5056563.213	0
526757.1449	5056309.314	0	526431.1188	5056581.959	0

Easting (m)	Northing (m)	Thickness (cm)	Easting (m)	Northing (m)	Thickness (cm)
526436.8567	5056608.559	0	526514.1557	5057209.016	0
526443.2525	5056628.784	0	526534.8471	5057208.482	0
526451.674	5056650.796	0	526555.3283	5057206.07	0
526459.7579	5056666.04	0	526569.172	5057220.305	0
526467.3172	5056683.748	0	526569.3514	5057238.538	0
526468.3064	5056696.663	0	526566.5689	5057255.402	0
526474.6952	5056718.499	0	526568.3749	5057272.142	0
526477.4984	5056746.331	0	526563.9256	5057287.111	0
526481.1739	5056766.867	0	526555.3086	5057298.529	0
526482.3759	5056779.16	0	526553.4724	5057323.663	0
526488.858	5056778.977	0	526557.9653	5057347.836	0
526503.9218	5056801.528	0	526563.6372	5057376.814	0
526501.3325	5056820.571	0	526566.859	5057404.947	0
526500.005	5056837.841	0	526567.7081	5057428.727	0
526496.7929	5056856.782	0	526556.8076	5057436.802	0
526489.6534	5056874.217	0	526545.0844	5057442.374	0
526485.8087	5056893.566	0	526534.8055	5057454.518	0
526483.4276	5056913.132	0	526528.0702	5057466.777	0
526480.9495	5056935.375	0	526530.101	5057480.107	0
526479.0017	5056950.154	0	526540.934	5057487.864	0
526480.1247	5056971.869	0	526556.9812	5057496.676	0
526482.5404	5056991.866	0	526577.641	5057494.175	0
526478.4625	5057018.458	0	526590.7637	5057503.808	0
526473.165	5057035.09	0	526598.8578	5057516.331	0
526467.2223	5057056.929	0	526614.9268	5057521.821	0
526455.3242	5057065.023	0	526636.629	5057526.913	0
526441.093	5057070.373	0	526662.4376	5057526.19	0
526426.419	5057082.81	0	526681.676	5057522.739	0
526412.029	5057101.792	0	526695.1026	5057508.631	0
526403.161	5057124.664	0	526713.2131	5057501.209	0
526395.7881	5057142.142	0	526736.0106	5057496.107	0
526391.9834	5057154.003	0	526754.8437	5057489.111	0
526393.9855	5057174.21	0	526776.7605	5057478.706	0
526412.2206	5057198.207	0	526794.1455	5057467.948	0
526402.641	5057190.467	0	526810.0816	5057453.595	0
526436.008	5057206.018	0	526820.8078	5057437.198	0
526424.9253	5057207.427	0	526832.1536	5057421.626	0
526459.6125	5057207.363	0	526843.7421	5057398.555	0
526488.4646	5057207.452	0	526854.9115	5057376.95	0

Easting (m)	Northing (m)	Thickness (cm)	Easting (m)	Northing (m)	Thickness (cm)
526862.8418	5057353.275	0	527244.4873	5056916.93	0
526875.2532	5057332.707	0	527251.6636	5056937.927	0
526892.0685	5057309.671	0	527258.6969	5056954.201	0
526906.3167	5057285.9	0	527250.4606	5056974.363	0
526918.9404	5057264.923	0	527243.8896	5056994.944	0
526930.2991	5057248.318	0	527234.224	5057008.856	0
526943.0972	5057228.486	0	527206.5718	5057024.568	0
526953.8089	5057215.622	0	527183.2785	5057048.209	0
526967.5244	5057196.238	0	527163.5289	5057072.065	0
526974.712	5057176.904	0	527156.2399	5057098.398	0
526978.5467	5057158.389	0	527164.7133	5057120.3	0
526973.1741	5057145.245	0	527178.8926	5057139.482	0
526960.0158	5057143.832	0	527189.0836	5057149.726	0
526943.5377	5057137.306	0	527197.8119	5057159.552	0
526929.1409	5057132.244	0	527204.0361	5057170.201	0
526918.4615	5057137.609	0	527214.3042	5057162.746	0
526918.9342	5057125.534	0	527233.5955	5057161.786	0
526921.5215	5057107.225	0	527255.5484	5057159.593	0
526926.2031	5057087.369	0	527269.9429	5057156.201	0
526932.3155	5057075.318	0	527291.4374	5057160.883	0
526945.836	5057056.056	0	527313.1491	5057165.767	0
526963.2395	5057041.343	0	527336.9915	5057169.693	0
526979.04	5057028.079	0	527353.501	5057168.932	0
526989.3423	5057012.714	0	527363.7661	5057163.977	0
526999.4012	5056990.593	0	527372.7885	5057154.64	0
527008.468	5056972.722	0	527377.2133	5057145.705	0
527021.4418	5056950.291	0	527375.8219	5057129.044	0
527027.2554	5056937.14	0	527367.3088	5057118.174	0
527044.6791	5056919.716	0	527356.8539	5057104.219	0
527063.2711	5056905.932	0	527345.4218	5057091.047	0
527090.065	5056894.182	0	527342.8704	5057075.993	0
527118.2824	5056882.928	0	527336.4679	5057058.055	0
527149.9	5056867.244	0	527330.6872	5057042.209	0
527178.8339	5056859.66	0	527319.3119	5057024.927	0
527209.3372	5056860.215	0	527312.6836	5057010.521	0
527243.3762	5056864.53	0	527308.7861	5056995.094	0
527263.7307	5056868.263	0	527299.9681	5056979.046	0
527263.0684	5056877.215	0	527292.2935	5056966.935	0
527251.0886	5056892.994	0	527289.6296	5056954.425	0

Easting (m)	Northing (m)	Thickness (cm)	Easting (m)	Northing (m)	Thickness (cm)
527302.2307	5056939.07	0	527820.3049	5057280.076	0
527326.0743	5056925.131	0	527809.9244	5057265.454	0
527353.2792	5056915.673	0	527795.7825	5057250.603	0
527384.4447	5056907.266	0	527779.1333	5057235.53	0
527427.35	5056900.577	0	527759.1368	5057221.697	0
527458.4816	5056912.302	0	527738.9317	5057207.442	0
527487.4558	5056927.429	0	527713.2074	5057190.596	0
527520.4198	5056945.772	0	527690.3155	5057170.918	0
527546.0575	5056959.629	0	527669.9057	5057157.084	0
527570.3573	5056971.247	0	527641.7738	5057140.294	0
527589.5612	5056976.12	0	527614.9507	5057125.187	0
527622.1939	5056967.098	0	527590.1437	5057112.167	0
527648.2963	5056953.371	0	527576.1992	5057100.029	0
527673.2129	5056941.815	0	527555.1213	5057094.514	0
527696.6975	5056931.72	0	527545.1205	5057087.182	0
527717.6289	5056924.736	0	527537.7964	5057091.104	0
527740.7037	5056919.239	0	527546.7253	5057103.021	0
527767.8343	5056926.648	0	527552.736	5057114.291	0
527795.5137	5056941.992	0	527535.3257	5057130.246	0
527820.3973	5056962.357	0	527525.5353	5057122.915	0
527835.4609	5056976.79	0	527515.4252	5057140.369	0
527856.8918	5056997.506	0	527528.8202	5057164.048	0
527884.5315	5057014.628	0	527544.1454	5057188.08	0
527906.3676	5057037.013	0	527567.4593	5057207.549	0
527923.3086	5057051.343	0	527588.2752	5057228.206	0
527931.8512	5057072.835	0	527621.009	5057243.549	0
527935.5502	5057087.006	0	527648.4988	5057261.003	0
527920.6254	5057106.083	0	527663.8246	5057291.78	0
527903.7607	5057123.495	0	527678.7549	5057316.833	0
527887.1605	5057147.985	0	527710.6208	5057339.795	0
527874.0272	5057170.636	0	527737.5799	5057359.069	0
527876.0832	5057177.722	0	527758.7949	5057380.817	0
527870.4138	5057184.363	0	527779.5775	5057398.175	0
527864.9982	5057179.55	0	527811.5007	5057408.105	0
527867.1774	5057206.136	0	527827.0311	5057411.952	0
527859.4492	5057218.556	0	527840.327	5057429.499	0
527857.2333	5057247.288	0	527887.6905	5057442.42	0
527852.0934	5057274.941	0	527914.704	5057445.863	0
527835.7135	5057293.822	0	527943.9338	5057451.827	0
528017.4531	5057456.112	0			

Appendix C: After Filtering of Sample Data and Grouping

Easting (m)	Northing (m)	Thickness (cm)	Up to Grouping	Easting (m)	Northing (m)	Thickness (cm)	Up to Grouping
526769.6	5057122	35	50	527080.9	5056688	68	50
526781.9	5056427	48	50	527549	5056668	64	50
527432.7	5056877	15	50	526893.3	5057124	4	50
526637.4	5057478	5	50	526672.4	5057220	28	50
527926.6	5056918	20	50	527838.2	5056883	4	50
526918.7	5056716	17	50	527447.5	5056745	56	50
526775.1	5056390	41	50	527070	5056466	7.2	50
527785.1	5056817	87	50	527125.4	5056474	19	50
527473	5056737	20	50	527170.4	5056660	170	50
527210.7	5056657	101	50	527227.5	5056657	109	50
527919.7	5057370	18	50	527011.3	5056828	25	50
527409	5056726	58	50	527075.7	5056576	13	100
527971	5057121	84	50	526672.2	5056672	25	100
527318	5056713	3	50	527634.1	5056629	12	100
526614.2	5057378	26	50	526728.6	5056524	32	100
527614	5056700	37	50	527530.5	5056700	11	100
526576.7	5056764	29	50	527428.6	5056720	26	100
526755.7	5056335	6	50	527655.2	5057219	21	100
527401.4	5056675	29	50	527156.6	5056826	9	100
527297.3	5056672	106	50	527568.4	5056831	12	100
528053.3	5057363	25	50	528023	5057036	22	100
527244.9	5056665	111	50	527023.2	5056483	22	100
527226.5	5056715	10	50	527565.8	5057170	4	100
526634.3	5056632	39	50	526714.9	5056474	41	100
526789.4	5057433	17	50	527122.2	5056702	8	100
526839.1	5056426	38	50	526709.7	5057224	39	100
527167.8	5056684	19	50	528078.5	5057288	26	100
527237.1	5056786	14	50	526917.1	5057162	0.6	100
527049.3	5056474	9	50	527383.7	5056719	64	100
526787	5056578	18	50	527521.4	5056885	10	100
527644.4	5056722	29	50	527785.8	5057362	18	100
526922.2	5057030	22	50	526676.4	5056787	33	100
527971.2	5057417	16	50	527473.1	5056719	6	100
526912.6	5057028	18	50	527985.3	5056787	9	100
526810.8	5057159	42	50	527021.9	5056520	39	100
527327.1	5056613	9	50	527127.1	5056677	56	100
527622.8	5056683	69	50	527501.6	5056468	35	100
528061.1	5056772	12	50	527845.3	5056932	50	100
526614	5057128	8.5	50	526769.1	5056614	29	100

Easting (m)	Northing (m)	Thickness (cm)	Up to Grouping	Easting (m)	Northing (m)	Thickness (cm)	Up to Grouping
526930.9	5056822	28	100	528075.3	5057385	17	200
527933.7	5057220	34	100	527928.6	5057024	21	200
527763.9	5056885	9	100	527929.5	5057436	29	200
526682.6	5057021	29	100	527754.9	5056784	67	200
527717.5	5056730	10	100	526576.4	5057466	4	200
527083.1	5056706	11	100	527869.9	5057372	21	200
527266.4	5056674	83	100	526822.2	5056833	50	200
527257.9	5056680	18	100	526771.3	5056878	36	200
527955.6	5057171	24	100	527193.8	5057101	23.35	200
526668.1	5057177	33	100	526719.9	5056967	37	200
526721.6	5056772	36	100	527128.4	5056653	7	200
526934.2	5056866	15	100	527371.7	5056761	12	200
527031.7	5056695	13	100	528096.7	5057355	23	200
527780	5057328	19	100	526523.1	5057115	28	200
527808.9	5056827	10	100	527774.8	5056624	12	200
527256.4	5057134	5	100	526916.2	5056432	29	200
526465.8	5056574	40	100	527279.5	5056648	88	200
527269.9	5056966	8.8	100	526951.1	5056967	26	200
526881.4	5056573	21	100	527122.8	5056777	17	200
527577.5	5056669	69	100	526557.2	5056860	30	200
526568.2	5056560	74	100	526623.6	5056833	28	200
527890.3	5057357	14	100	528052.5	5057421	0	200
527427.4	5056573	7.5	200	526579.2	5056716	19	200
527262.5	5057030	10	200	526685.6	5056818	53	200
526775.2	5057021	33	200	527035.9	5056731	11	200
527310.8	5057134	14	200	527232.3	5056735	15	200
526672.3	5056885	46	200	527820.3	5057374	24	200
526589.8	5057268	11	200	527270.9	5056474	25	200
527709.5	5056795	13	200	527621.2	5056653	8	200
527884.4	5057221	30	200	527738.5	5057283	22	200
527574.5	5056713	59	200	526625.5	5056719	29	200
527928.6	5056830	11	200	526727.1	5056871	34	200
526524.5	5056822	0	200	526643.3	5056568	33	200
527323.4	5056875	1.25	200	527971	5057317	28	200
527014	5056681	16	200	527639.8	5056511	21	200
526595	5056605	18	200	527864.2	5056984	20	200
527824.5	5056913	59.5	200	526608.2	5057324	29	200
526887.7	5057222	31	200	527523.1	5056629	10	200
526664.7	5056476	16	200	526677	5057330	27	200

Easting (m)	Northing (m)	Thickness (cm)	Up to Grouping	Easting (m)	Northing (m)	Thickness (cm)	Up to Grouping
527503.5	5056423	20	200	527272.1	5056775	24	200
527083.3	5056700	14	200	528016.9	5057404	28	200
526828.3	5056721	27	200	527125	5056630	11	200
526775.3	5057366	29	200	526759.9	5056684	18.5	200
527784.1	5056917	4	200	527236.9	5057099	17	200
527577.3	5056686	52	200	527713.2	5056766	60.5	300
528065.3	5057315	15	200	527432.1	5056667	21	300
527281.1	5056429	10.35	200	527694.6	5056710	19	300
526974.4	5056879	12	200	526971.1	5056412	36	300
527137	5056719	11	200	527369.3	5056677	14	300
526925.7	5056773	15	200	527439.1	5056822	14	300
526721.1	5057336	26	200	527893.6	5057425	21.75	300
526679.9	5056382	14.5	200	527917	5057325	13	300
527980.3	5057029	78	200	527675.2	5056566	27	300
527482.2	5056662	60	200	526620.7	5056928	41	300
528013.1	5057366	30	200	526810.8	5057410	2	300
526624.8	5056772	47	200	527262.2	5056650	88	300
527374.4	5056826	24	200	527568.6	5056491	25	300
526732.4	5057264	24	200	527891	5056955	16	300
527316.6	5056664	108	200	526831.4	5057375	23	300
526728.4	5056374	43	200	526717.2	5057170	28	300
527473.8	5056758	73	200	526708.8	5057124	43	300
527995.9	5057437	38	200	527724.8	5056709	5	300
527875.7	5057323	24.75	200	526865.1	5056760	25	300
527022.6	5056898	28	200	527687.6	5056752	96	300
526525.2	5056515	35	200	527009.4	5056413	22	300
527164.5	5056467	29	200	528018.2	5057438	32	300
526675.8	5056989	31	200	527992.9	5057049	102	300
526723.9	5057062	31	200	527069.7	5056622	24	300
527740.5	5056750	7	200	526793.3	5057400	31	300
527315.6	5056772	17	200	527905.7	5057225	30	300
527729	5056575	24	200	527511.7	5056666	66	300
527921	5057129	31	200	526863.1	5057120	17	300
526910.8	5056637	13	200	526672.3	5056715	26	300
527542.1	5056674	78	200	527701.5	5057256	18	300
527714.2	5056735	12	200	527272.1	5057081	10	300
527227.1	5056625	9	200	526863.1	5056916	47	300
526855.9	5057158	35	200	526718.6	5056831	44	300
527677.4	5056727	44	200	527500.5	5056734	59.5	300

Easting (m)	Northing (m)	Thickness (cm)	Up to Grouping	Easting (m)	Northing (m)	Thickness (cm)	Up to Grouping
527577.4	5056648	8	300	526873.4	5056726	17	300
527976.1	5056976	27	300	526754.2	5056984	48	300
528062.5	5056787	15	300	527611.3	5056584	19	300
527425.8	5056692	13	300	527662	5056738	34	300
528050.2	5057295	13	300	526575.1	5057068	29	300
527922.5	5057176	40	300	526631.8	5057179	15	300
527777.2	5056674	16	300	527083.8	5056824	34	300
527200.1	5056527	25	300	526865.1	5057081	13.5	300
527346.1	5056735	12	300	527645.7	5056716	75	300
527428.5	5056757	65	300	527726	5056673	13	300
527265.7	5056723	10	300	526588.5	5057332	17	300
527628.4	5056919	7	300	527836.5	5056858	11	300
527315.8	5056650	28	300	527870.6	5056919	16	300
526878.9	5056467	16	300	528075.7	5057415	30	300
527469.1	5056778	9	300	527499.2	5056827	30	300
526564.4	5056656	0	300	526635.7	5056957	30	300
527066.8	5056778	20	300	526909.2	5056528	8	300
527853.7	5057359	18	300	527133.3	5056525	35	300
527825.1	5057321	21	300	527726.5	5056810	19	300
526774.3	5056831	28	300	526522.1	5056924	32	300
527304.6	5056837	14	300	528023.2	5056971	9	300
527323.9	5056426	8	300	527312.8	5056701	5	300
527339.3	5056684	96	300	527125.8	5056728	12	300
526818.9	5056965	29	300	527835.7	5056701	4.7	300
527627.2	5056731	11	300	526512.9	5056617	25	300
527922.5	5056988	51	300	527949.2	5057012	44	300
526862.5	5057025	22	300	527193.5	5056727	18	300
527553.7	5056707	31	300	527170.3	5056638	7	400
527287.4	5056914	20	300	527885.2	5057271	31	400
527040.9	5056620	18	300	527992.4	5057276	22	400
526992	5056609	25	300	526822.2	5057351	33	400
526630.5	5057075	18	300	527222.2	5056477	15	400
526823	5056924	67	300	527069.3	5056663	14	400
527761	5056832	93	300	526972.7	5056675	15	400
528018.8	5056874	13	300	526832.9	5057286	33	400
527826.7	5056766	10	300	526633.6	5057320	26	400
526869.5	5056967	35	300	527613.6	5056778	6	400
526613.6	5057122	14	300	526732.2	5057382	27	400
527671.6	5056830	10	300	526620.2	5056521	37	400

Easting (m)	Northing (m)	Thickness (cm)	Up to Grouping	Easting (m)	Northing (m)	Thickness (cm)	Up to Grouping
526640.1	5056868	15	400	526963.1	5056577	13	400
526777.7	5056776	23	400	526651.3	5057215	31	400
527526.2	5056719	79	400	526736.2	5056618	58	400
526724	5057028	39	400	527221.5	5056526	22	400
527807.5	5056877	36	400	526721.7	5056730	47	400
526824.7	5057027	33	400	527426.9	5056777	9	400
526769.4	5057233	25	400	527977.7	5057377	25	400
527362.7	5056698	96	400	527663.5	5056694	12	400
526816	5057110	38	400	527171.1	5056733	18	400
526923.4	5056485	11	400	527878	5056870	13	400
526572.4	5056917	2	400	527617.1	5056664	6	400
527242.8	5056816	17	400	527904.7	5057011	18	400
527952.5	5057214	19	400	526780.9	5057074	23.5	400
526819.5	5056866	62	400	527515	5056527	32	400
527556.7	5056417	24	400	527360.9	5056706	72	400
527862.9	5057269	19	400	527096.4	5056508	12	400
527529.8	5056733	59	400	526821.6	5056416	42	400
527189.1	5056657	75	400	527900	5057425	29.25	400
527266.8	5056626	17	400	527011	5056561	18	400
527219.7	5057062	16	400	527322.2	5056673	130	400
527376.7	5056576	21	400	527711.5	5056622	15	400
526552.5	5056600	40	400	526671.4	5056920	48	400
527668	5056769	4	400	526673.4	5057422	21	400
527893.9	5057167	70	400	527222	5056566	17	400
526520.4	5057017	10	400	527347.7	5056552	18	400
526775.5	5056720	26	400	528018.9	5056929	12	400
527316	5056634	6	400	527939.5	5057062	1.5	400
527731.3	5057327	24	400	526759.4	5057162	35	400
527778.7	5057284	26	400	527571.4	5056574	14	400
527537.9	5056771	6	400	527639.9	5057177	10	400
526776.2	5057269	35	400	526619.8	5056434	45	400
527609.8	5056717	8	400	526673.5	5057076	28	400
527486.1	5056577	25	400	527281.7	5056581	17	400
527183.7	5056703	15	400	527471.7	5056690	11	400
526871.7	5057268	20	400	526754.4	5056555	14	400
527169.1	5056529	13	400	528024.7	5057318	30	400
527949.2	5057126	47	400	527035.5	5056670	39	400
526924.6	5056973	23	400	527433.7	5056744	38	400
526829.5	5056525	25	400	527657.8	5056765	9	400

Easting (m)	Northing (m)	Thickness (cm)	Up to Grouping	Easting (m)	Northing (m)	Thickness (cm)	Up to Grouping
527478.5	5056626	6	400	527726.3	5056876	12	460
526689.5	5056577	50	400	526633.2	5057269	18	460
527576.5	5056735	8	400	527921.6	5056960	22	460
527902.1	5056774	11	400	527038.2	5056575	31	460
527177.7	5056573	17	400	527425.6	5056626	14	460
527953.9	5057287	21	400	526722.6	5056417	41	460
526667.6	5057369	30	400	526727.3	5056928	26	460
526826.9	5057220	49	400	527877.7	5056967	60	460
526827.9	5056386	52	400	527173	5056771	26	460
527589	5056696	45	400	526776	5056916	27	460
526870.7	5056665	33	460	526525.7	5056732	32	460
526876.5	5056834	22	460	527725.8	5056826	2	460
527073.1	5056668	12	460	526671.8	5056624	26	460
527791.5	5056857	59	460	527319.5	5056486	20	460
527683.2	5056717	48	460	527013	5056605	50	460
527637	5056862	11	460	526769.9	5057324	35	460
526476.4	5057154	23	460	527585.8	5056658	5	460
526825.6	5056621	27	460	527580	5056623	12	460
526680.8	5057124	33	460	527018.1	5056641	19	460
527036.5	5056526	14	460	527378.6	5056659	9	460
527061	5056872	10	460	526981.2	5056473	28	460
528019	5056768	3	460	527934	5057262	25	460
526636	5057017	36	460	527995.1	5057335	29	460
526722.7	5056665	37	460	526578.1	5056516	26	460
528025.8	5057281	16	460	527072.1	5056724	13	460
526846.4	5057066	25	460	526782.2	5056477	19	460
527947.1	5057248	31	460	526924.1	5056923	10	460
526724.9	5057469	12	460	526884.6	5056804	33	460
528025.6	5056816	5.5	460	527168.4	5056432	20	460
527807.2	5056938	17	460	527685.9	5056784	9	460
527961.9	5057068	68	460	526675.5	5057268	26	460
526569.1	5056968	32	460				
526914.6	5057168	12	460				
526868.7	5056885	30	460				
526577.7	5057166	0	460				
526970.2	5056763	20	460				
527973.5	5056880	9	460				
527543.8	5056925	10	460				
527765	5056774	8	460				

Appendix D: Summary of Correlation Length Results

Sample Size (#)	Square (#)	X-direction	Y-direction	Isotropic
50	1	118.03	113.68	115.21
50	2	52.4	168.23	93.37
50	3	84.71	142.71	106.8
50	4	370.25	81.35	154.87
50	5	230.85	65.01	90.8
50	6	115.25	60.03	78.66
100	1	109.06	118.42	114.06
100	2	58.44	285.92	119.3
100	3	119.39	220.06	142.95
100	4	229.72	72.06	121.13
100	5	117.06	62.09	80.76
100	6	65.1	64.39	64.55
200	1	385.08	54.71	134.62
200	2	154.94	124.33	135
200	3	113.15	117.43	115.05
200	4	489.2	38.67	147.18
200	5	183.07	56.25	84.21
200	6	47.82	45.99	46.79
300	1	236.6	51.83	102.15
300	2	175.88	100.97	116.07
300	3	104.58	202.68	134.39
300	4	321.98	36.48	115.36
300	5	136.45	48.2	66.51
300	6	105.1	53.84	73.27
400	1	56.7	96.12	77.29
400	2	87.83	237.19	132.79
400	3	108.27	276.81	146.76
400	4	323.69	32.85	105.91
400	5	124.95	37.56	59.52
400	6	114.3	50.35	72.32
460	1	57.34	101.63	80.75
460	2	71.22	141.04	97
460	3	102.91	254.44	135.81
460	4	280.55	34.08	104.42
460	5	141.4	37.69	61.03
460	6	156.16	43.93	75.73

Appendix E: Krige and Averaged LAS Thickness Maps

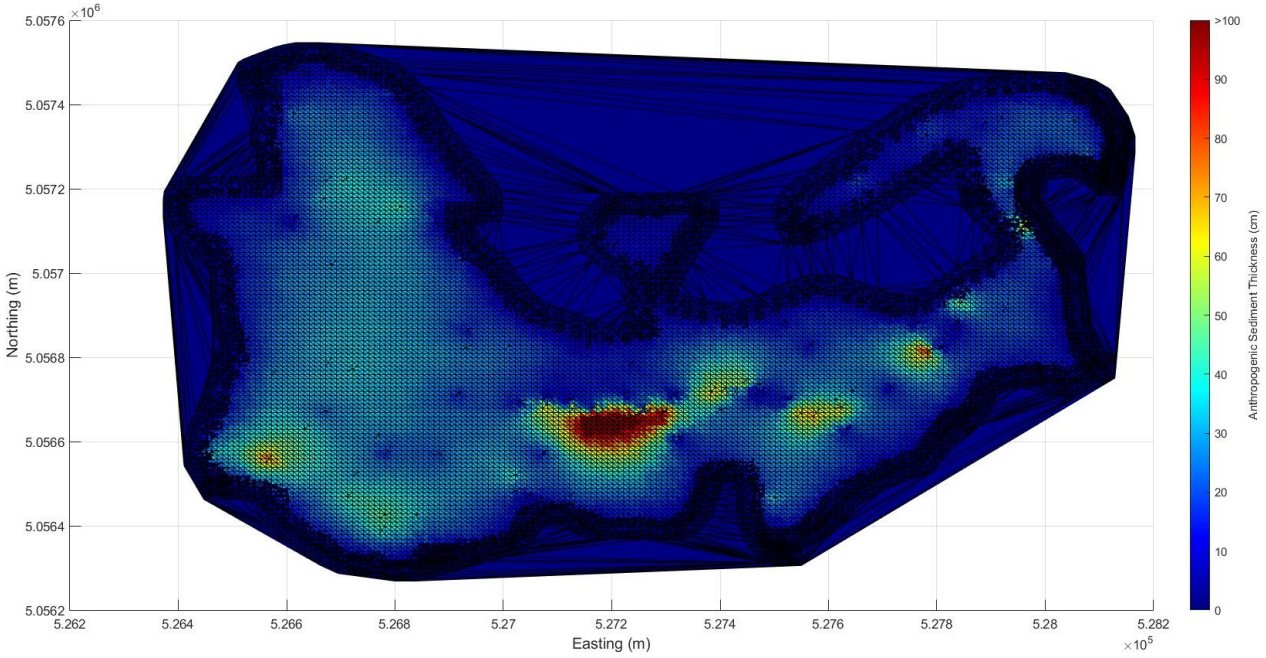

Figure 21: Sim2d averaged simulation thickness at the average correlation length and sample size of 100.

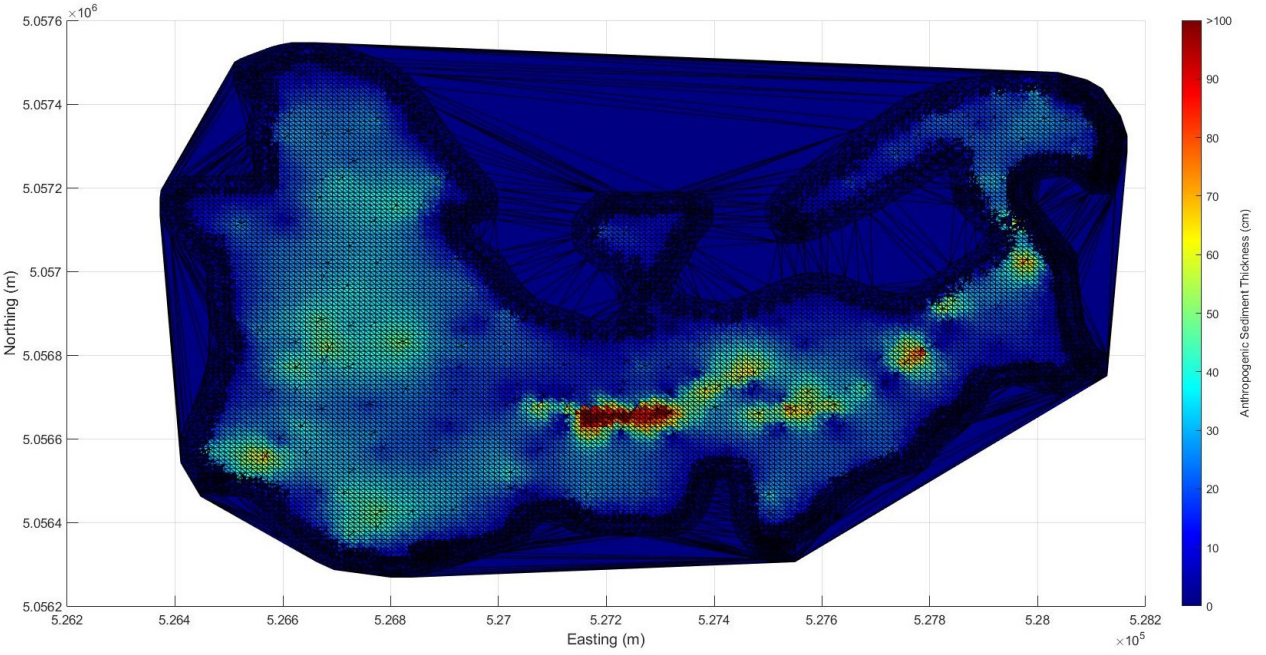

Figure 22: Sim2d averaged simulation thickness at the average correlation length and sample size of 200.

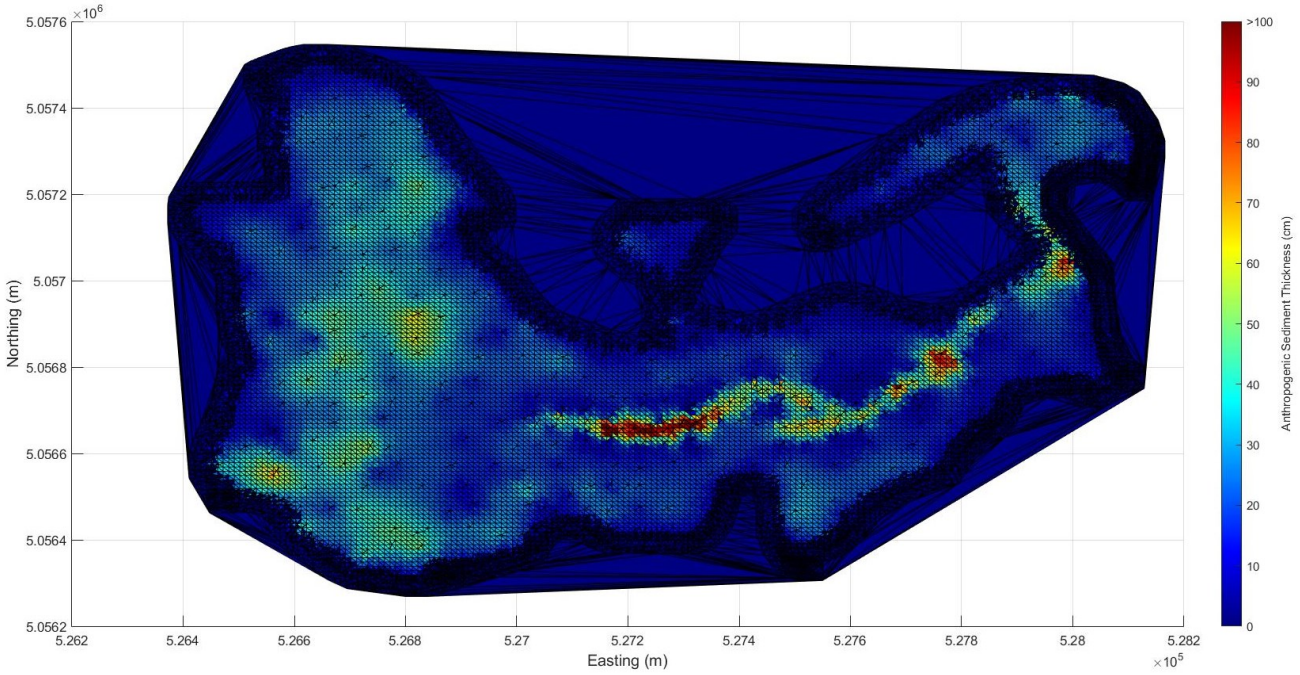

Figure 23: Sim2d averaged simulation thickness at the average correlation length and sample size of 400.

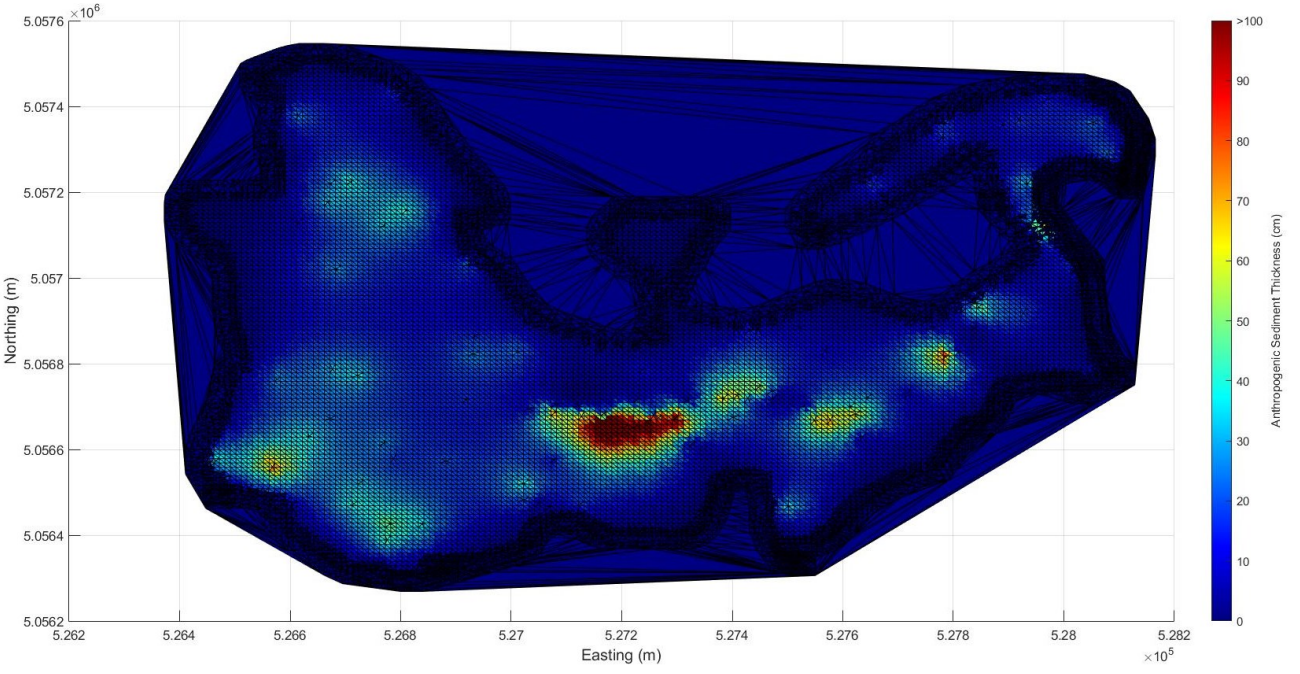

Figure 24: Krige simulation thickness at the average correlation length and sample size of 100.

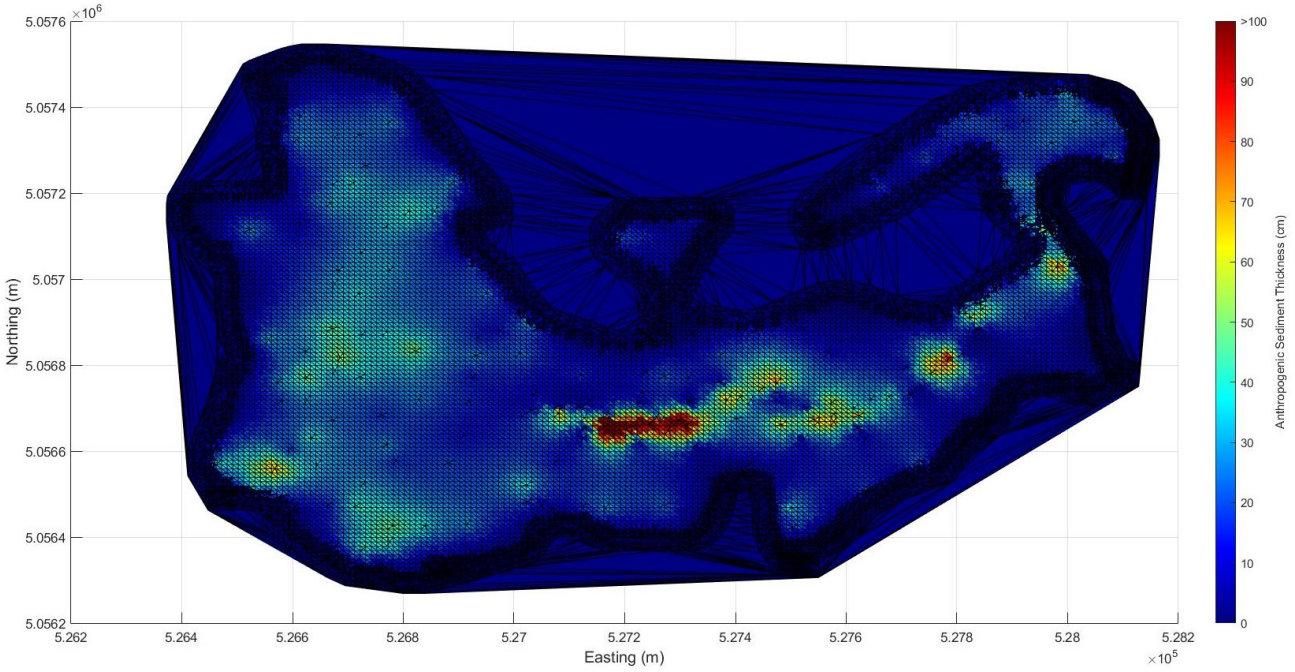

Figure 25: Krige simulation thickness at the average correlation length and sample size of 200.

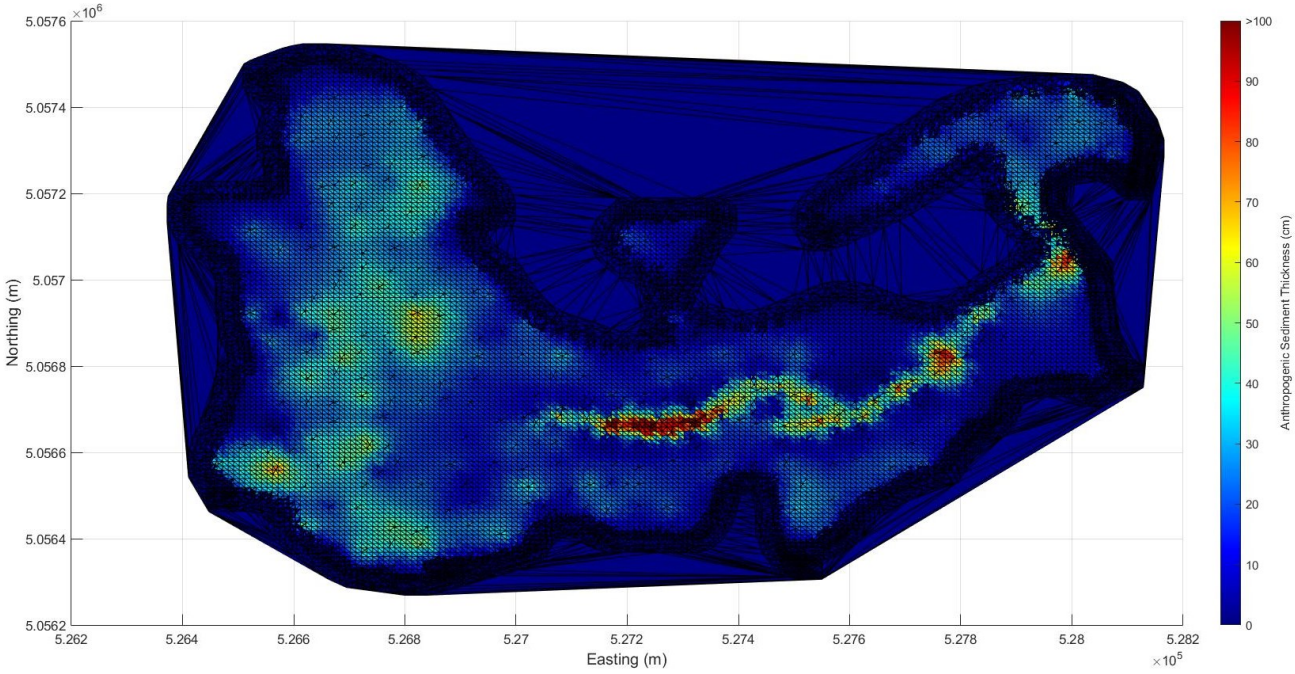

Figure 26: Krige simulation thickness at the average correlation length and sample size of 400.